

R  
E  
S  
E  
A  
R  
C  
H  
E  
S  
T  
A  
B  
L  
I  
S  
H  
M  
E  
N  
T  
L  
I  
B  
R  
A  
R  
Y



MINISTRY OF DEFENCE (PROCUREMENT EXECUTIVE)

AERONAUTICAL RESEARCH COUNCIL

REPORTS AND MEMORANDA

A Comparison of Wing Pressure Distributions Measured  
in Flight and on a Windtunnel Model of the  
Super VC.10

By Miss G. C. BROWNE, T. E. B. BATEMAN, M. PAVITT and A. B. HAINES

Aircraft Research Association Limited

LONDON: HER MAJESTY'S STATIONERY OFFICE

1972

PRICE £2.50p NET

## LIST OF CONTENTS

1. Introduction
2. Aircraft Details and Flight Tests
3. Details of Model and Tunnel Tests
4. Presentation of Results
5. Effects of Wing Surface Tubing
6. Discussion of Flight-Tunnel Comparison
  - 6.1 Middle and Outer wing
  - 6.2 Inner wing
7. Conclusions

References

Tables—1 to 5

Illustrations—Figs. 1 to 17

Detachable Abstract Cards.

## 1. Introduction

It is generally assumed—or at least, hoped—that pressure distributions measured on windtunnel models apply directly to the full-scale aircraft and that they can therefore be used for aerodynamic appraisal and for stressing or loading calculations. There are however various reasons why exact correspondence may not always be achieved and there is a continuing need for direct comparison between full-scale and model data for typical practical cases; only in this way can one obtain final validation of the techniques used in the tunnel tests. This report presents one such comparison—between pressure measurements in flight over the wing of a Super VC.10 and correspondingly, for a 1/15 scale half-model tested in the A.R.A. 9 ft × 8 ft transonic tunnel at a Reynolds number of  $5.4 \times 10^6$ .

This comparison is of particular interest because all the flight results (consisting of ten combinations of  $M$  and  $C_L$ ) were obtained for conditions where the flow over the wing upper surface was already supercritical, i.e., shock waves were present, and in at least two of the ten conditions, a significant flow separation was observed aft of the shock. A recent paper<sup>1</sup> by Pearcey, Osborne and Haines has discussed the nature of the scale effect likely to be observed under such conditions and how this scale effect can be minimised through the use of roughness bands on the windtunnel models. The position and size of the bands must be chosen to ensure that the boundary layer is turbulent ahead of the shock and has a thickness not so increased or a profile not so distorted as to provoke a separation not present full-scale, or to modify any separation that is present full-scale. Obviously, the magnitude of any scale effect remaining after following this advice is likely to vary from one wing design to another. In one respect, the Super VC.10 wing should not be unduly sensitive. The pressure distributions are such that no incipient rear separation should be observed even at the model test Reynolds number of  $5.4 \times 10^6$  and hence, in the language of Ref. 1, the relevant flow model should be Class A rather than Class B. On the other hand, the chordwise pressure distribution over much of the upper surface includes an adverse pressure gradient far forward and hence, transition tends to occur before 0.1  $c$ , whether or not a roughness band is used. This means that particularly at a Reynolds number as high as  $R = 5.4 \times 10^6$ , it is not possible to adopt the 'under-fixing' technique recommended in Ref. 1. Also, it is difficult to choose a position for the roughness band where it will not on the one hand interfere with the development of the high suction region near the leading edge nor, on the other hand, provoke a separation in the subsequent adverse pressure gradient. In these senses, therefore, the Super VC.10 wing is a sensitive example. In the present report, the main comparisons are between the flight results and tunnel data obtained with a 'standard' roughness band. This is of the type normally used in past routine testing where one of the test aims is usually to obtain drag data that can be interpreted accurately. The 'standard' bands extend over the complete span on both surfaces and are coarse enough to provoke a turbulent boundary layer immediately downstream of the band. Tests were also made with what was called a 'minimum roughness' band; this only extended over the region (outer wing, upper surface) where there was a risk that without a band, there might be laminar flow back to the shock. Some comparisons between the results for the two types of band are mentioned in the report; in general, any differences are small in this instance but for other wings where flow model B (with an incipient rear separation) applies, more substantial effects might be observed. Hence, the word 'standard' in this report refers to the past; it is now common practice, as suggested in Ref. 2, even in routine tests, to obtain comparative data with two or more roughness bands, accepting the data from whichever appears more appropriate. In principle, the 'minimum roughness' band of this report would be judged more appropriate when obtaining pressures in conditions near or beyond the  $C_L$ - $M$  boundary for flow separation.

The comparison of the pressure measurements made in flight and in the tunnel can be influenced by various factors quite apart from genuine scale effect and the transition-fixing in the tunnel tests. For example,

- (i) The technique used for the actual pressure measurements. Under this heading, perhaps the most significant point is that the pressure measurements in flight were made with the pressure tubing laid externally to the wing surface. Previous low speed tunnel tests at B.A.C. had suggested that the interference of this tubing should not be appreciable, but nevertheless, as will be seen later, the possible effects at high speeds are now thought to be important.

- (ii) The model representation of the full-scale geometry. Under this heading, there are general points such as whether the model wing which simulated the estimated twist in 'lg' cruising flight is sufficiently close to the twist of the aircraft wing in the actual flight test conditions. Also, there are more specific points such as the representation of the vortex generators over the outer wing upper surface: for these tests, these were scaled geometrically but it has often been argued that allowance should be made for the different relative boundary layer thicknesses in flight and tunnel.
- (iii) Doubts due to the use of the half-model technique for the tunnel tests. The model was designed with the aircraft centre-line 1.5 in.\* above the tunnel floor with an extra parallel-sided insert in the fuselage below this line.
- (iv) Factors affecting the correct setting up of the  $C_L$ ,  $M$  conditions for comparison. This is not merely a question of the experimental accuracies in both flight and tunnel. The values of  $C_L$  depend on whether the tail lift in flight has been estimated correctly to give the required  $C_L$  for the wing-fuselage-nacelle configuration in the tunnel, and on the aeroelastic and half-model effects mentioned under (ii) and (iii) above. The values of  $M$  depend on whether the blockage corrections for the tunnel tests have been assessed correctly.

The effects mentioned under (i-iv) have to be assessed and allowed for before one can arrive at reliable conclusions regarding scale effect. In the present instance, it was found that the external pressure tubing used in flight was the most significant extraneous factor. This is therefore discussed in some detail in Section 5 before turning to the main discussion of the flight-tunnel comparison in Section 6.

## 2. Aircraft Details and Flight Tests

The flight data used in this flight-tunnel comparison were obtained from pressure measurements carried out on the Super VC.10 G-ARTA. A comprehensive series of flight tests was carried out during the early part of 1965, but all the information used here was obtained on flight 425 made from Wisley on 29th March 1965. The data from this test were recommended by B.A.C. Flight Test Department as being very representative and reliable. The measurements at all ten combinations of Mach number and  $C_L$  were made in the same flight and details of these, with altitude and Reynolds number are given in Table 1.

The aircraft configuration (Fig. 1) was the B.U.A. type with a Standard fuselage and Super wing having 3 ft Küchemann tips and a small leading edge fence at Station 476 (Fig. 4). This wing had a leading edge sweepback of 36 degrees, and trailing edge sweepback of 0 degrees inboard and 23 degrees outboard of Station 179. The thickness chord ratio was  $12\frac{1}{2}$  per cent at the root and  $9\frac{1}{2}$  per cent on the outer wing. For flight 425 the large fence at Station 89 was removed and the leading edge slats were bolted down to prevent distortion under load. Aircraft G-ARTA was not available for examination at the time of preparation of this report but the surface finish was stated to be good and this was borne out by examination of some Super VC.10 aircraft. One point of interest was the condition of the spoilers in the wing upper surface. It was not always possible to fit these absolutely flush but where steps would have occurred, balsa fairings were used to keep the wing surface smooth. The auxiliary air intake in the wing leading edge between Stations 6 and 80, required on the aircraft for the freon cooling system, was blanked off.

The aircraft was otherwise in a normal flight configuration, with ailerons upswept by 2.5 degrees. There were vortex generators between Stations 476 and 752 with one removed near Station 576, leaving a total of 34 in position. They were of the cropped delta type of length 2.6 in. and height 0.75 in. (See Fig. 4) and were located at a chordwise position varying from approximately 0.22 c at Station 476 to 0.27 c at Station 752, and were toed out by 30 degrees.

The method used for sensing wing surface pressures on the aircraft in flight was by the use of multiple tube runs on the surface of the wing (Fig. 2). There were full-chord Stations at 6, 80, 179, 358, 576 inches from the wing-root and partial chord Stations at 110, 198, 240, 456 inches from the root, but pressure results are not available for all the latter.

---

\* Since the experimental work was carried out using precise measurements in inches, it has been thought better to retain these rather than convert to SI units.

It can be seen that the tubes at the rear of Stations 80 and 358 were slightly outboard of those at the front of the chord, but it is considered that the chordwise pressure distributions are not significantly affected by this. The rear part of Station 80 should in fact correlate better with the tunnel pressures (at Station 89), and the only noticeable effect at Station 358 would be the influence of the flap track fairing. However, even this does not show in the flight-tunnel comparisons because it only affects the pressures on the lower surface, at the rear, and these were not measured in flight aft of 0.45 c at this station. The tubes were 0.2 in. outside diameter with a 0.12 in. bore and were manufactured in P.V.C. as strips of multibore tubing in sets of ten. At the required pressure plotting positions, holes 0.075 in. in diameter were punched into the tubes normal to the tube surface. The punch used for this operation was tapered slightly, giving an effective chamfer to the edges of the holes. Since the diameter of the holes was of the same order as that of the tubing the sides of the holes were lower than the front and back.

The banks of tubes were run chordwise along the pressure plotting stations to the region of 0.6–0.8 of the local chord for the upper surface, and 0.3–0.5 c for the lower surface, and then they were run inboard to the fuselage (see Fig. 2 and Table 5). The upper surface tubes were taken round the leading edge to eliminate discontinuities in this region and the lower surface holes up to 0.025 c were included in these upper surface tubes. Due to the fact that the leading edge was swept back 36 degrees the sets of tubes had to swing outboard away from the pressure plotting station to avoid being kinked, and back again on the lower surface. There was a discontinuity in the tube runs at 0.05 c on the lower surface in the form of a rearward-facing step about 4.25 in. wide and 0.2 in. high and a similar forward-facing step slightly further aft at the beginning of the lower surface tubes. Each of these was faired with a cold setting filler compound P.R.1422 B.T. This compound was also used to fair in the step at the edges of the sets of tubes.

The upper surface tubes entered the fuselage at about 0.7 root chord through the apertures created by the removal of three windows. These window apertures were then sealed and balsa blocks were shaped to fit round the bunches of tubes to give a firm base for sheets of heavy gauze which were fastened over the whole area. The resulting bulge on the fuselage was about 6 ft long, by 2 ft wide, and about 3 in. thick.

On the lower surface, the tubes again ran spanwise at about 0.35 c to the underbody fairing and then forward along this fairing, finally rising up the fuselage side, clearing the root leading edge by about 2 ft and entering the fuselage through a window aperture forward of the leading edge.

The tubes were attached to the wing surface using Research Bostick. At low temperatures the P.V.C. tubes became very brittle so that at places where flexing was necessary i.e. over the aileron-wing joint, silicon rubber tubing was used and joined to the P.V.C. tube well away from any pressure hole. Over the spanwise tube runs, gauze sheets were stretched to give as smooth a surface as possible. The chordwise runs were left uncovered but strips of gauze 2 in. wide were stretched over the tubes about 2 in. either side of the pressure holes. The forward-facing edges only of these strips were held down and faired in with filler compound. Where the sets of tubes had to negotiate fairly tight bends i.e. at the change from chordwise to spanwise runs, metal straps were fastened where tubes had a tendency to kink.

The pressures were measured on capsule-type dial-gauges mounted in sets of fifty on four observer panels. Each panel also included a reference static gauge, a clock giving G.M.T. and a time base giving aircraft time from take-off in tenths of a second. The reference static came from a specially modified window blank set into a window about 10 ft forward of the wing leading edge. From the reservoir at the back of this 'window static', tubes led to the observer panels. This static was also referred to the second pilot's static which takes a mean of readings from two pitot static tubes below the pilot's windows on each side of the fuselage.

The majority of gauges had a range of +1 p.s.i. to -5 p.s.i. with one revolution of the pointer being equivalent to 1 p.s.i. However, for the leading edge and the 0.001 c pressure holes at each station the pressures were read on +3 p.s.i. to -2 p.s.i. gauges having 5 p.s.i. per revolution.

The actual pressure recording was made by taking synchronized photographs of all observer panels, together with a master panel giving general flight information such as Mach number, altitude etc. On average about three sets of readings were taken over a period of perhaps ten seconds at a given flight condition. About thirty seconds elapsed before recording to allow conditions to stabilise.

In an attempt to estimate the reliability of surface multibore tubing for pressure plotting, McIntosh at B.A.C. Weybridge (Ref. 3) carried out tests on a model in a low speed (120 ft/sec) wind tunnel comparing flush pressure tappings and multibore tubes. The tubing used was of outside diameter 0.075 in., as compared with the 0.2 in. of the tubes in the G-ARTA flight tests. In relation to the wing chord this represents a difference of ten times the scaled down size. In general, use of the multibore tubing reduced the observed suction ahead of 0.2–0.3 chord, the leading edge suction peak being reduced by the order of 20 per cent. It was concluded, however, that the multibore method of testing should be satisfactory for flight tests since the relative size of tubing would be less at full scale than in the model test, thus modifying the effect of the disturbance from the tubes. On the other hand at the higher flight Reynolds numbers ( $30 \times 10^6$ ) the flow will be more sensitive to disturbances than at the model test Reynolds number ( $1 \times 10^6$ ) of McIntosh's tests. How far these ideas are borne out in practice can be seen from the later discussions in Section 5.

The accuracies for flight should be about 0.005 for  $C_p$  and 0.002 for  $C_L$ . The estimated uncertainty of Mach number quoted by R.A.E. Aero. Flight Department was  $\pm 0.005 \rightarrow \pm 0.01$  at low M (0.7  $\rightarrow$  0.8) and  $\pm 0.02$  at high M (0.8  $\rightarrow$  0.9) for production aircraft. Greater accuracy than this would be expected for flight test aircraft, since in this case the G-ARTA was calibrated against the Farnborough Javelin and more efficient instrumentation procedures were used. Therefore a total maximum possible error in Mach number was suggested as  $\pm 0.005$ .

Although, in the present flight tests, fabric strips were placed across the tubes near the pressure plotting holes, there was still an area of undulating surface immediately surrounding the holes. When the tubes were in essentially chordwise flow this would produce little disturbance, but at the leading edge and within the spanwise bank of tubes where the tubes would be subject to cross-flow, it was possible that local disturbances could produce errors in the pressure results. In addition to the immediate effect of the tubes on the pressures, there was the further possible effect on the general boundary layer development and the influence of the spanwise tubes on the shock position.

Although for flight testing in general it is recommended that the tubes at the edge of the runs should not be used, in this case some edge tubes had to be used, but only aft of 0.6 chord.

Estimates had been worked out at B.A.C. Weybridge of the spanwise twist distribution for various values of dynamic head at  $M = 0$  and 0.86. The total variation between these two extreme cases at an all-up-weight of 230 000 lb, which is an average for flight 425, was about 1.6 degrees at the wing tip. The tip twist over the range of flight conditions was estimated to vary from  $-0.2$  to  $+0.3$  degrees from the value at the design condition at  $M = 0.81$ ,  $C_L = 0.45$ .

### 3. Details of Model and Tunnel Tests

The model used for these tests was a 1/15 scale pressure plotting wing-body half-model modified to conform with the flight configuration. It had the Standard V.C.10 fuselage and nacelle assembly but no tail, and a Super V.C. 10 port wing with the 4 per cent leading edge extension out as far as  $0.65 \times$  semispan (Station 476) where there was the small leading edge fence. As on the aircraft it had a Küchemann tip, five flap-track fairings (see Fig. 3) and aileron upsweep of 2.5 degrees. The vortex generators were positioned as in flight and scaled down from full-size. For these tests four of the vortex generators had been removed, as they were very near the pressure-plotting stations. These were two near Station 576 and two near Station 677 so that finally, there were only 31 as shown in Fig. 3. There was a fillet at the root extending from about 0.6 c back to the trailing edge. It was of increasing thickness with a constant radius of about one inch. This was to correspond with a similar root fairing on the aircraft.

In order to simulate the flight configuration, the windtunnel model was manufactured with a twist distribution which was that estimated to be present at the aircraft design condition. Calculations have been made on a cantilever representation of the tunnel model and these showed that the model tip twist varied from  $-0.6$  to  $-0.5$  degrees from its design value over the M,  $C_L$  range corresponding to the flight tests. Since the aircraft tip twist varied from  $-0.2$  to  $+0.3$  degrees from the design condition, the difference in twist between the model and the aircraft varied from  $-0.4$  to  $-0.8$  degrees.

Transition was fixed on the model with roughness bands of 0.005–0.006 inch ballotini:  
0.15 in. wide at 0.05 chord on upper and lower wing surfaces  
0.5 in. wide at 1.5 in. back from the fuselage nose  
0.4 in. wide at 0.4 in. back from the lip on the nacelles.

For the 'minimum roughness' case most of the roughness on the wing surfaces was removed, leaving it only on the upper surface outboard of Station 358. Over the rest of the wing natural transition was checked at  $M = 0.7$ ,  $C_L = 0.55$  and  $M = 0.87$ ,  $C_L = 0.38$ . It was found to occur near 0.07 chord on the upper surface and 0.3 chord on the lower surface, and hence always in front of the main shock waves. For the 'minimum roughness' test the vortex generators were also removed. Any comparisons between this and the 'standard roughness' test may therefore include other effects as well as those due to transition fixing.

Chordwise pressure-plotting runs were located at six stations corresponding to 6, 89, 179, 358, 456, 576 inches from the root of the aircraft. The spanwise and chordwise positions of these pressure plotting points and those used in flight are given in Tables 2 and 3.

Initially the aim of the tests was to repeat the flight Mach numbers and the values of  $C_L$  appropriate to the Wing + Body + Nacelle configuration. The tunnel tests included a small range of  $C_L$  above and below the flight value, in order to assess whether any discrepancies between the flight and tunnel pressures could be interpreted as being due to an error in  $C_L$  (bearing in mind that the  $C_L$  values for the tunnel tests are dependent on a calculation of the tailplane contribution to  $C_L$  in trimmed flight).

These initial tests are reported in Ref. 4; these showed that under some conditions there were differences between the shockwave positions in flight and in the tunnel and that these were very sensitive to Mach number. In order to investigate this further and to gain evidence on the accuracy of measurement of Mach number in flight and in the tunnel, a third series of tunnel tests was made. It is the results of these tests which are given in the present report. They include measurements at closely spaced steps in Mach number between 0.7 and 0.92 at several fixed values of  $C_L$ , as well as repeating the basic measurements over a small  $C_L$  range which are required for the actual comparison with flight conditions.

This final series of tunnel tests was also used to investigate the effects of flight pressure measurement techniques, in particular the banks of tubing attached externally to the wing surface (as described in Section 2 above). This tubing was simulated on the model by strips of Cobroc transparent plastic, of thickness 0.02 in., cut to the appropriate shape and attached to the wing surface with Evostick. The pressure plotting holes were satisfactorily re-drilled through these strips. The thickness of 0.02 in. was chosen to represent the same percentage of the boundary layer displacement thickness (43 per cent) as the tubing did on the aircraft. The calculation of boundary layer thickness was made at 0.6 chord at Station 358, i.e. a representative location of the main spanwise bank of tubing, and the values of  $\delta^*/c$  were found to be 0.002 for the aircraft and 0.003 for the model at this position.

Tests were made on three new model configurations with this surface tubing simulated, and most of the flight combinations of  $M$  and  $C_L$  were included. The first configuration included a complete representation of all the aircraft tubing on both upper and lower surfaces. The second was with the chordwise bands removed in order to investigate the spanwise ones alone. The third configuration was with a fairing extending 0.5 in. in front of and behind the spanwise band (on the upper surface only) in an attempt to minimise the disturbances due to actual steps on the surface. It was hoped that this last test might provide a pointer to a possible improvement in flight technique.

The tests were carried out in the A.R.A. 9 ft  $\times$  8 ft transonic tunnel under standard conditions which would normally be used to provide data relevant to the aircraft. The blockage ratio of the model in this tunnel was 1.0 per cent. Forces were measured and pressure scans were taken at all data points. The local incidence of the tunnel flow over most of the wing was accurate to within  $\pm 0.2$  degrees. In other respects it is estimated that the accuracy of the tunnel data should be:

$C_p$  within  $\pm 0.005$ , i.e. within the plotting accuracy,

$C_L$  within  $\pm 0.002$  and

$M$  (uncorrected for blockage) within  $\pm 0.002$ .

The blockage corrections applied to the results varied from  $-0.001$  at  $M = 0.7$  to  $-0.008$  at  $M = 0.9$ . While the analysis has been in progress, evidence has been obtained from other tests that for complete

model tests in the tunnel with four perforated walls, the blockage corrections can be assumed to be zero up to at least  $M = 0.86$ . This suggests that the corrections for half models (tested in a working section with three perforated and one largely solid wall) should also be trivial or possibly slightly positive rather than slightly negative. If this is so, the corrected Mach numbers quoted in the present report might be as much as 0.005 too low at say,  $M = 0.84$ . It will be seen later that any changes in this direction would tend to increase the differences between the tunnel and flight data.

#### 4. Presentation of Results

Chordwise pressure distributions for the five pressure plotting stations common to the aircraft and tunnel model are presented in Figs. 5 to 9. The pressures measured in the tunnel at Station 89 are compared in these graphs with flight data for Station 80. Flight measurements were also made for Station 110 and so it would have been possible to interpolate between the results for Stations 80 and 110 to produce a strict comparison for 89 but this would not have notably altered the pictures. The pressures on the model at Station 456 are not shown as there are no comparable aircraft data, but they have been taken into account in drawing the isobar patterns.

The chordwise distributions are only shown here for four out of the ten available flight combinations of  $M$  and  $C_L$ , i.e. those at  $M = 0.696$ ,  $C_L = 0.576$ ;  $M = 0.804$ ,  $C_L = 0.455$ ;  $M = 0.839$ ,  $C_L = 0.482$  and  $M = 0.885$ ,  $C_L = 0.431$ . The Mach numbers quoted on the figures are from the tunnel tests and may be 0.002 different from the above values; however, the true values of test Mach number are used in any derived figure such as that showing the variation of shockwave position with Mach number. In an earlier interim report<sup>4</sup>, all ten data points were shown, but all the important aspects of the comparison can be illustrated from the four conditions chosen in the present case and it is desirable to avoid unnecessary repetition.

The next set of graphs in Fig. 10 compare pressure distributions from the tunnel tests on the clean wing, the wing with the spanwise banks of tubing simulated and finally the wing with both the spanwise and chordwise banks simulated. Results are compared for all stations at  $M = 0.806$ ,  $C_L = 0.45$ , and for Stations 358 and 576 at  $M = 0.883$ ,  $C_L = 0.431$ . This selection is sufficient to show all the main effects of the external tubing. Results from the test carried out with a fairing on the spanwise band are not shown since there was no significant effect visible. The hatched areas shown on Figs. 10a to g denote the position of the spanwise bank of tubing on the upper and lower surfaces at each station.

Figure 11 compares the tunnel\* and flight results for Stations 358 and 576 at a typical cruise condition for the Super VC.10,  $M = 0.805$ ,  $C_L = 0.45$ . This picture is intended to illustrate the order of agreement that was achieved in a representative non-extreme condition. It is well known that the shock position is a good parameter by which to judge the extent of any scale effect and Figs. 12a and b compare the shock positions for the full range of test conditions, for Stations 358 and 576. Obviously it is difficult to derive the shock position precisely for any particular pressure distribution with a finite number of pressure holes and some scatter is to be expected. The mean curves from the tunnel data for the variation of shock position with Mach number at a given  $C_L$  should however be reliable because the scatter has been eliminated by taking a large number of data points at close intervals in Mach number. The flight points are compared with these curves.

The pressure distributions were also integrated to give values of local  $C_L$ ; the resulting spanwise lift distributions are shown in Figs. 13a and b. The values derived from the tunnel data should be reasonably accurate, but integration of the flight data was less satisfactory because of the smaller number of pressure holes, particularly on the lower surface. It will be noted in the later discussion that the discrepancies in the integrated local  $C_L$  values are sometimes not a good guide to the genuine differences in the upper surface pressure distributions and it is these pressure distributions that one would expect to reveal any scale effect that may be present. Hence, Figs. 18 and 19 should never be used in isolation; one should always refer back to the pressure distributions to assess the source of any discrepancy. Integration for

---

\* The tunnel distributions in Fig. 11 are not the same as in Figs. 8b and 9b but this point is discussed later.

Station 6 was particularly difficult since there was no pressure tapping in flight aft of 0.45 c on the lower surface and the curves drawn through the upper surface data are very sensitive to the values recorded at 0.65 c which may be in error due to the spanwise bank of tubing which lies just behind this position.

Isobar patterns based on the pressure distributions are shown in Figs. 14a and b to 17a and b, the first of each pair being the pattern from the flight data and the second being from the nearest test condition in the tunnel.

## 5. Effects of Wing Surface Tubing

Analysis of the data soon showed that the flight-tunnel comparison, certainly for individual pressure tappings, was being confused by apparent effects of the external pressure tubing used in flight. As noted earlier, supplementary tunnel tests were therefore made, simulating this tubing on the model. These results (Fig. 10) confirmed that the effects were significant. One must have a clear picture of the nature of these effects before entering into the general discussion.

Broadly, the effects can be divided into three categories.

- (i) Local effects on the pressures at individual tappings situated either near a discontinuity in the bank of tubing, or because the tapping is just ahead of, on or just behind the spanwise bank of tubing which forms a forward-facing step followed by a backward-facing step to the flow over the wing,
- (ii) Effects which at first sight, may not appear to be local and yet probably arise because the pressure tappings are in the middle of a chordwise bank of tubing, i.e. effects which would not be observed to the same extent if the pressures had been measured elsewhere on the wing surface, and
- (iii) Effects which arise because the presence of the tubing has modified the overall flow over the wing. Let us consider each category in turn.

### (i) The Local Effects

As noted earlier, there is a discontinuity in the tubing in flight at about 0.05 c on the lower surface. This appears to be responsible for some small discrepancies recorded at 0.02 to 0.08 c at all stations out-board of Station 89 (see Figs. 7c, 8c, 9c for example). There are definite signs in the tunnel tests of a difference in this region between the results with and without the chordwise plastic strips (Figs. 10d and f) and so the tunnel tests appear to support the flight data in this respect. Fortunately, the effects occur downstream of the stagnation point and so should be irrelevant when studying the flow over the wing upper surface.

There are several locations where clearly the local pressures have been affected by the spanwise bands of pressure tubing and two main effects can be distinguished, i.e.

- (a) An increase in pressure just ahead of the bands.

This can be seen for example by comparing the data with and without bands on the tunnel model at

Station 358, Fig. 10d, 0.5 c upper surface and

Station 576, Fig. 10e, 0.4 c upper surface

and in the flight-tunnel comparison at

Station 6, Figs. 5a to d, 0.65 c upper surface and

Station 89, Figs. 6a to d, 0.57 c upper surface.

- (b) An increase in suction on and just behind the bands.

The tunnel model shows this at:

Station 6, Fig. 10a, 0.35 c lower surface,

Station 358, Fig. 10d, 0.6 c, upper surface and

Station 576, Fig. 10e, 0.45 c, upper surface

and the flight-tunnel comparison provides examples at

Station 6, Figs. 5a to d, 0.45 c, lower surface and

Station 179, Figs. 7a to d, 0.65 c, upper surface.

Precise correlation of these effects between the tunnel/simulated tubing and flight tests would not be expected because the magnitude of the effects depends critically on the exact position of the pressure holes

in relation to the front of the spanwise band of tubing and this is not necessarily the same on the model and on the aircraft. Clearly, the suction alters very sharply in the neighbourhood of the forward-facing step, and a strongly marked 'dip and bump' becomes obvious when the pressure plotting holes are suitably placed. Figure 10e shows an example of this. In other cases, however, the positioning of the holes is such that practically no effect of the tubing becomes apparent (*see* for example Fig. 10b, Station 89, upper surface). Again, this probably accounts for the fact that at Station 179 there is a very high suction recorded on the spanwise band in flight whereas at Station 358, 0.6 c, there appears to be little effect. Despite these remarks, the general order of both the average and maximum effects is much the same in the tunnel/simulated tubing and in the flight tests. Generally, the errors are about 0.05 to 0.10 in  $C_p$  while the worst examples are about 0.2 in  $C_p$ , viz., at Station 576 in the tunnel test (Fig. 10e) and at Station 179, 0.65 c upper surface in the flight test (Fig. 7). In the latter case, the flight pressure distributions have been drawn to omit this point; otherwise, the curves would have been grossly misleading.

One final point is that the data from the tunnel tests shows that the addition of the chordwise tubing strips modifies the effect of the spanwise bands.

### (ii) Quasi-local Effects

The wrapping of the chordwise bands of tubing round the wing leading edge and the presence of these chordwise bands over the forward part of the chord clearly modifies the development of the local supersonic region on the wing upper surface. This is shown in Fig. 10. For Stations 89 and 179, where the pressure distribution is of a peaky type, the addition of the chordwise tubing reduces the peak suction. At Stations 358 and 576 where the supersonic region is of a more nearly roof-top type, the tubing reduces the level of suctions, usually leaving the shape of the pressure distribution much the same but sometimes, for example Fig. 10d, accentuating the tendency for an isentropic recompression. Typically, the reduction in suction level is about 0.05 in  $C_p$  although occasionally it can be as much as 0.15. It is argued later in Section 6.1, that the general average effect in flight may have been substantially greater than 0.05.

### (iii) Overall Effects on the Flow

In general, the tunnel tests suggest that the simulated tubing has relatively little effect on the shockwave position but that it reduces the pressure recovery over the rear of the surface upstream of the trailing edge. This is observed in nearly every condition with the chordwise tubing; it is even present at lower combinations of  $M$ ,  $C_L$  not shown in this report such as  $M = 0.7$ ,  $C_L = 0.5$  and  $M = 0.8$ ,  $C_L = 0.2$ . In some cases the spanwise tubing alone has the same effect. When the shock has moved back onto the spanwise bank of tubing in the extreme flight test conditions, it appears that a major interaction between the tubing and the flow can occur. This is shown best in Fig. 10f for Station 358 at  $M = 0.883$ ,  $C_L = 0.43$ . The shock is just ahead of 0.6 c near the front of the spanwise bank of tubing. It is plausible to interpret the curves by saying that for the clean wing in the absence of the tubing, a shock-induced separation bubble has formed but is reattaching ahead of the wing trailing edge, whereas the addition of the tubing has the effect of accentuating this separation to the extent that there is already a divergence in trailing-edge pressure.

The effects under (ii, iii) as determined by the model tests with simulated tubing are therefore significant and the additional tunnel tests showed that they were not reduced by adding a fairing over the spanwise bands. The discussion in Section 6 below suggests that the effects of the actual external tubing in the flight tests could well have been even greater.

## 6. Discussion of Flight-Tunnel Comparison

There are several reasons why it is convenient to start the discussion by considering the results for the middle and outer wing, i.e. for Stations 358 and 576. First, the analysis is more straightforward than for the inner wing. For most of the test  $M$ ,  $C_L$  conditions, there is a single swept shock varying in strength across the span but otherwise quasi-two-dimensional, whereas on the inner wing there is a forward

shock followed by another supersonic region related to the flow past the root of the three-dimensional wing. Second, the shock strength is greater on the middle and outer wing and it is therefore on this part of the wing that a shock-induced separation first appears as  $M$  or  $C_L$  is increased; hence there is a greater chance of arriving at conclusions of general interest regarding the scale effect. Third, the flow over the inner wing is more affected by other extraneous factors such as the half-model technique and the precise representation of the wing-fuselage junction geometry.

In summary, therefore, the comparison for the middle and outer wing is likely to yield conclusions of general validity; the inner wing may also lead to important conclusions but they may be more peculiar to the present wing and the present model. The two areas are considered in this order in Sections 6.1 and 6.2 below.

The results for Station 179 at the planform crank are referred to in both sections.

## 6.1 Middle and Outer Wing

The flight and tunnel pressure distributions for Station 358 are compared in Fig. 8 and for Station 576 in Fig. 9. It is convenient to divide the flight test points into three groups.

(a) Points at  $M \leq 0.75$  for which the shockwave is near or ahead of 0.1 c. In the present report, this group is represented by the results for  $M = 0.694$ ,  $C_L = 0.576$  in Figs. 8a and 9a.

(b) Points at  $0.80 \leq M \leq 0.84$  for which the shockwave position is in the range 0.25 to 0.50 c and where the shockwave is moving aft with increasing Mach number at a given  $C_L$ . In this report this range is represented by the points at  $M = 0.806$ ,  $C_L = 0.455$  and  $M = 0.838$ ,  $C_L = 0.482$  in Figs. 8b, c and 9b, c and also by the comparison in Fig. 11.

(c) The two extreme points at  $M \geq 0.85$  and  $C_L > 0.4$  where there tends to be a flow separation over the rear of the upper surface in flight. In this report, this group is represented by the data for  $M = 0.883$ ,  $C_L = 0.431$  in Figs. 8d and 9d.

In the first range (a), the agreement between flight and tunnel is relatively good even as plotted, without allowing for the effects of the external pressure tubing. The peak suction measured in flight are somewhat lower than in the tunnel and the shock position is slightly further forward, 0.08 c rather than 0.10 c. The tunnel tests with simulated tubing show that these two differences are consistent with the effects to be expected from the chordwise banks of tubing in flight. For example, the addition of the chordwise tubing on the model for  $M \leq 0.75$  tends to move the shock forward and decrease the peak suction by typically 0.1 in  $C_p$  (these results are not shown here). Having allowed for the effects of the tubing, therefore, one can say that the flight and tunnel data in range (a) are in good agreement.

The standard of agreement in the second range (b) is best introduced by looking at Fig. 11 which compares the data for  $M = 0.805$ ,  $C_L = 0.45$  which is a typical cruise condition for the Super VC.10. The main points are,

(i) The shock position is in good agreement at Station 576 and is slightly further aft in flight at Station 358,

(ii) The suction level upstream of the shock is lower in flight particularly at Station 358, and

(iii) The pressure recovery at the rear of the upper surface at Station 358 is not quite as good in flight.

These are therefore the issues that have to be discussed in detail. There are however some difficulties in arriving at general conclusions about scale effect and the order of agreement between flight and tunnel merely on the basis of a comparison of the plotted pressure distributions for individual data points. In the first place, in looking at these, one has to mentally subtract any local tubing effects as described in Section 5. Second, the agreement may appear to be sensitive and non-repeatable if the shockwave is lying close to a particular pressure plotting hole. The results for  $M = 0.805$ ,  $C_L = 0.45$  at Station 358 are a good illustration of this last point. The agreement in shock position in Fig. 11a appears close but if one refers to Fig. 8b where the same flight data point is compared with three distributions from the tunnel at increasing  $C_L$ , the discrepancy in shock position appears somewhat greater at about 0.06 c. The two tunnel distributions for  $C_L = 0.45$  were obtained in different tests and a small difference in shock position can be overemphasised because the pressure hole at 0.25 c is apparently ahead of the shock in one test (Fig. 11a) and just behind the shock in the other test (Fig. 8b). In practice, in a case

such as this, the shock position could have been oscillating slightly and therefore, despite the sizeable apparent discrepancy as plotted, the genuine change in mean position between the two tests may have been quite trivial. It is therefore preferable to judge the agreement in shock position between tunnel and flight from the graphs in Fig. 12a and b. The mean curves drawn through the large number of tunnel data points should eliminate most of any scatter and one is merely left with the risk of some scatter in the flight values. This in turn can be lessened by drawing conclusions based on the eight relevant flight points in the Mach-number ranges (a, b) rather than concentrating on a single point. It is worth noting from Fig. 12 that the shock position from the distribution plotted in Fig. 11 lies on the mean curve and that therefore presenting Fig. 11 as a typical comparison was justified.

Figures 12a and b show that in the range  $0.80 \leq M \leq 0.84$ , the shockwave moves aft with increasing Mach number at a given  $C_L$ . The shockwave tends to be slightly further aft in flight but generally by not more than 0.05 c. This is more noticeable at Station 358 than at Station 576, and there is just one case showing a significantly larger discrepancy than 0.05 c, this is at Station 358 at  $M = 0.838$ ,  $C_L = 0.480$  where the shock is about 0.10 c further aft in flight (Figs. 8c and 12a).

Earlier, the accuracy of the test Mach numbers was quoted as  $\pm 0.005$  for both flight and tunnel and thus, relatively speaking, there could be an error of 0.01 in Mach number. If the flight Mach numbers were increased relative to the tunnel values by 0.01, the agreement in shock position would have been very close and better than that shown in Figs. 12a and b. This seems improbable however; a full additive effect is statistically unlikely and further, there is evidence from other models that any uncertainty in the tunnel value due to model blockage effects would be in the opposite sense. After due consideration therefore of the possible errors it was felt that Figs. 12a and b are presenting the correct picture. It is possible that the relative shock positions are affected slightly by the presence of the external pressure tubing in flight but as noted earlier these effects should be small. One is therefore left with the hypothesis that the discrepancy in shock position, generally not more than 0.05 c, is an example of genuine 'scale effect', this term including the effects of transition fixing in the tunnel test. The discrepancies are certainly in the right direction to be explained in terms of the effects of a greater boundary layer thickness, model scale. These effects are discussed in detail in Ref. 1. This distinguishes between 'Class A flows' where there is a bubble separation at the foot of the shock with the re-attachment point moving rearward with increases in  $M$  or  $C_L$  and 'Class B flows' where there is a rear-separation with the point of separation moving forward from near the trailing edge. 'Scale effects' in shock position are usually 'small' for Class A flows (assuming that the boundary layer on the model is turbulent ahead of the shock and that the test Reynolds number is greater than say,  $R = 2 \times 10^6$ ) and possibly 'large' for Class B flows. 'Large' in this context can be as much as 0.3 c. The shape of the pressure distributions over the rear of the upper surface in the present case tend to suggest a Class A situation and hence the scale effect affecting the shock position by only about 0.05 c is perhaps the result one might expect.\*

The fact that the difference in shock position is more apparent at Station 358 than at 576 could be related to the effects of the vortex generators which are on the upper surface outboard of Station 476. It could indicate that these generators are less effective in flight but this seems very unlikely; in fact, prior to the tests, any doubts concerned their effectiveness in the tunnel rather than in flight, on the grounds that the vortex generators had been scaled on the model without any allowance for the increased boundary layer thickness. A more probable interpretation is that the scale effect on shock position is smaller at Station 576 because the vortex generators have reduced the mean boundary layer thickness near the trailing edge at this station and hence any remaining differences in boundary layer thickness between model and full-scale are less significant.

Turning now to the difference in suction level in the supersonic region ahead of the shock, this can be at least partly explained in terms of the effects of the external pressure tubing in flight. Assuming however that these are the same as for the simulated tubing in the special tunnel tests (Fig. 10), they do not provide the full explanation. One is still left with sizeable discrepancies which appear to be different

---

\* It is true that some of the distributions suggest that the chordwise banks of tubing may tend to provoke a rear separation but if so, it might be merely localised and not affect the wing between the banks of tubing.

in character at Station 358 and 576. At 358, the shape of the pressure distribution in the supersonic region is similar in flight and tunnel but the suction level is lower in flight by about 0.1 in  $C_p$  even after making the corrections. At 576, the mean level in flight and tunnel is more nearly the same but the shape differs: in flight, the peak suction is greater and there is then an isentropic recovery to a suction level upstream of the shock that is again lower than in the tunnel (*see* Figs. 8b, c; 9b, c: remember that these plotted curves for the flight data do not include any correction for the tubing). Scale effect may be partly responsible for these differences but it seems unlikely that this can be the major factor. Rather, it seems that the effects of the external pressure tubing in flight may be substantially larger than those measured in the tunnel with the simulated tubing. It is arguable that the tubing has been moulded better to the wing surface on the model, particularly in cranking it to wrap round the leading edge at the outer section with its smaller leading-edge radius. This could account for the results at Station 576. The more substantial difference in suction level at 358 is more unexpected although Figs. 8b and c suggest that the relevant point is that at 358 in flight, there is a loss in pressure recovery over the rear of the upper surface which could imply a loss in circulation over this part of the span. It should be noted that this argument is not invalidated by the spanwise lift distributions in Figs. 13a and b which show higher lift in flight than in the tunnel at Station 358. This is because the comparison of the integrated  $C_L$  is dominated by the effect of the more rearward shock position in flight; also, the effect of the suction level discrepancy on the upper surface is partly cancelled by a smaller and less consistent difference on the lower surface.

It is worth pointing out that relative errors in Mach number between tunnel and flight even if they exist (and this has been doubted in the earlier discussion) could not provide the explanation for the differences in suction level upstream of the shock. Earlier, when considering the small discrepancies in shock position, it was noted that a relative change of 0.01 in Mach number, increasing the flight value or decreasing the tunnel value would improve the agreement, and it is tempting to look at the pressure distribution comparisons and suggest that this change would also help with regard to the suction level since  $(-C_p)$  is decreasing with Mach number in the range in question. However, this argument is completely fallacious. If the test Mach numbers were in error relatively speaking, this would certainly imply that the wrong data points are being compared in the figures but also it would mean that the actual  $C_p$  values had been computed incorrectly. When one allows for both these effects, one finds that the two almost cancel and hence the final standard of agreement would be substantially unaffected, the comparisons would merely be labelled with a different Mach number. This argument depends on the fact that in the range of the present data,  $(-C_p)$  in the supersonic region decreases with Mach number at a given  $C_L$ ; at lower Mach numbers,  $(-C_p)$  would increase with Mach number and the effects would have been additive.

To summarise the comparison for range (b), the shockwave position tends to be further aft in flight but in general by not more than 0.05 c. This is assessed as a genuine scale effect. Secondly, the suction levels in the supersonic region ahead of the shock are generally lower in flight and this is assessed as being largely due either to the chordwise tubing modifying the flow development around the leading edge or else, reducing the circulation round the wing.

Let us now turn to range (c), the extreme  $M - C_L$  conditions where there is apparently a shock-induced separation in flight but not in the tunnel, as shown in Figs. 8d and 9d for  $M = 0.883$ ,  $C_L = 0.431$ . The shock positions are now in good agreement but this is somewhat coincidental; if it were not for the premature separation in flight, the 0.05 c average discrepancy might still have been observed as at lower  $M$ ,  $C_L$ .

The most likely source of the premature separation in flight is once again, the effects of the external pressure tubing. As noted in Section 5, the simulated tubing on the tunnel model produces an effect of this nature when the shock moves back to near the spanwise band of tubing. However, again, the effects in flight appear to be similar in character but larger in magnitude. Also, the correlation between the appearance of the separation and the arrival of the shockwave near the tube bank is not so clear-cut at Station 576 as at 358; at 576, the spanwise bank of tubing is further forward and on this argument, one might have expected a separation at  $M = 0.838$ ,  $C_L = 0.482$ , Fig. 9c, but the flow appears to be still attached in this condition.

The greater severity of the apparent separation in flight at  $M = 0.883$ ,  $C_L = 0.431$  may indicate that as for the effects discussed earlier, the simulated tubing is not fully representing the effects in flight, (Figs. 10f and g). One must however consider whether there could be any other explanation and two ideas are worthy of discussion: first, does it suggest that the vortex generators are less effective in flight and second, is there any possibility of an adverse scale effect?

Regarding the vortex generators, other tunnel tests with and without these generators showed that they were effective in delaying trailing-edge pressure divergence to a higher  $C_L - M$  boundary. Also, even in the absence of a flow separation, they improved the pressure recovery at the trailing edge by about 0.04 in  $C_p$ . No flight data, vortex generators off, are available but it seems likely that the vortex generators would have a similar effect in flight—at least qualitatively, e.g., comparison of the pressures at 0.99 c in Figs. 8 and 9 shows that in general  $C_p = 0.12$  at Station 576 in flight as compared with only 0.08 at Station 358. The comparative tunnel data (with and without generators; not presented in this report) suggest that this change can be ascribed to the generators. Also, the flight data even for the extreme test conditions show a less well developed separation and a more rearward shock position than in the tunnel test without generators. These comparisons suggest that the premature separation in flight, relative to the tunnel, generators on, should not be linked with the action of the generators. In any case, the discrepancy is observed not only at Station 576 but at 358 which is inboard of the inner end of the line of generators.

Turning to the possibilities for scale effect, there are in principle, various mechanisms by which the  $C_L - M$  boundary for the separation to extend from the shock to the trailing edge might vary with Reynolds number. In two-dimensional flow, one would look for a favourable effect with increasing Reynolds number that could be substantial if the flow is of Class B type (interaction with a rear separation) or small if it is Class A. With a three-dimensional wing, however, with the scale effect varying across the span, the overall consequences could be either favourable or adverse. Consider for example the isobar patterns in Figs. 16 and 17. As noted earlier, the shockwave tends to be slightly further aft in flight than in the tunnel and this difference is more pronounced at Stations 179 and 358 than at Station 576. As a result the sweep of the shock front particularly near Station 358 is lower in the flight isobar pattern than in the tunnel. It follows that for a given pressure distribution, the local Mach-number component normal to the shock would be greater in flight, i.e. the shock strength would be greater and the separation boundary would for this reason be degraded. In principle, therefore, one could have an adverse scale effect on the separation boundary. However, as discussed earlier, the suction level ahead of the shock appears to be lower in flight in general and taking into account both the change in suction and the change in isobar and shock sweep, one finds that the local value of Mach number normal to the isobars at Stations 358 and 576 at  $M = 0.883$ ,  $C_L = 0.431$  is between 1.28 and 1.34 in flight as compared with about 1.36 in the tunnel and hence, numerically one might predict a trivial favourable scale effect on this argument. This quantitative assessment however depends on accepting as genuine the different suction levels in flight and tunnel. Earlier it was argued that this difference might only apply on the chordwise banks of tubing and would not be observed on the wing surface in between these banks. Therefore if one allows for the difference in shock sweep but not the difference in suction level, one would predict an adverse scale effect on the shock strength and trailing-edge pressure divergence boundary. Hence it is suggested that this hypothesis should not be excluded and should be accepted as a partial explanation. Certainly, in the future, on wings with a greater measure of scale effect between model and full-scale it is more than likely that the magnitude of this scale effect will vary across the span with important consequences on the overall behaviour. This point is developed in some detail in Ref. 6.

To summarise therefore, the premature separation in flight observed at the two extreme  $M$ ,  $C_L$  conditions is being assessed as being largely but not entirely caused by the effects of the external pressure tubing with the possibility that there is some adverse scale effect arising from a change in sweep of the shock front between model and full-scale.

## 6.2 Inner Wing

One might have expected that the root station (6) would have been the most difficult at which to obtain good agreement between flight and tunnel. On the one hand, the flight data could be affected by the

banks of tubes emerging from the windows in the fuselage side and running down onto the surface of the wing. However, the tunnel tests with simulated tubing did not suggest that it had any greater effect on the pressure distributions at the root than at the other stations further from the fuselage side (see Fig. 10a). Also, the tunnel data near the root could in principle be affected by the use of the half-model technique. Admittedly, the half-fuselage has been raised out of the tunnel floor boundary layer, but even so, the fuselage effects on the wing root pressures could still be incorrect. This could be important particularly bearing in mind that the wing is mounted in an off-centre position. This is a possible explanation for the different suction levels in flight and tunnel near the leading edge on the upper surface at the root, where perhaps the most important discrepancy is that aft of about 0.1 c, the suction is generally higher in the tunnel by an amount which increases from about 0.05 to about 0.15 in  $C_p$  as the flow becomes more supercritical (see Figs. 5b, c, d). Judging from the erratic nature of the pressure distributions measured both in flight and in the tunnel this is a sensitive region. It is also important to note that the tunnel tests with simulated tubing (Fig. 10a) indicate that the flight tubing may be responsible for some of the differences between flight and tunnel measurements near 0.1 c at Station 6, i.e. an increase in suction just ahead of 0.1 c and a decrease in suction further aft.

At Station 89 there is quite good agreement between the leading edge peak suction measured in flight and in the tunnel (Fig. 6). This may be somewhat fortuitous since it would be expected from the tests with simulated tubing (Fig. 10b) that the peaks in flight would be about 5 per cent lower than in the tunnel. Incidentally, the chordwise bank of tubing in the tunnel test was added at Station 89 since the pressure holes are at this station. In flight, the holes were at Station 80.

Despite the fears that it would be difficult to obtain good agreement between the flight and tunnel measurements at the root itself the general order of agreement is nevertheless quite good. Even the apparently striking differences over the rear of the upper surface are largely illusory. As already noted the suction recorded in flight at 0.65 c at the root is decreased by the spanwise bank of tubing, and further aft at 0.85 c the flight-tunnel difference is considered to be at least partly due to possible small differences in the wing-root fillet present on both the aircraft and the model. The measurements here are very sensitive to the precise size and shape of the fillet; this has been shown by some non-repeatability in the tunnel results from one test series to another, in spite of the fact that the fillet has been nominally the same. The 0.85 c pressure holes on the upper surface are in fact located in the root fillet and not merely just outboard of it, so these are probably very susceptible to small changes. However it is worth noting that the measurements close to the trailing edge on both the upper and lower surfaces appear to repeat well between different tests.

At Station 89 also, the differences between flight and tunnel measurements over the rear of the chord are probably partly due to the presence of the surface tubing in flight. Although the tunnel tests with the simulated tubing only show a small effect of the tubing at 0.75 c and no effect at 0.85 c on the upper surface at Station 89 (Fig. 10b), it is still considered that in the light of the effects at other stations the flight-tunnel difference at 0.85 c is due to the spanwise tubing. It should always be remembered that the simulation of the tubing effects in the tunnel tests may not be entirely correct. In this case the effect becomes more pronounced at extreme  $M - C_L$  conditions (e.g.  $M = 0.883$ ,  $C_L = 0.431$ , Fig. 6d) and the pressure at 0.99 c is also beginning to fall ( $C_p = 0.13$  compared with 0.15–0.16 at lower  $M$ ).

Turning now to the region between 0.25 c and 0.6 c on the upper surface, the apparent discrepancies between tunnel and flight in this region are of more general interest.

At Mach numbers above 0.8 a region of supercritical flow develops more noticeably on the tunnel model at Stations 6 and 89 than in flight. It is particularly conspicuous at Station 6 at high Mach number (Figs. 5b to d) and the suction reaches a maximum near 0.35 c.

Fig. 10a shows that the presence of the chordwise surface tubing causes a significant decrease in the suction level near 0.35 c and this would account for at least some of the flight-tunnel difference here. It is also relevant that in earlier tunnel tests the suction was not quite so high in this region as in the present tests and yet there is no obvious reason for this change to have occurred, since no differences could be found in the local model surfaces or in the model assembly. It therefore appears that near the root this region is very sensitive to small local changes as well as being influenced by the addition of the surface tubing in flight.

Nevertheless the supercritical type expansion can also be related to differences in the isobar patterns in flight and tunnel. For example, when comparing the patterns in Figs. 16a, b it will be seen that outboard of Station 6 (i.e. near Station 89), the rear of the isobar loops near 0.25–0.5 c are more swept in flight, thus leading, on this argument, to a less pronounced supercritical development in the pressure distribution at Station 6. The extra sweep is due partly to the isobars having to loop round to the pressure maximum near 0.12 c, (which is discussed below) and partly to the further aft shock position on the wing outboard of Station 89. Similarly, the further aft pressure rise (0.5 c rather than 0.4 c in Fig. 6c for example) is also just an inward extension of the same discrepancy.

Another discrepancy between flight and tunnel which appears at Station 89 is that the pressure rise aft of the forward peak suction is both steeper and greater in magnitude in flight than in the tunnel. To some extent, the plotting of some of the graphs may have artificially exaggerated this discrepancy; there was no pressure plotting hole on the model at 0.12 c, the position where the maximum pressure recovery occurs in flight. However, the data from other pressure holes confirm that to some extent at least, there is a genuine discrepancy between flight and tunnel.

It is possible in principle to suggest three types of explanation, firstly a change in the shock wave–boundary layer interaction, secondly a change in the supercritical development upstream of the shock, and thirdly a change in the direction (in plan view) of this shock. The fact that the flight pressures were for Station 80 and the tunnel were for 89 is not important. There were also some flight measurements at Station 110 and interpolating between 80 and 110 to produce a direct comparison for 89 does not materially alter the pictures. Examining each of these explanations in turn,

(i) A change in the shock-boundary layer interaction or expressed more precisely, the flight results are closer to the pressure rise that would be expected in inviscid flow, while in the tunnel, the pressure rise is interrupted by a bubble separation at the foot of the shock. There is evidence that suggests that this is not the correct explanation. First, oil flow tests (admittedly limited in number) have failed to reveal the bubble separation in the appropriate  $C_L - M$  range; second, in most conditions the component normal to the shock of the upstream local Mach number does not appear to be high enough to induce a separation even at the Reynolds number of the tunnel tests and third, calculations of the boundary layer thickness near 0.10 c (for the tunnel test Reynolds number and a transition position of 0.05 c, and for the flight Reynolds number and transition at the leading edge) have given very similar values for the two cases.

(ii) A change in the supercritical development upstream of the shock viewed on a quasi-two-dimensional basis. A connected point analysis for one particular case  $M = 0.806$ ,  $C_L = 0.455$ , Fig. 6b, appeared to support this suggestion; it showed that 0.04 c and 0.12 c were connected points<sup>5</sup>, but for two other cases, the analysis appeared less relevant. If it had looked encouraging in every case, the changes in apparent shock strength might have been related to the differences in magnitude and position of the peak suction near the leading edge, just as if the comparison had been between pressure distributions over two different aerofoil sections in two-dimensional flow. However, as the analysis does not appear to apply in every case, it seems that this type of explanation should also be rejected.

(iii) A change in shock direction; this would imply a change in the pressure rise through the shock even if the local Mach number ahead of the shock was the same. On this explanation, the greater pressure rise observed in flight would denote a less swept shock; comparison of the isobar patterns near Station 89 (for example, Fig. 16a versus 16b) appears to support this suggestion. One cannot say that this is proven but it is at least an arguable hypothesis and more attractive than (i and ii) above.

Even if (iii) is accepted (tentatively), one still has to try and explain why the shock sweep is different in flight and in the tunnel. It is difficult here to decide what is 'cause' and what is 'effect' but it seems possible that the different suction levels (lower in flight) over the forward part of the chord (say 0.1–0.3 c) further inboard near the body side, e.g. Station 6, form the starting point. This has been established as resulting most probably from the chordwise pressure tubing, but another relevant factor may be that the tunnel tests were made on a half-model. As noted earlier, the half-fuselage was raised 1.5 in. above the floor of the tunnel (compared with a measured tunnel flow boundary layer displacement thickness of about 0.75 in.) but it is still possible that the influence of the body on the wing root pressure distributions is not being reproduced correctly. It is difficult to forecast even the sign of any such effect.

The results for Station 179 have not been discussed in detail because the pressure distributions at this station contain both the features that have been classed as 'middle and outer wing' and those that have been classed as 'inner wing'. It is the station at which the peak suction near the leading edge, particularly at moderate Mach numbers such as  $M = 0.7$ , is at its highest. It is therefore encouraging to find that the tunnel and flight data are in very good agreement as regards these peak suction once allowance has been made for the effects of the external pressure tubing. As plotted in Fig. 7a, the values from the tunnel tests are somewhat higher but the differences which are less than 5 per cent can be entirely accounted for by the surface tubing as shown in Fig. 10c. A further point of interest is that the magnitude of the pressure rise downstream of this forward peak suction is now about the same in flight and tunnel; in this respect, the agreement is much better than at Station 89. It is significant that the isobar sweep in flight and tunnel is much the same near Station 179 and so these results provide some support for the idea put forward earlier that the different pressure rises in flight and tunnel at Station 89 should be related to differences in isobar sweep near that station. The comparisons for Station 179 at the higher Mach numbers are similar to those discussed earlier for Station 358. On a detailed point, the suction on the lower surface near the trailing edge is increased by the presence of a flap track fairing.

## 7. Conclusions

It is clear that bearing in mind the extraneous effects due to the external pressure tubing used in the flight tests, the flight and tunnel data are generally in good agreement. Clearly the genuine scale effect is small; the shockwave tends to be further aft in flight but generally by not more than 0.05 c. Admittedly, the tunnel tests are at a relatively high Reynolds number ( $R = 5.4 \times 10^6$ ) and the results suggest a Class A flow in the tunnel i.e., no incipient rear separation, but on the other hand, over much of the span, transition even without a roughness band appears far forward and hence it is impossible to offset the change in Reynolds number between tunnel and flight by a major change in transition position, i.e., by the 'underfixing technique'.

Comparisons have been shown in this report for only four out of the ten available flight test combinations of  $M$  and  $C_L$ . However, these four provide examples of all the main differences between the flight and tunnel measurements that have been found. These differences are as follows.

(1) There is a more rearward shock position in flight over part of the outer wing, for  $M - C_L$  conditions between  $M = 0.80$  and  $0.86$  where the shock is moving rearward with increasing Mach number, prior to the appearance of the flow separation in flight. Only in one case is the discrepancy more than about 0.05 c. It is however more evident at Stations 179 and 358 than at 576 and it is postulated that this is because at Station 576, the vortex generators which only extend in to 476, are thinning the boundary layer and reducing the difference in boundary layer thickness between model and full scale. The difference in shockwave position although small is nevertheless thought to be a genuine scale effect.

(2) There is a flow separation in flight but not in the tunnel over the rear of the upper surface of the middle and outer wing at extreme test conditions,  $M \geq 0.85$ ,  $C_L > 0.4$  e.g.  $M = 0.858$ ,  $C_L = 0.486$  and  $M = 0.883$ ,  $C_L = 0.431$ , but not  $M = 0.864$ ,  $C_L = 0.377$ . This difference is assessed as being partly due to the presence of the external pressure tubing in flight but may also indicate an adverse scale effect due to the sweep of the shock front being lower in flight than in the tunnel (*see* (1) above).

(3) In the same range as for (1), the suction in the supersonic region upstream of the shock over the middle and outer wing are generally lower in flight. It seems likely that this difference is again due to the effects of the external pressure tubing which in this respect, appear more substantial in flight than in the tunnel tests with simulated tubing.

(4) There is a greater pressure rise in flight through the inner part of the forward shock over the inner wing. This appears to be related to this part of the forward shock being less swept in flight and may be partly caused by the fuselage effects on the inner wing flow not being represented exactly in the half-model test.

(5) In flight the supercritical expansion over the inner wing behind the forward shock is weaker than in the tunnel tests. This appears to be related to greater isobar sweep in this region in flight but it is also affected by the sensitivity of this region to any small changes in test conditions or geometry. The higher isobar sweep is a consequence of effects (1) and (4).

There are three main conclusions regarding technique issues.

(i) The external pressure tubing of the size used in the present tests (bands 0.2 in. high, full scale) has a major effect on the measured pressures. There are both local effects when the pressure tapings are just ahead, on or just behind the spanwise banks of tubing but more seriously, it can effect the flow development over the wing as a whole and the onset of separation. In the present tests, these effects were not alleviated by adding fairings in front of and behind the spanwise banks of tubing. Frequent reference has had to be made in the discussion in this report to these effects but it has still been possible to draw fairly precise conclusions about the scale effect. It is fair to say however that this would not have been possible if the flow in the model tests had been of the Class B type, with an incipient rear separation interacting with a shock-induced separation. A better flight technique is therefore required in future.

(ii) The use of a relatively large half model with a blockage ratio of 1.0 per cent has not in general invalidated the comparison. The use of such models should therefore be encouraged in the interests of higher test Reynolds number, at least for Mach numbers up to  $M = 0.88$ .

(iii) There is no indication in the data that direct scaling of the vortex generators without allowance for the increased boundary layer thickness on the model in the tunnel has led to any serious loss in effectiveness.

## REFERENCES

- | <i>No.</i> | <i>Author(s)</i>  | <i>Title, etc.</i>   |
|------------|---|--|
| 1          | H. H. Pearcey, J. Osborne<br>and A. B. Haines                   | .. The Interaction between Local Effects at the Shock and Rear Separation—a Source of Significant Scale Effects in Wind-Tunnel Tests on Aerofoils and Wings.<br>A.R.C. 30 477 (September 1968).  |
| 2          | A. B. Haines  | .. .. Recent Research into some Aerodynamic Design Problems of Subsonic Transport Aircraft.<br>A.R.A. Report No. 10. A.R.C. 30 929 (January 1969).   |
| 3          | J. F. McIntosh  | .. .. Measurement of Wing Surface Static Pressure Distribution using External Multibore Polyvinyl Tubing.<br>B.A.C. Weybridge W.T. Report No. 2468 (March 1962).   |
| 4          | Miss G. C. Browne, T. E. B. Bateman, M. Pavitt and A. B. Haines | A Comparison of Wing Pressure Distributions measured in Flight and on a Wind Tunnel Model of the Super V.C.10.<br>A.R.A. Model Test Note M.26/1. (July 1969).  |
| 5          | H. H. Pearcey   | .. .. The Aerodynamic Design of Section Shapes for Swept Wings. in von Karman, T., (ed.): <i>Advances in Aeronautical Sciences</i> , v. 3., pp. 277–322. Pergamon Press, (1962).   |
| 6          | A. B. Haines  | .. .. Possibilities for Scale Effect on Swept Wings at High Subsonic Speeds. Recent Evidence from Pressure Plotting Tests. Paper No. 14 AGARD Conference on Facilities and Techniques for Aerodynamic Testing at Transonic Speeds and High Reynolds Number at Göttingen. (April 1971.) |

TABLE 1  
*Details of Flight Tests*

M	$C_L$ Complete Aircraft	$C_L$ Wing, body, nacelle	Altitude ft.	$R \times 10^{-6}$
0.696	0.556	0.576	38 200	28.7
0.751	0.452	0.479	37 200	32.9
0.798	0.560	0.555	43 500	26.0
0.804	0.453	0.455	39 800	31.0
0.806	0.350	0.371	34 900	38.8
0.820	0.459	0.461	40 700	30.9
0.839	0.460	0.482	41 600	29.9
0.858	0.461	0.486	42 500	29.3
0.864	0.350	0.377	37 600	36.9
0.885	0.355	0.431	38 700	35.9

TABLE 2  
*Spanwise Positions of Pressure  
 Plotting Stations  
 Station (full scale inches from root)*

Tunnel	Flight	$\eta_{\text{gross}}$
6	6	0.088
	80	0.172
89		0.182
179	179	0.284
358	358	0.488
456		0.600
576	576	0.736

TABLE 3  
Chordwise Positions of Pressure Plotting Points

Station 6 Upper surface x/c		Station 89	Station 80	Station 179 Upper surface x/c	
Tunnel	Flight	Tunnel	Flight	Tunnel	Flight
0-001	0	0-03	0	0-001	0
0-0025	0-001	0-05	0-001	0-005	0-001
0-005	0-005	0-10	0-005	0-02	0-005
0-01	0-01	0-15	0-01	0-03	0-01
0-02	0-025	0-20	0-025	0-05	0-025
0-03	0-05	0-25	0-05	0-10	0-05
0-05	0-075	0-30	0-075	0-15	0-075
0-10	0-10	0-35	0-10	0-20	0-10
0-15	0-125	0-40	0-125	0-25	0-128
0-20	0-15	0-45	0-15	0-30	0-15
0-25	0-175	0-50	0-175	0-35	0-175
0-30	0-20	0-60	0-20	0-40	0-20
0-35	0-25	0-75	0-25	0-45	0-25
0-40	0-35	0-85	0-35	0-50	0-35
0-45	0-50	0-975	0-50	0-60	0-50
0-50	0-65		0-57	0-75	0-65
0-60	0-85		0-85	0-85	0-85
0-85	0-99		0-99	0-975	0-99
0-975					
Lower surface x/c		Lower surface x/c		Lower surface x/c	
0-005	0-001	0-001	0-001	0-005	0-001
0-01	0-005	0-005	0-005	0-01	0-005
0-025	0-01	0-01	0-01	0-025	0-01
0-075	0-025	0-025	0-075	0-075	0-025
0-10	0-075	0-075	0-10	0-10	0-075
0-15	0-15	0-15	0-15	0-15	0-10
0-25	0-25	0-35	0-25	0-25	0-15
0-35	0-45	0-50	0-45	0-35	0-25
0-50		0-65		0-50	0-45
0-65		0-85		0-65	0-66
0-85		0-975		0-85	
0-975				0-975	

TABLE 3 (Continued)

Station 358 Upper surface x/c		Station 456 Upper surface x/c	Station 576 Upper surface x/c	
Tunnel	Flight	Tunnel	Tunnel	Flight
0-001	0	0-001	0-001	0
0-002	0-001	0-002	0-002	0-001
0-005	0-005	0-005	0-03	0-005
0-01	0-01	0-01	0-10	0-01
0-03	0-025	0-02	0-15	0-025
0-05	0-05	0-05	0-20	0-05
0-10	0-075	0-10	0-25	0-075
0-15	0-10	0-15	0-35	0-10
0-20	0-129	0-20	0-40	0-131
0-25	0-15	0-25	0-45	0-175
0-30	0-175	0-30	0-60	0-20
0-35	0-20	0-35	0-85	0-35
0-40	0-25	0-40	0-975	0-50
0-50	0-35	0-45		0-65
0-60	0-50	0-50		0-85
0-75	0-60	0-60		0-99
0-85	0-85	0-85		
0-975	0-99	0-975		
Lower surface x/c		Lower surface x/c	Lower surface x/c	
0-001	0-001	0-001	0-001	0-001
0-005	0-005	0-01	0-005	0-005
0-01	0-01	0-025	0-01	0-01
0-025	0-025	0-10	0-025	0-025
0-075	0-075	0-15	0-10	0-10
0-10	0-10	0-25	0-25	0-45
0-15	0-15	0-50	0-35	0-72
0-25	0-25	0-65	0-50	
0-35	0-45	0-85	0-65	
0-50		0-975	0-85	
0-65			0-975	
0-85				
0-975				

TABLE 4  
*List of Tunnel and Flight Points for Which Pressure Distributions are Compared*

Tunnel results			Corresponding flight results
M	$R \times 10^{-6}$	$C_L$	$C_L$
0.694	5.36	0.528	0.576
	5.31	0.580	
	5.26	0.623	
0.806	5.60	0.402	0.455
	5.58	0.450	
	5.56	0.493	
0.838	5.61	0.421	0.482
	5.60	0.466	
	5.59	0.517	
0.883	5.54	0.392	0.431
	5.54	0.438	
	5.52	0.479	

TABLE 5  
*Positions of Spanwise Banks of Tubes on Wing Surface*

Station	Upper surface	Lower surface
6	0.70-0.83 c	0.30-0.37 c
80	0.68-0.79 c	0.31-0.37 c
179	0.62-0.70 c	0.34-0.38 c
358	0.56-0.64 c	0.40-0.44 c
576	0.43-0.49 c	0.54-0.57 c

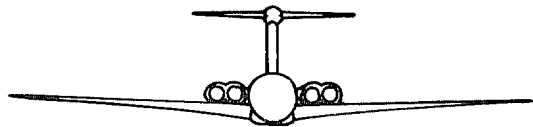
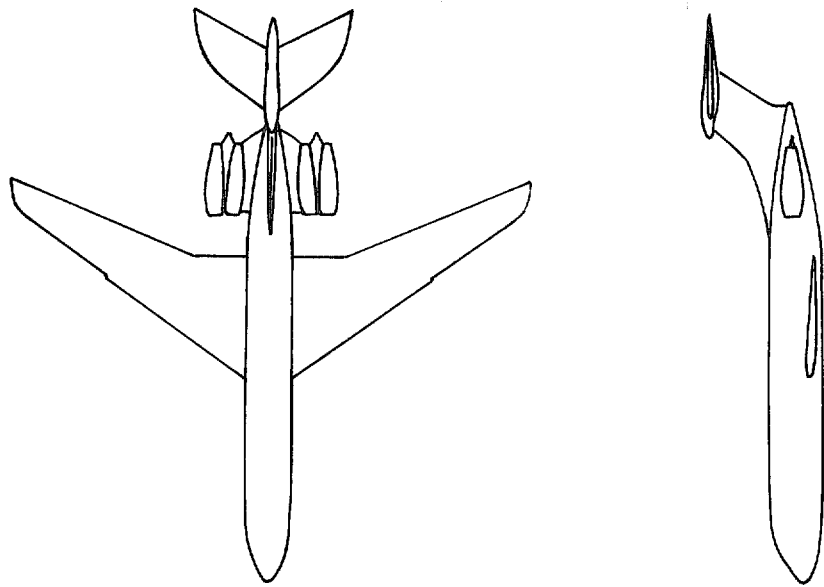


FIG. 1. G.A. of test aircraft (Super V.C.10 wing, standard fuselage).



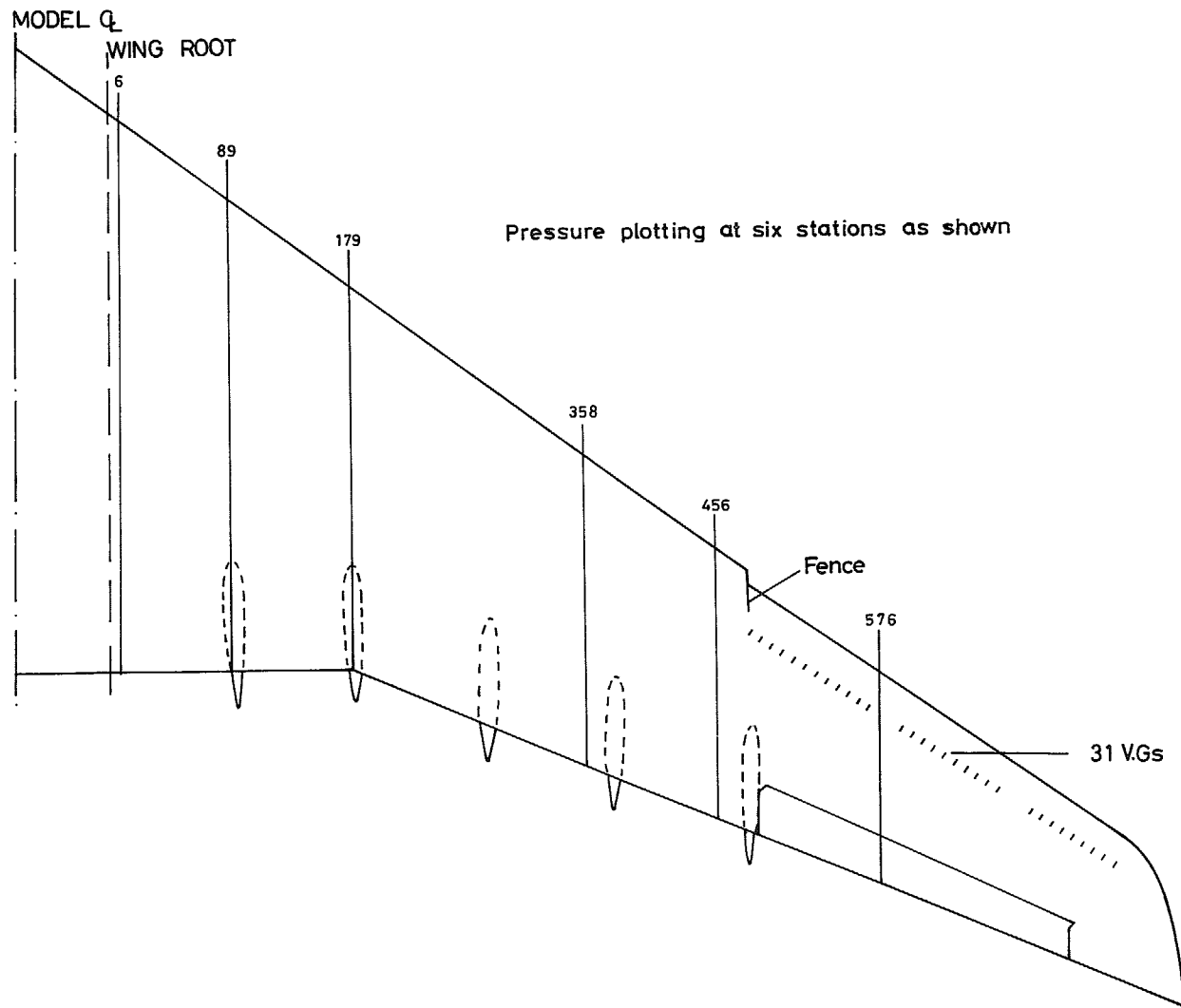


FIG. 3. Details of model wing upper surface.

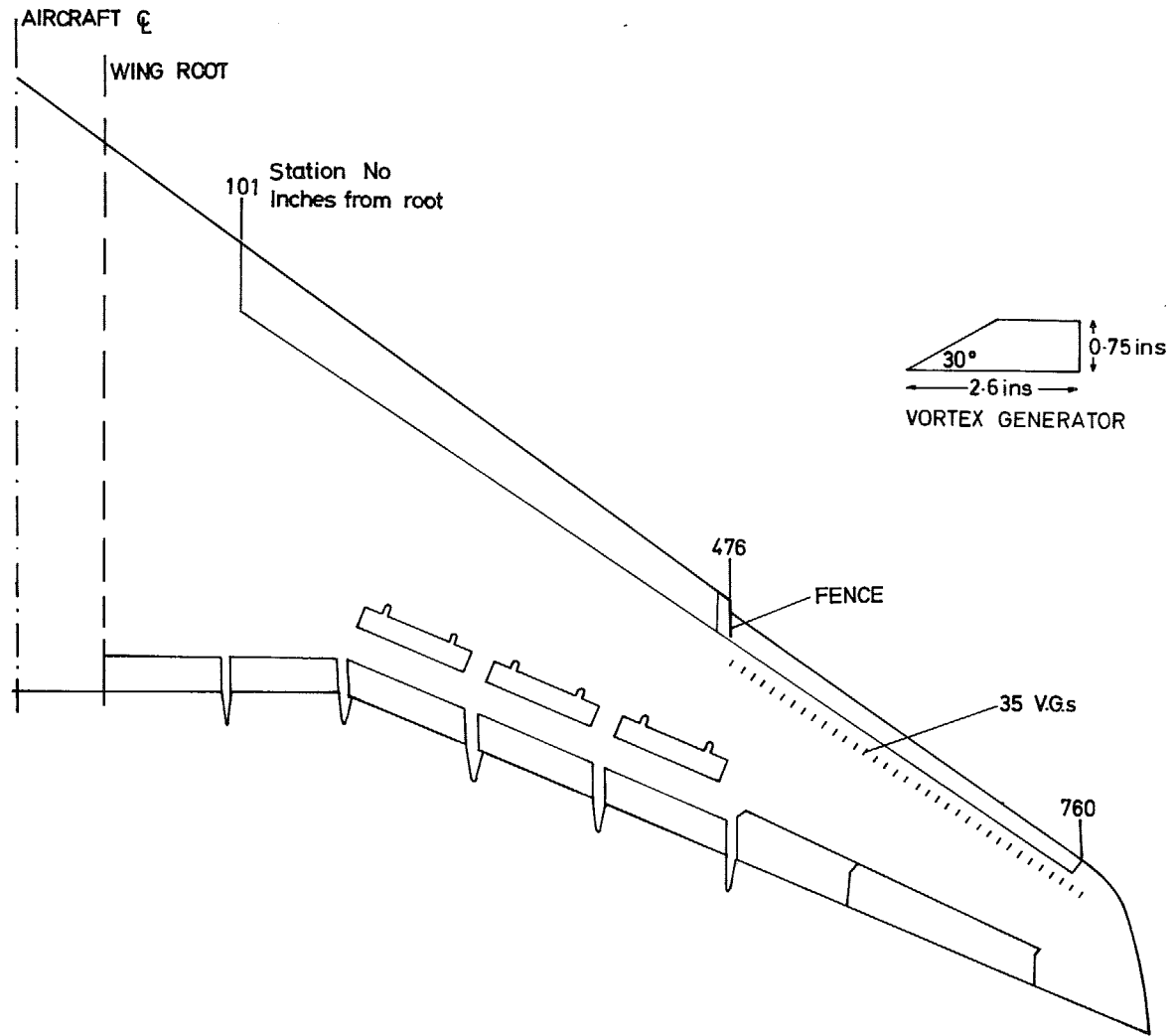


FIG. 4. Details of aircraft controls.

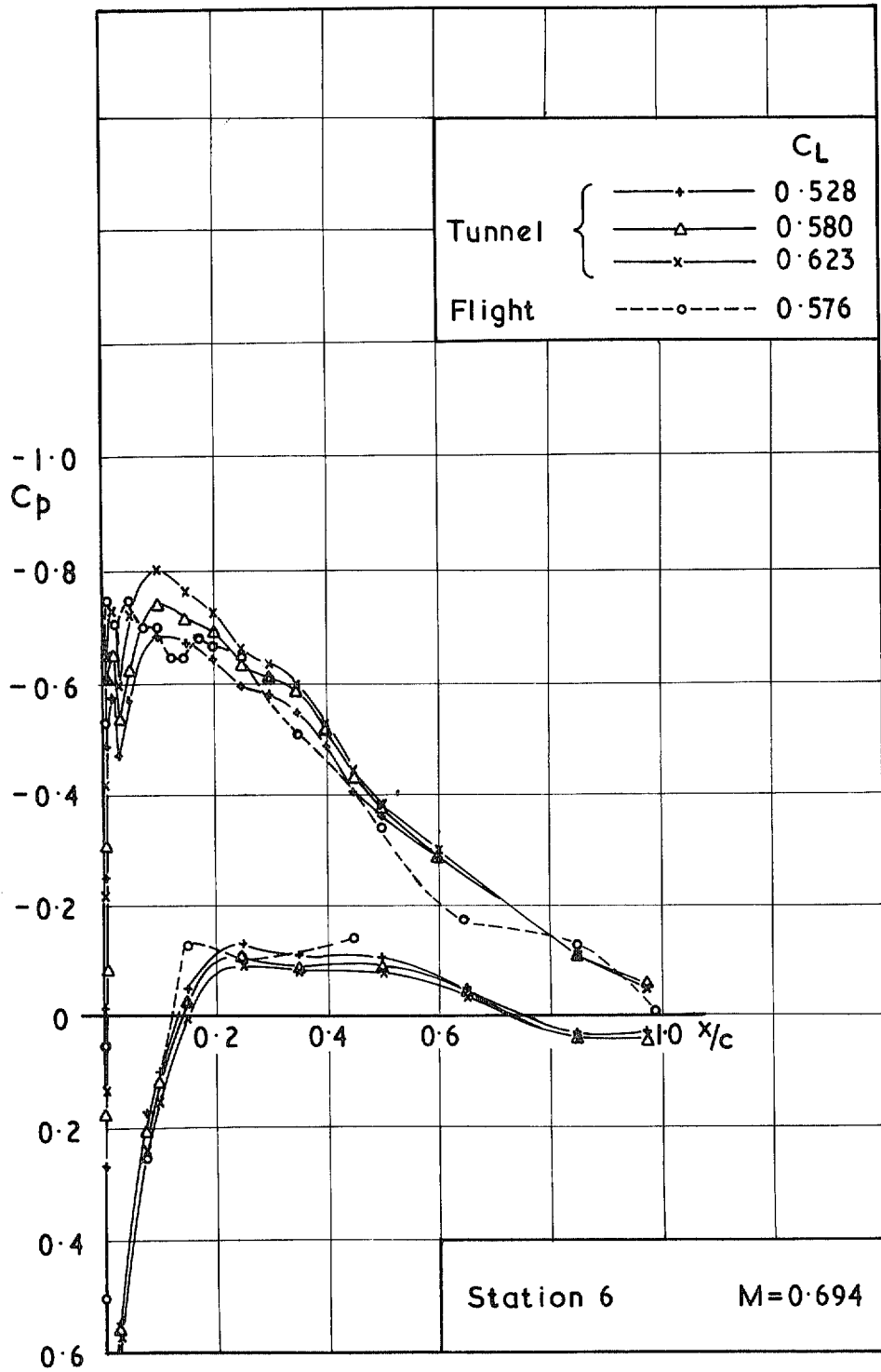


FIG. 5a.  $C_p \sim x/c$  for Station 6.  $M = 0.694$ .

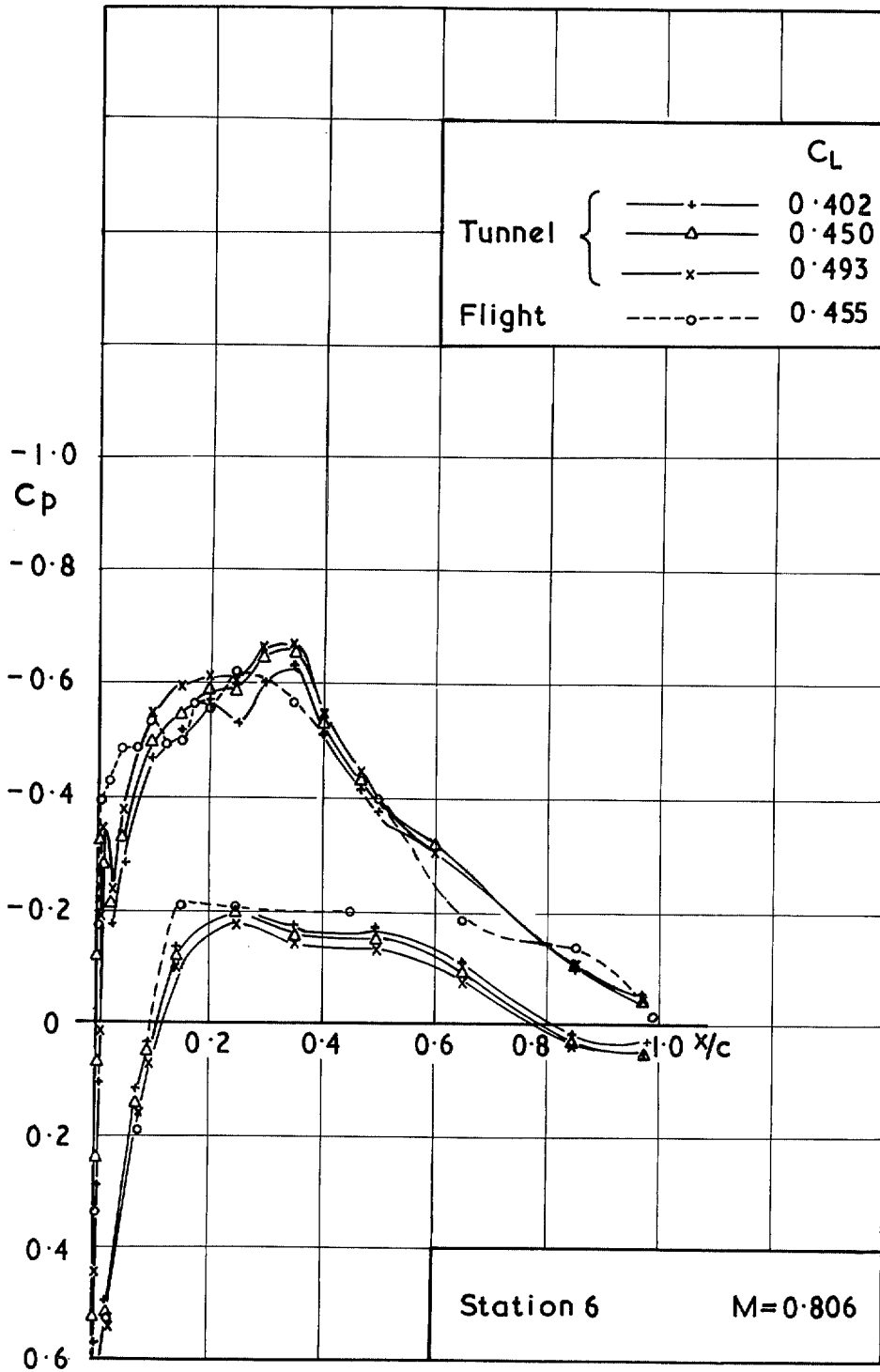


FIG. 5b.  $C_p \sim x/c$  for Station 6.  $M = 0.806$ .

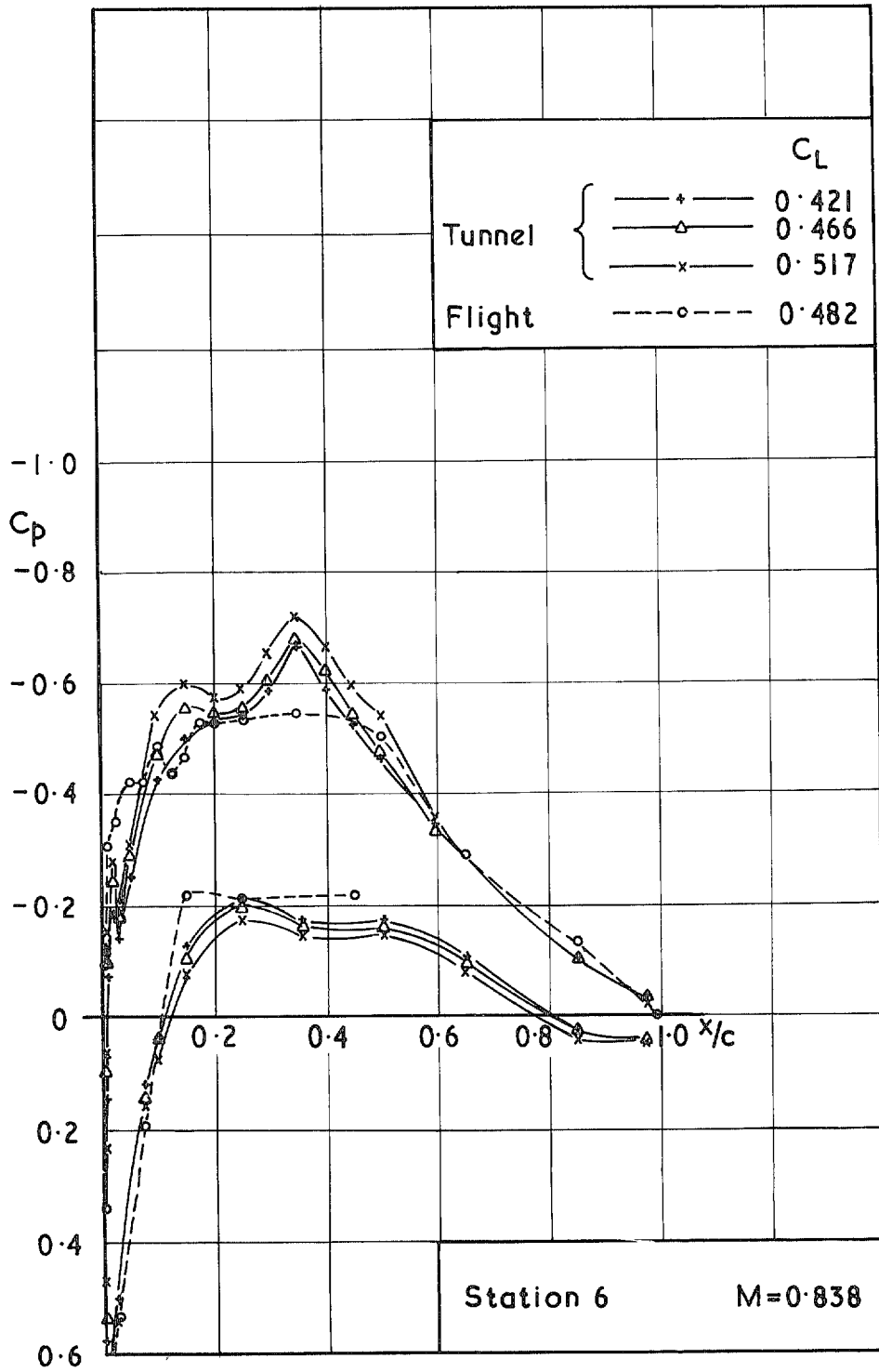


FIG. 5c.  $C_p \sim x/c$  for Station 6.  $M = 0.838$ .

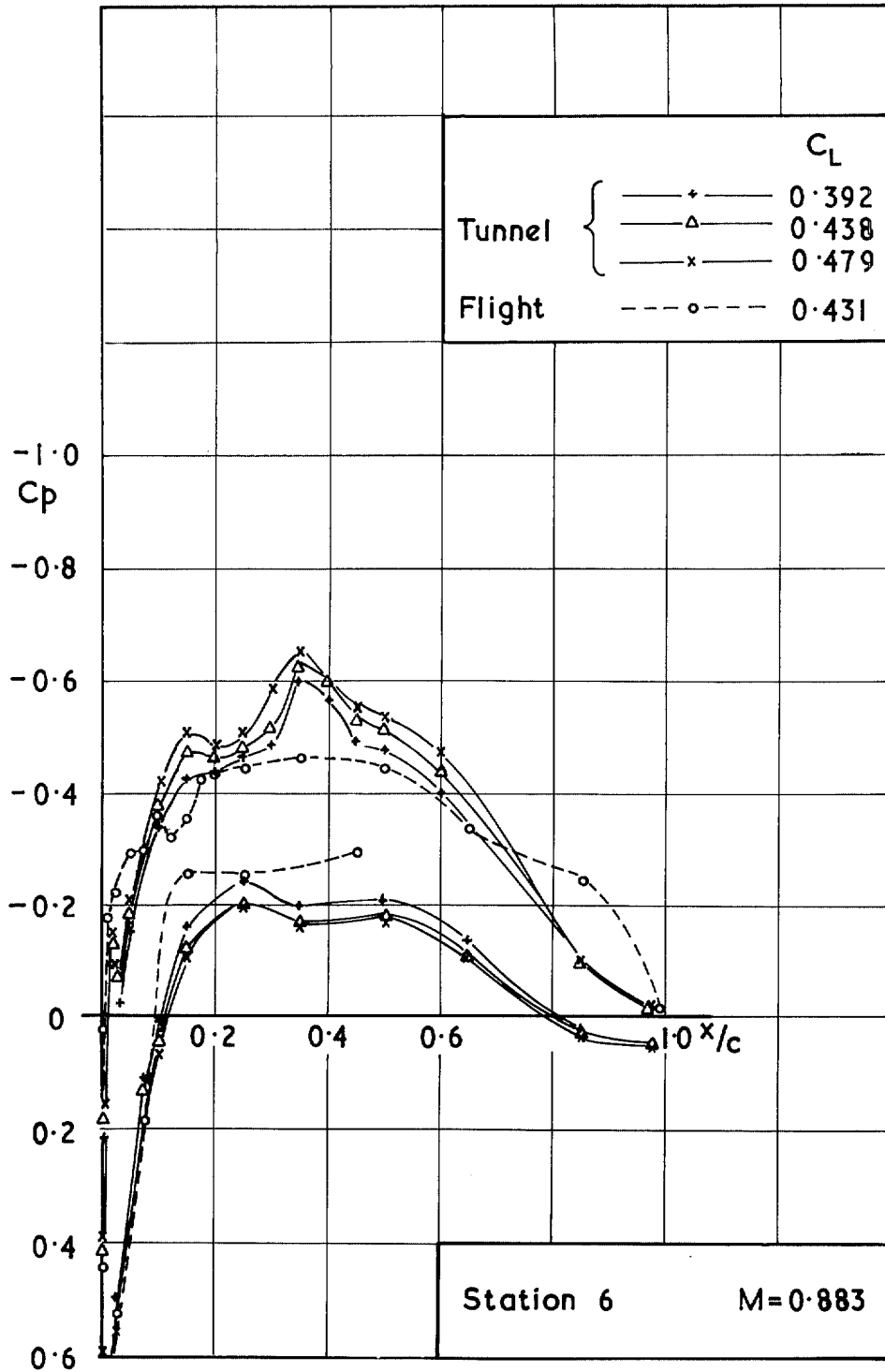


FIG. 5d.  $C_p \sim x/c$  for Station 6.  $M = 0.883$ .

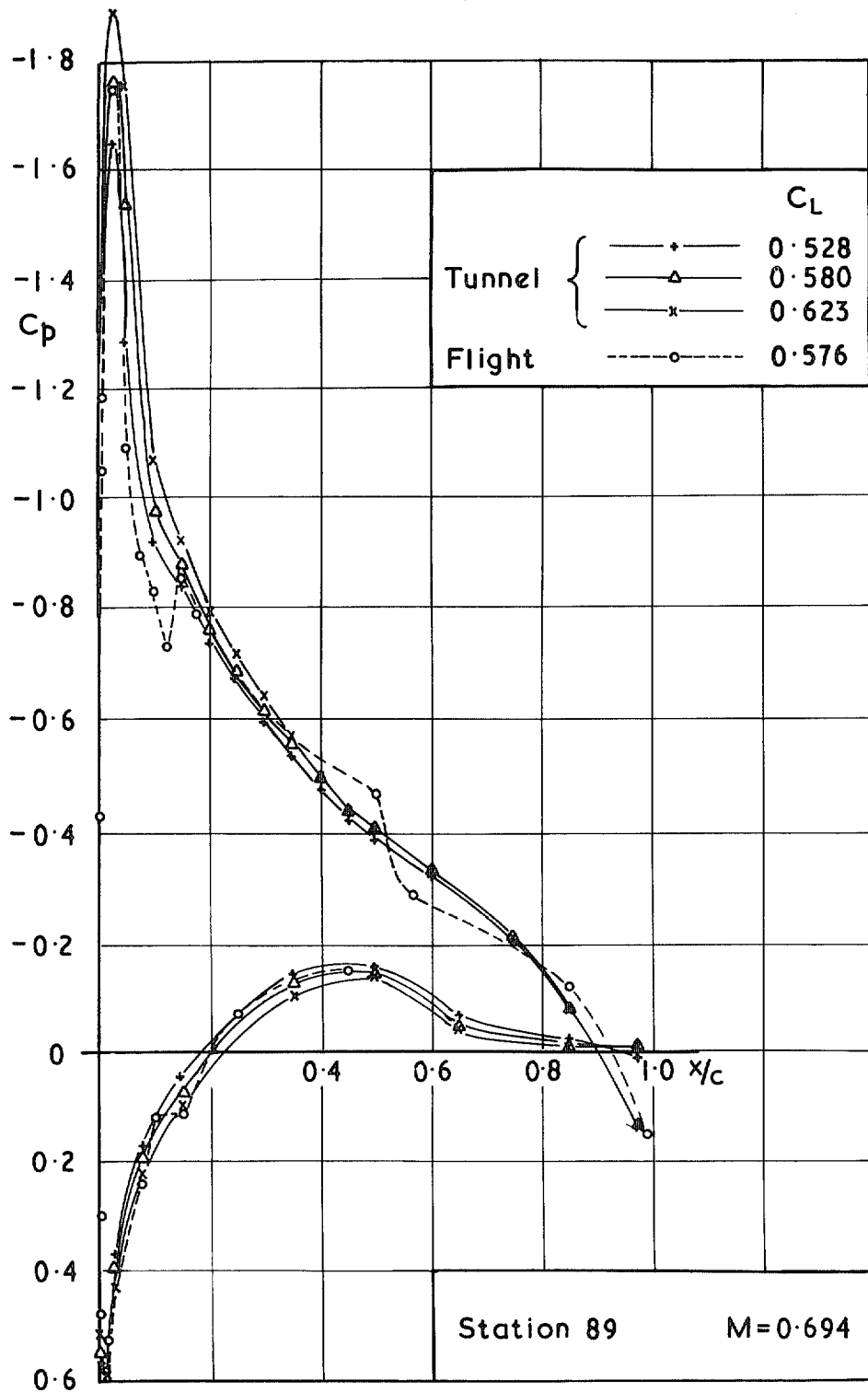


FIG. 6a.  $C_p \sim x/c$  for Station 89.  $M = 0.694$ .

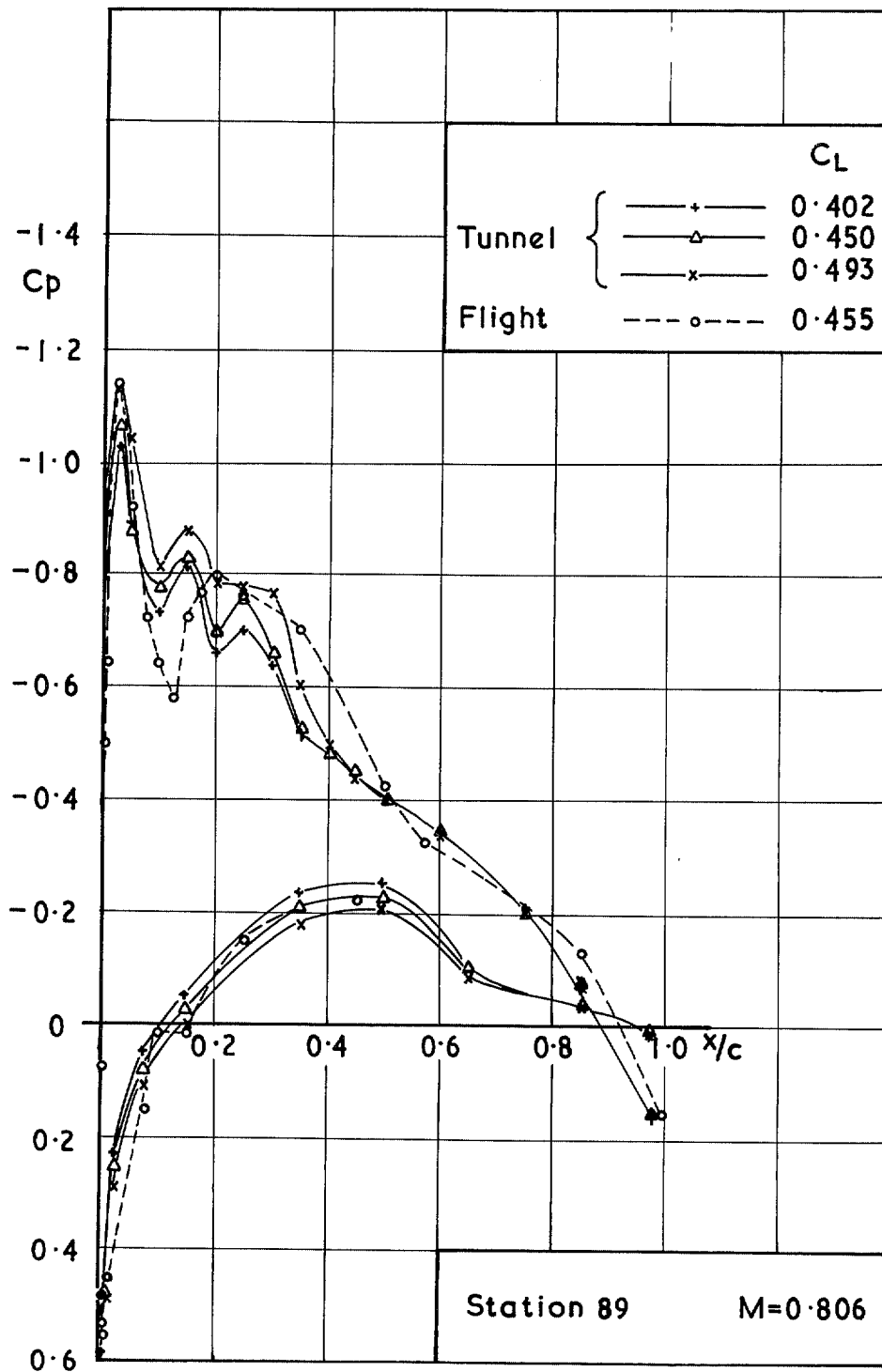


FIG. 6b.  $C_p \sim x/c$  for Station 89.  $M = 0.806$ .

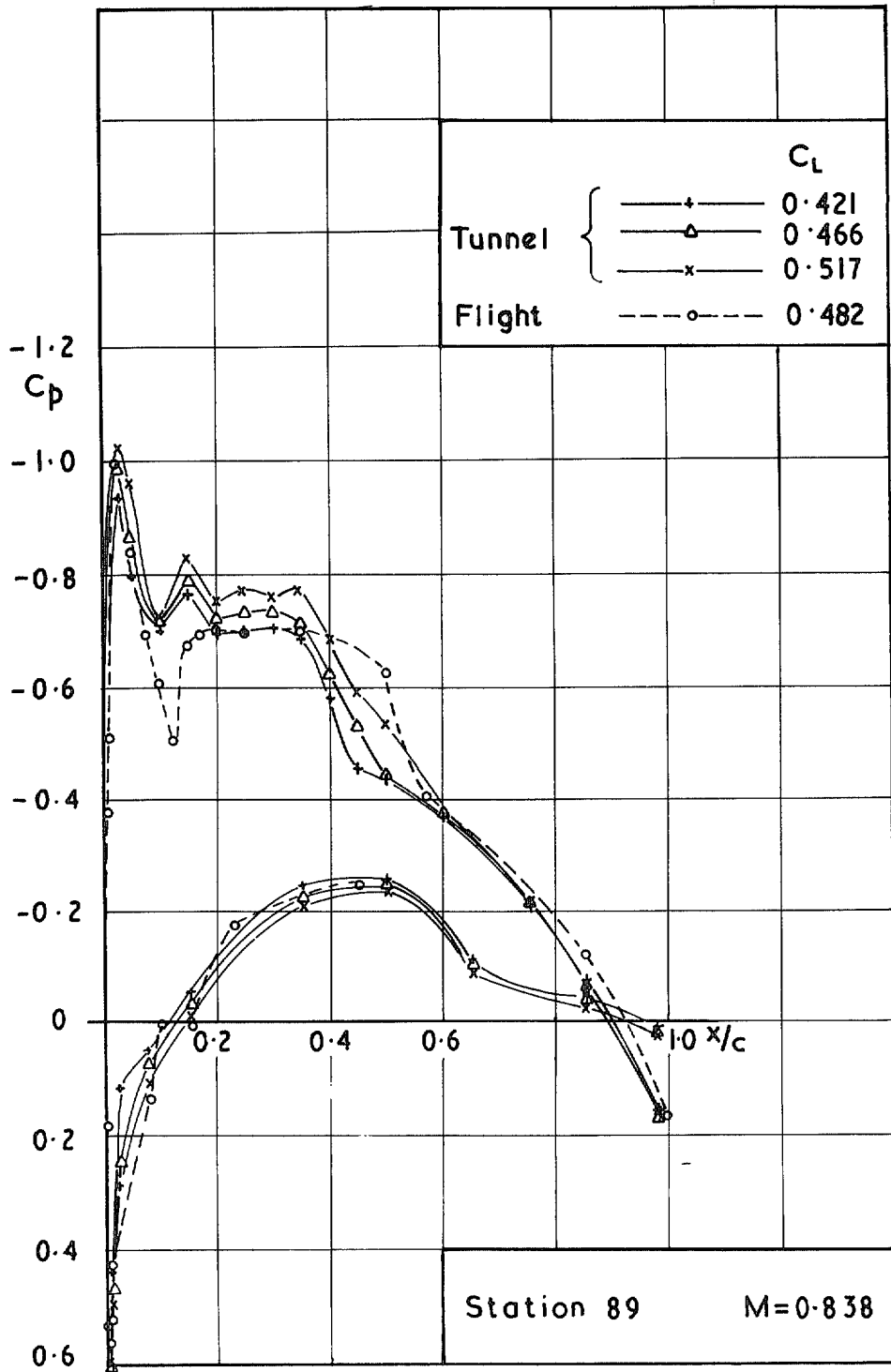


FIG. 6c.  $C_p \sim x/c$  for Station 89.  $M = 0.838$ .

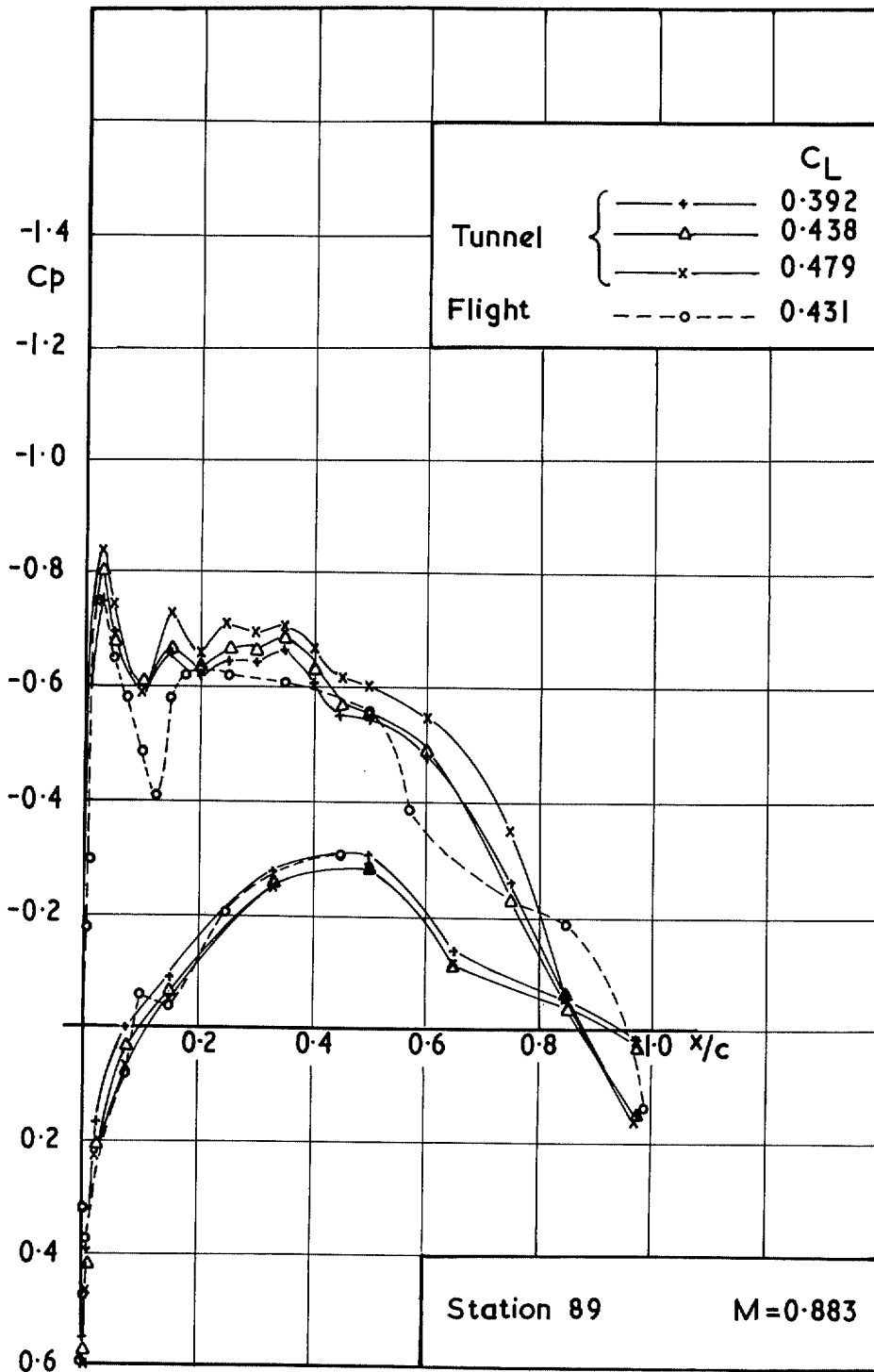


FIG. 6d.  $C_p \sim x/c$  for Station 89.  $M = 0.883$ .

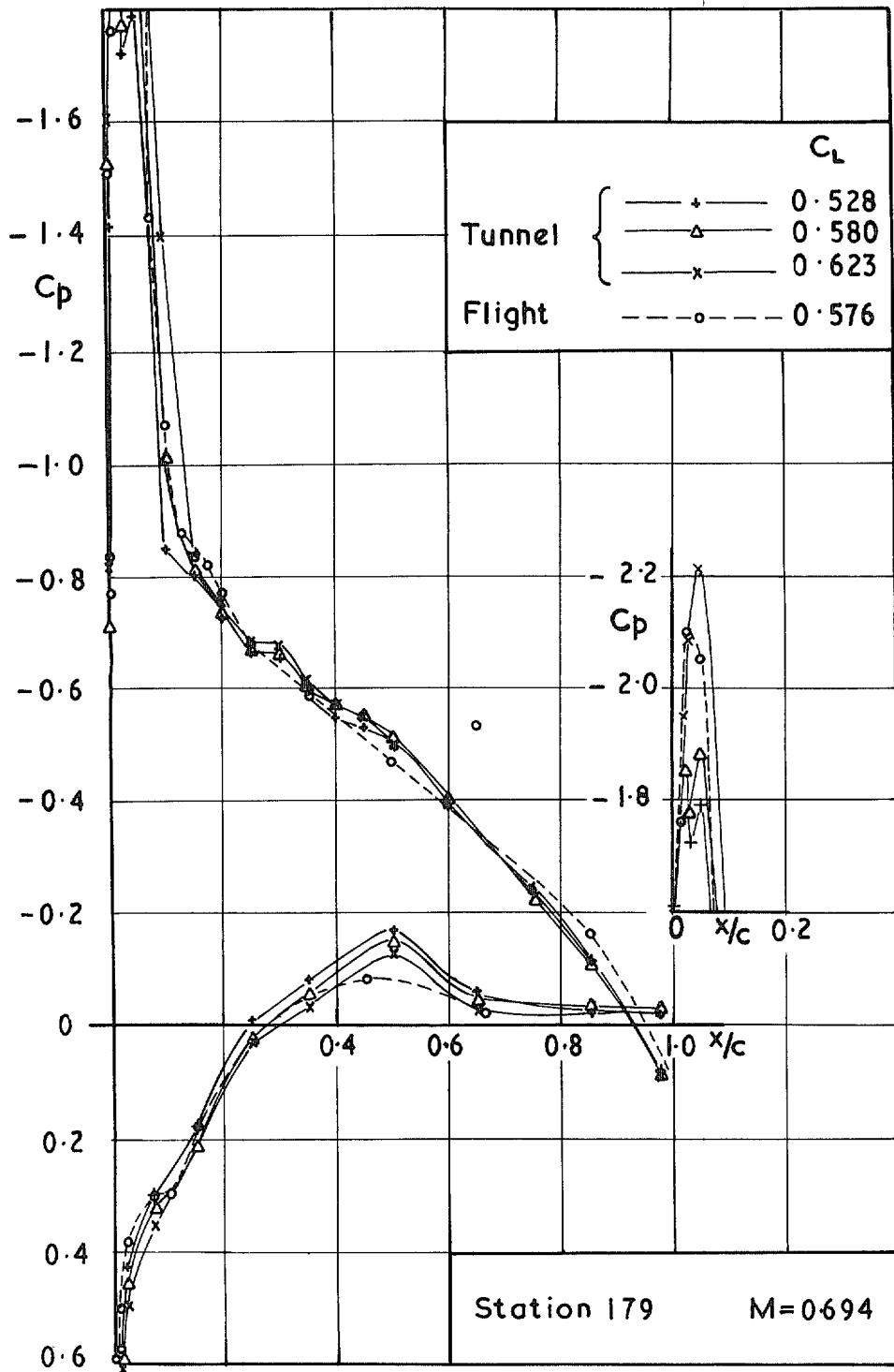


FIG. 7a.  $C_p \sim x/c$  for Station 179.  $M = 0.694$ .

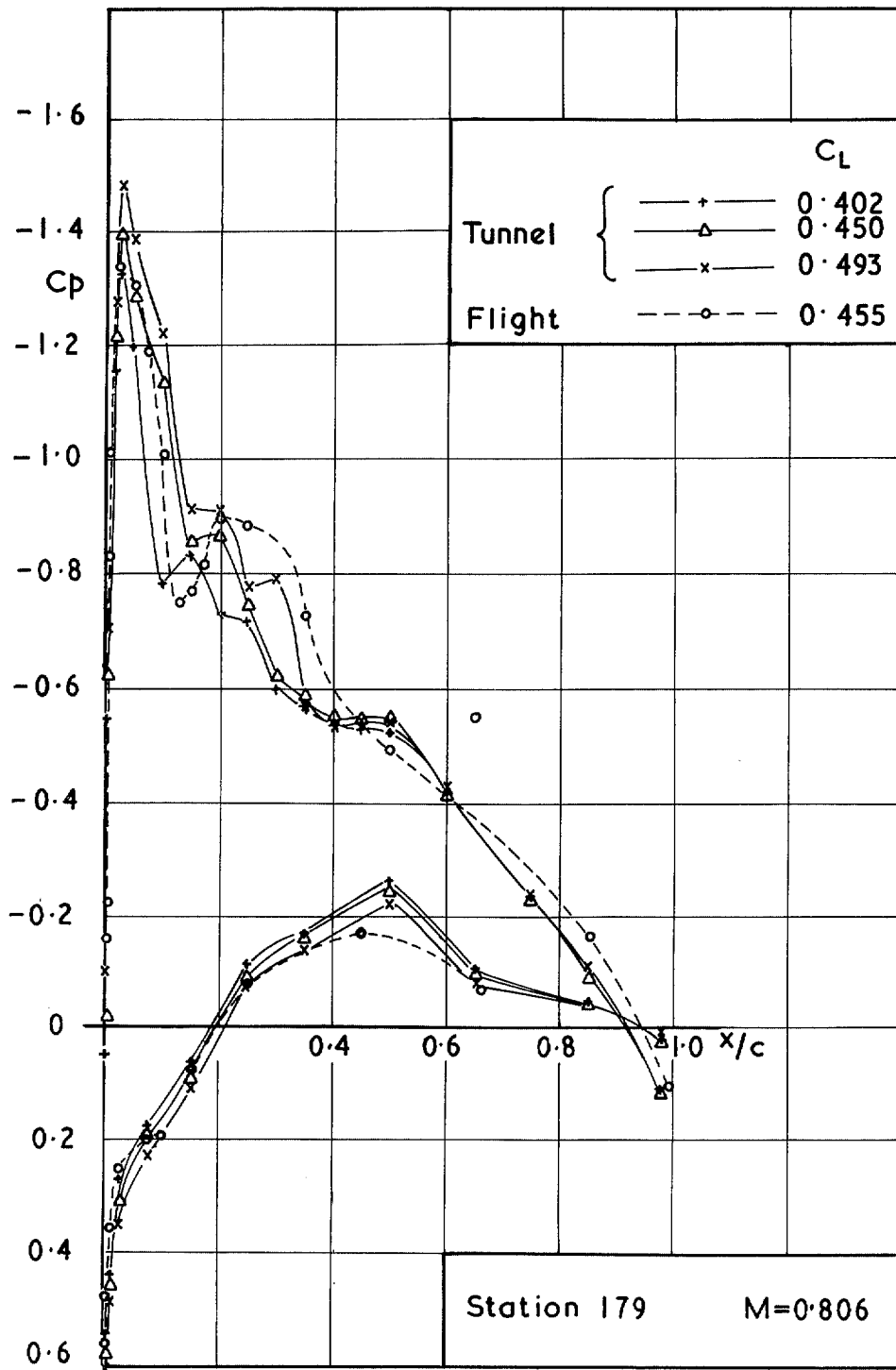


FIG. 7b.  $C_p \sim x/c$  for Station 179.  $M = 0.806$ .

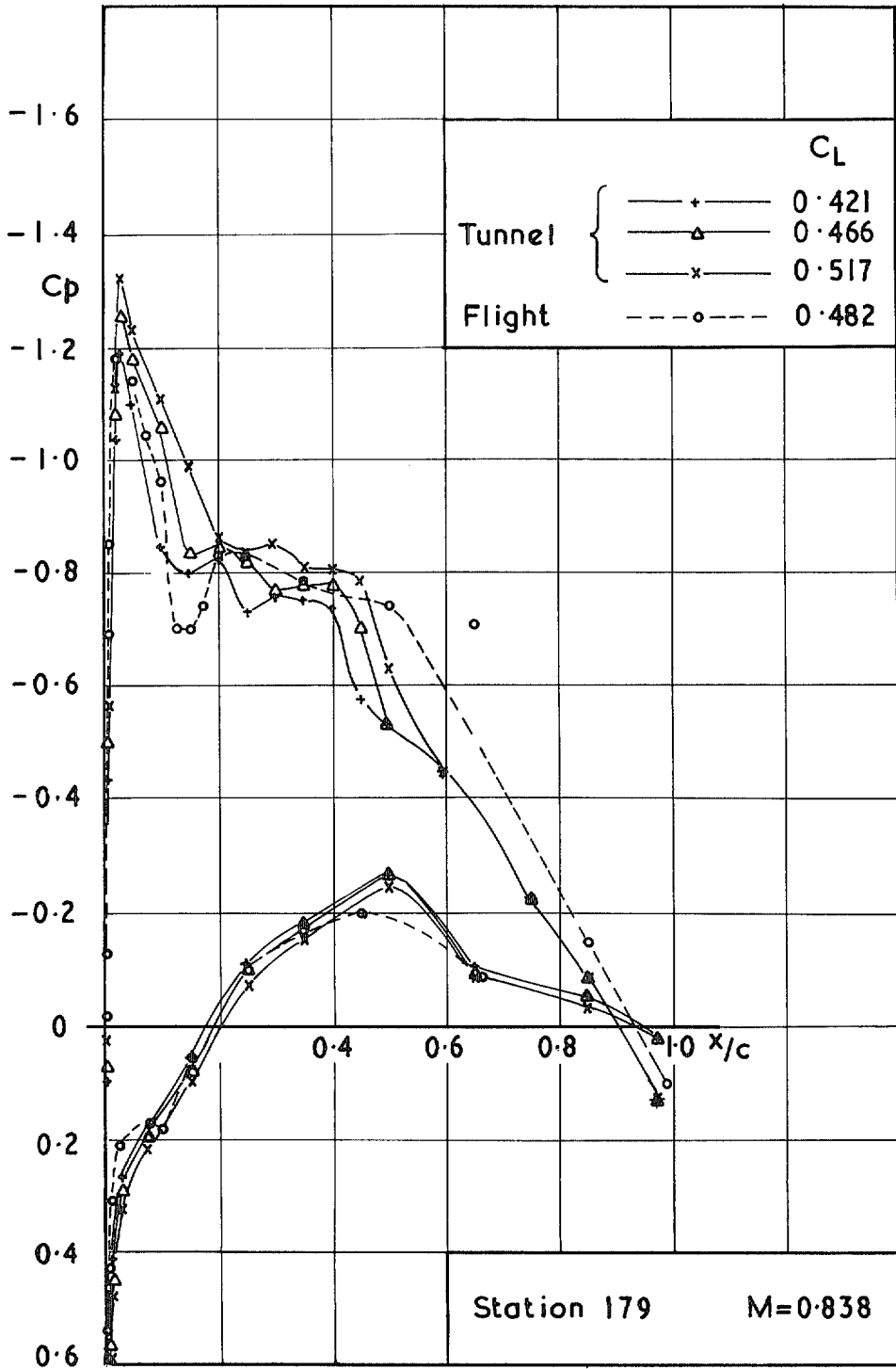


FIG. 7c.  $C_p \sim x/c$  for Station 179.  $M = 0.838$ .

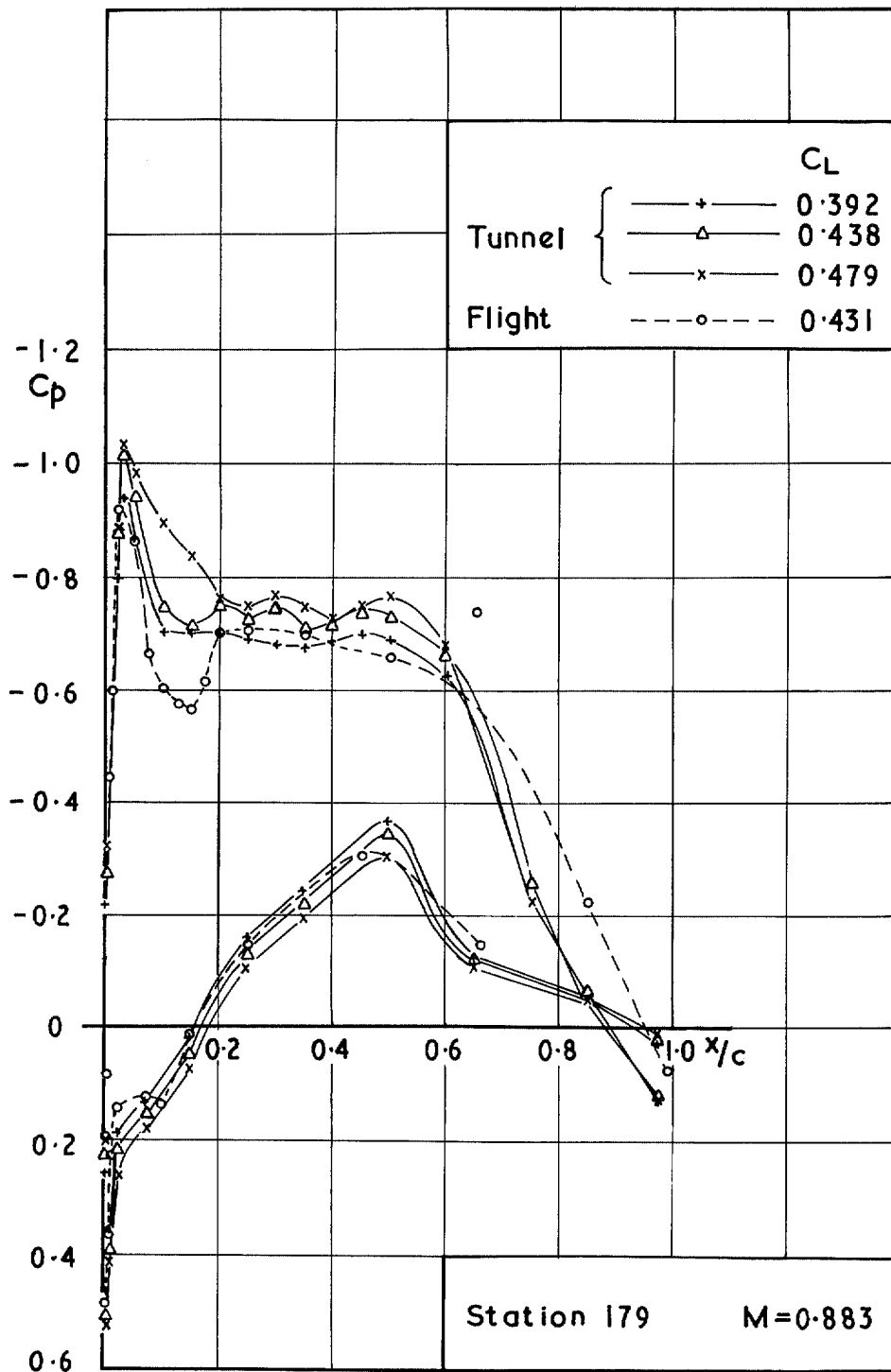


FIG. 7d.  $C_p \sim x/c$  for Station 179.  $M = 0.883$ .

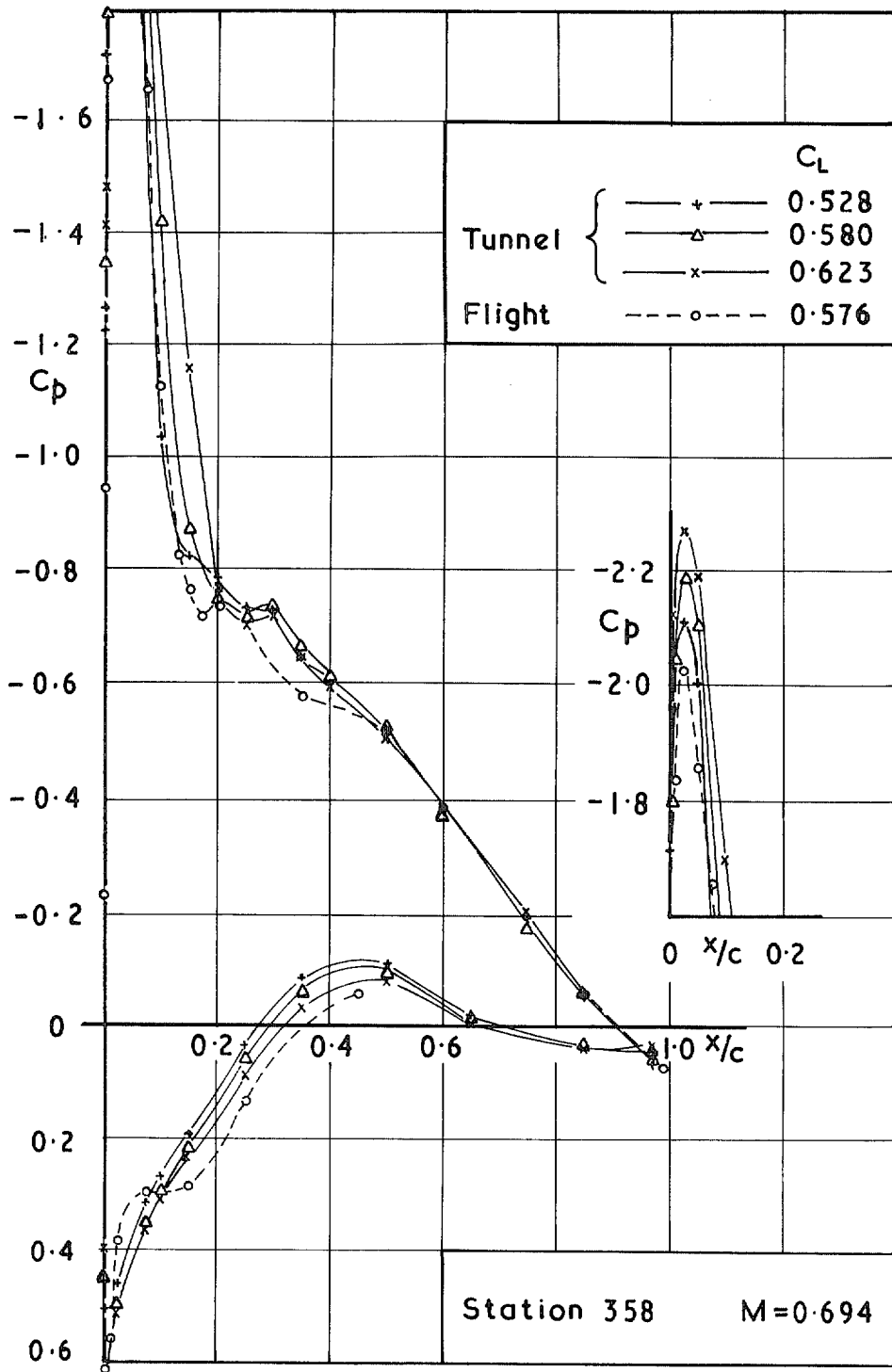


FIG. 8a.  $C_p \sim x/c$  for Station 358.  $M = 0.694$ .

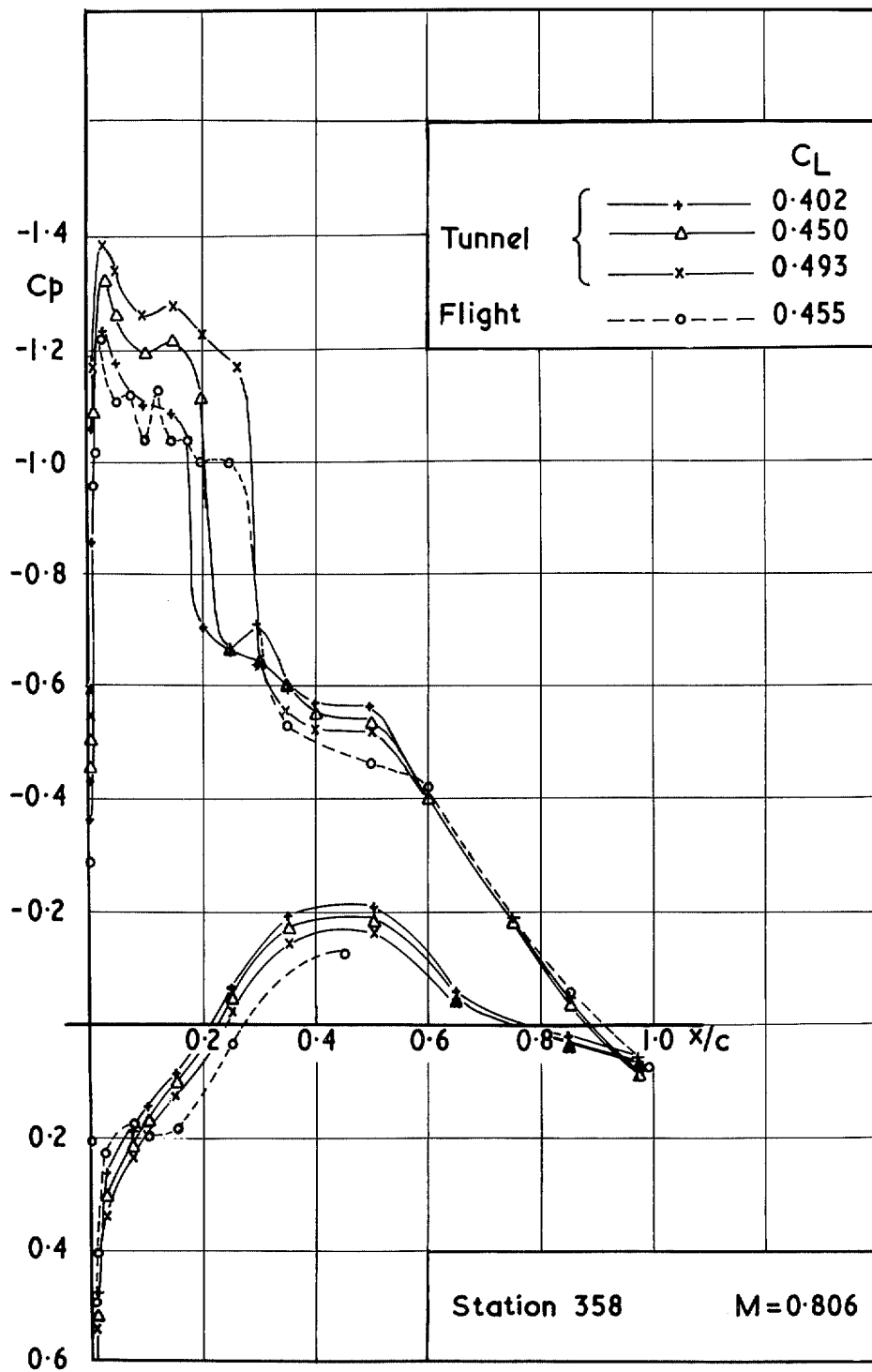


FIG. 8b.  $C_p \sim x/c$  for Station 358.  $M = 0.806$ .

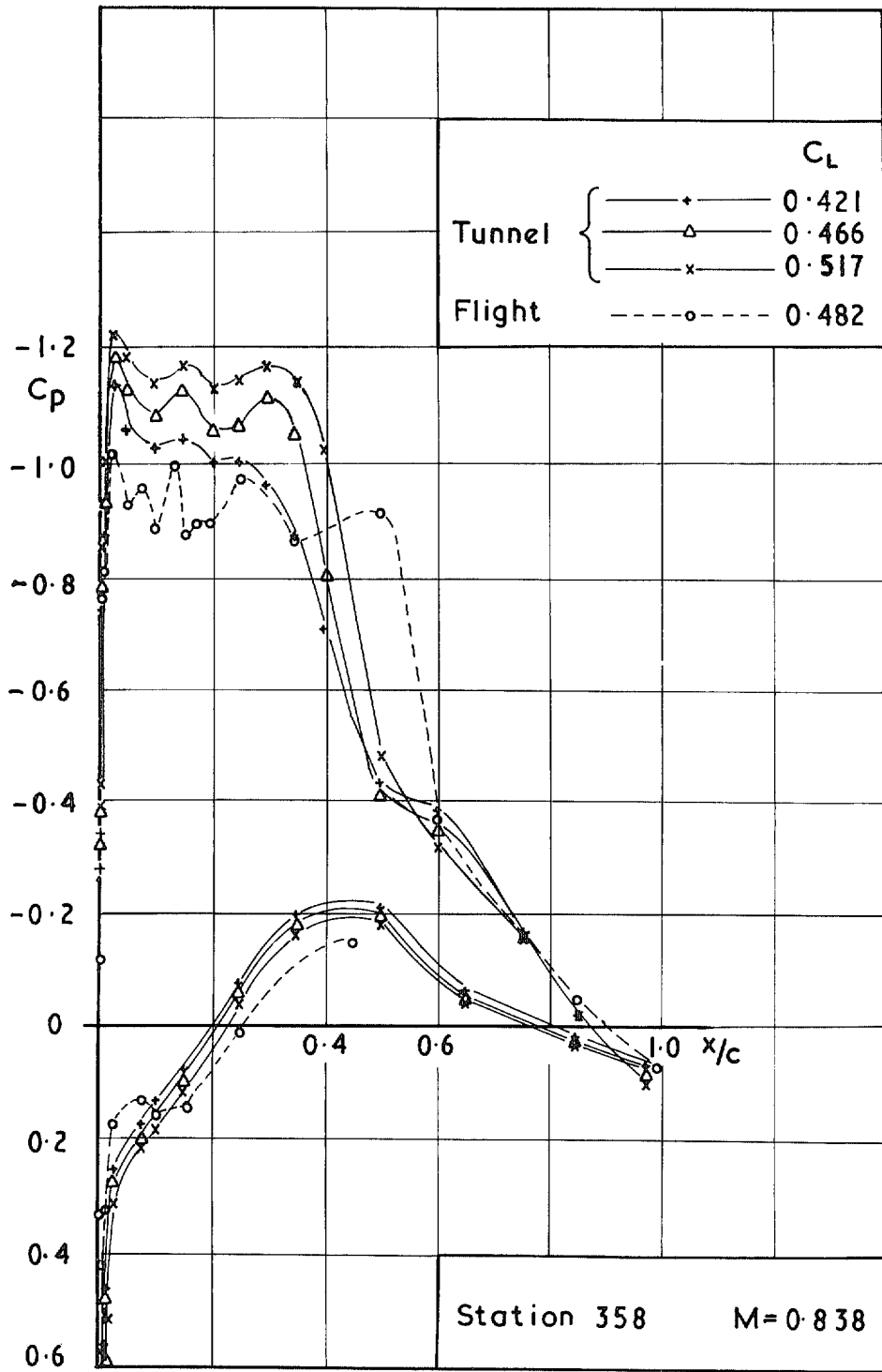


FIG. 8c.  $C_p \sim x/c$  for Station 358.  $M = 0.838$ .

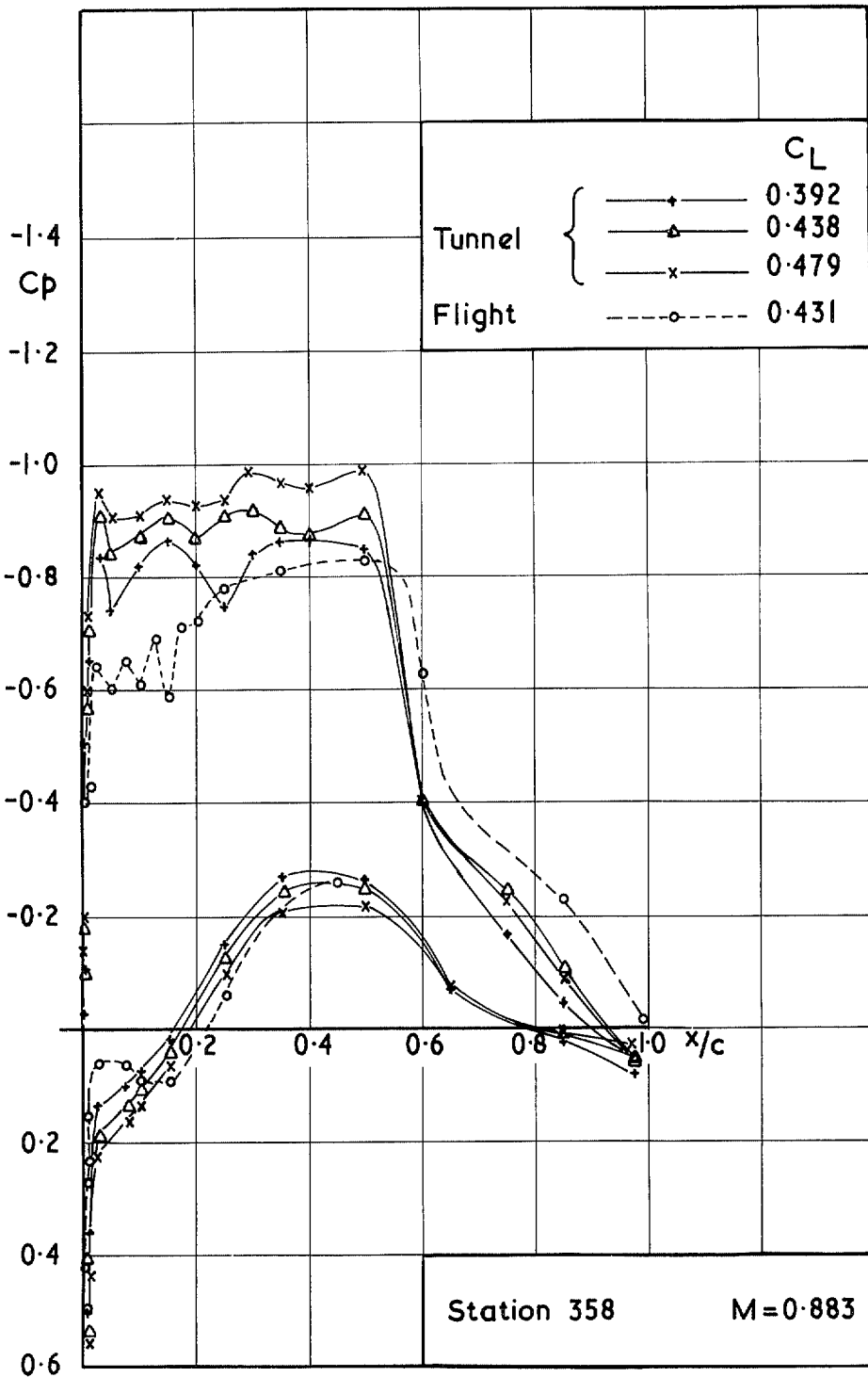


FIG. 8d.  $C_p \sim x/c$  for Station 358.  $M = 0.883$ .

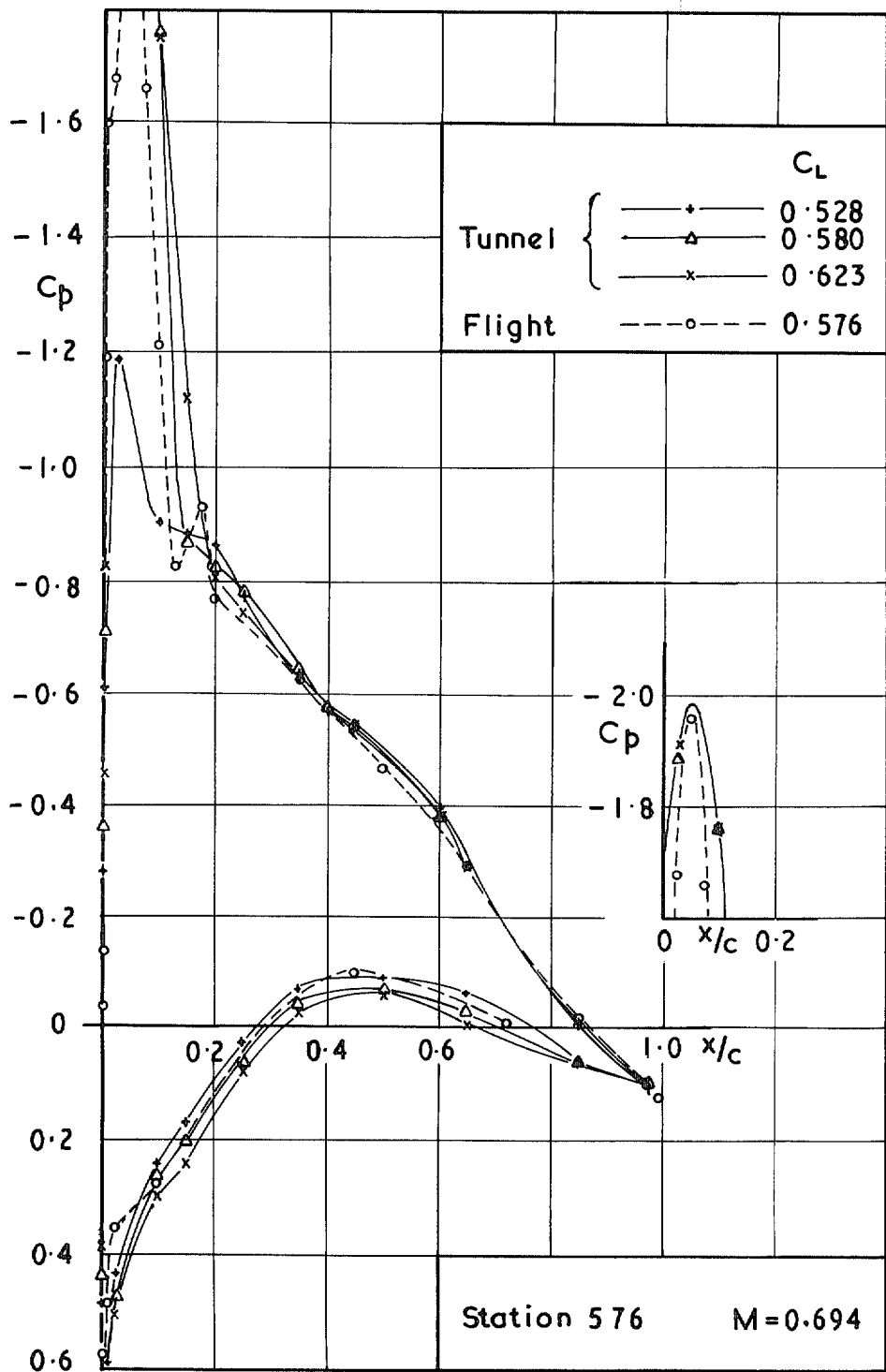


FIG. 9a.  $C_p \sim x/c$  for Station 576.  $M = 0.694$ .

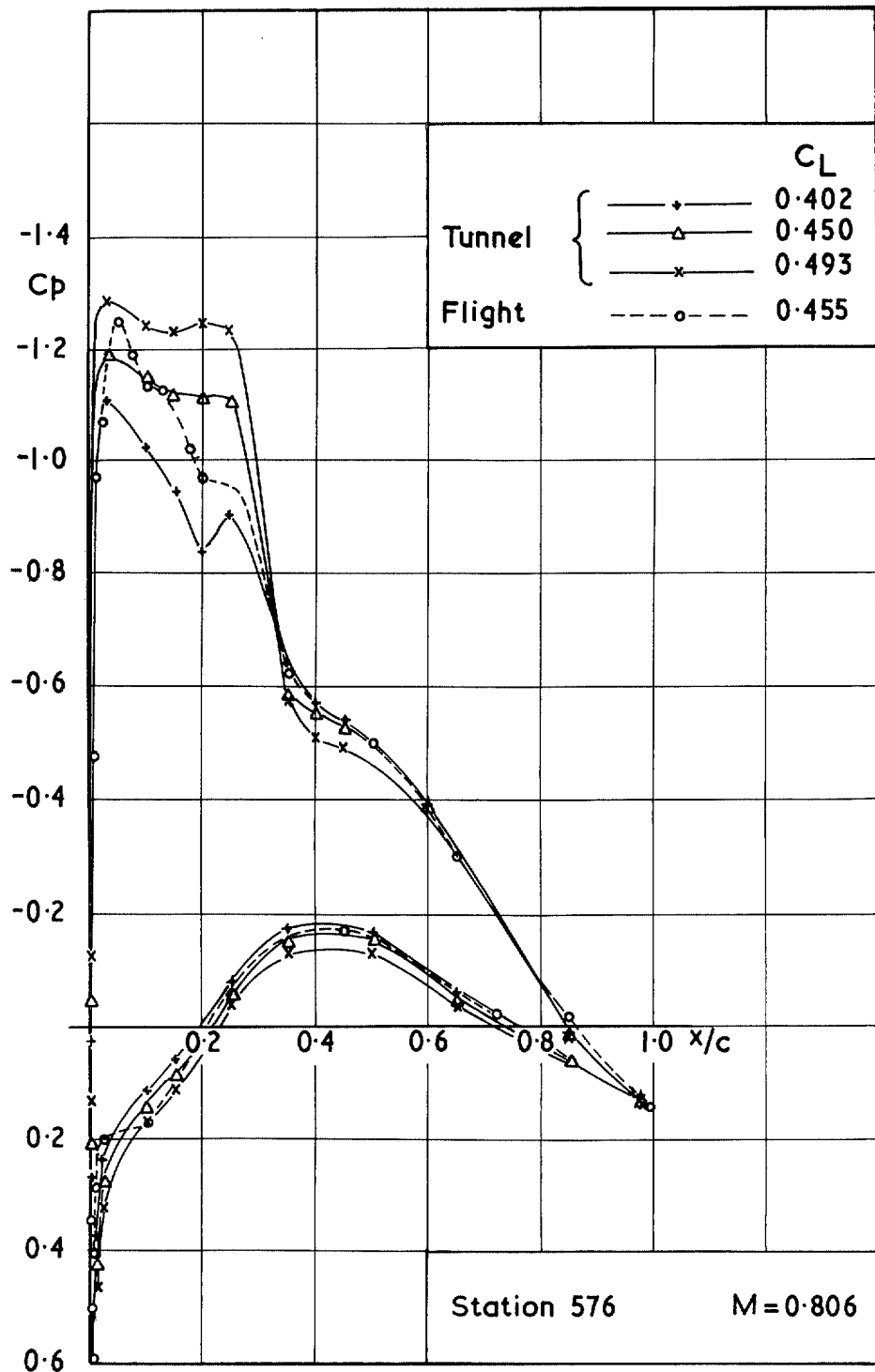


FIG. 9b.  $C_p \sim x/c$  for Station 576.  $M = 0.806$ .

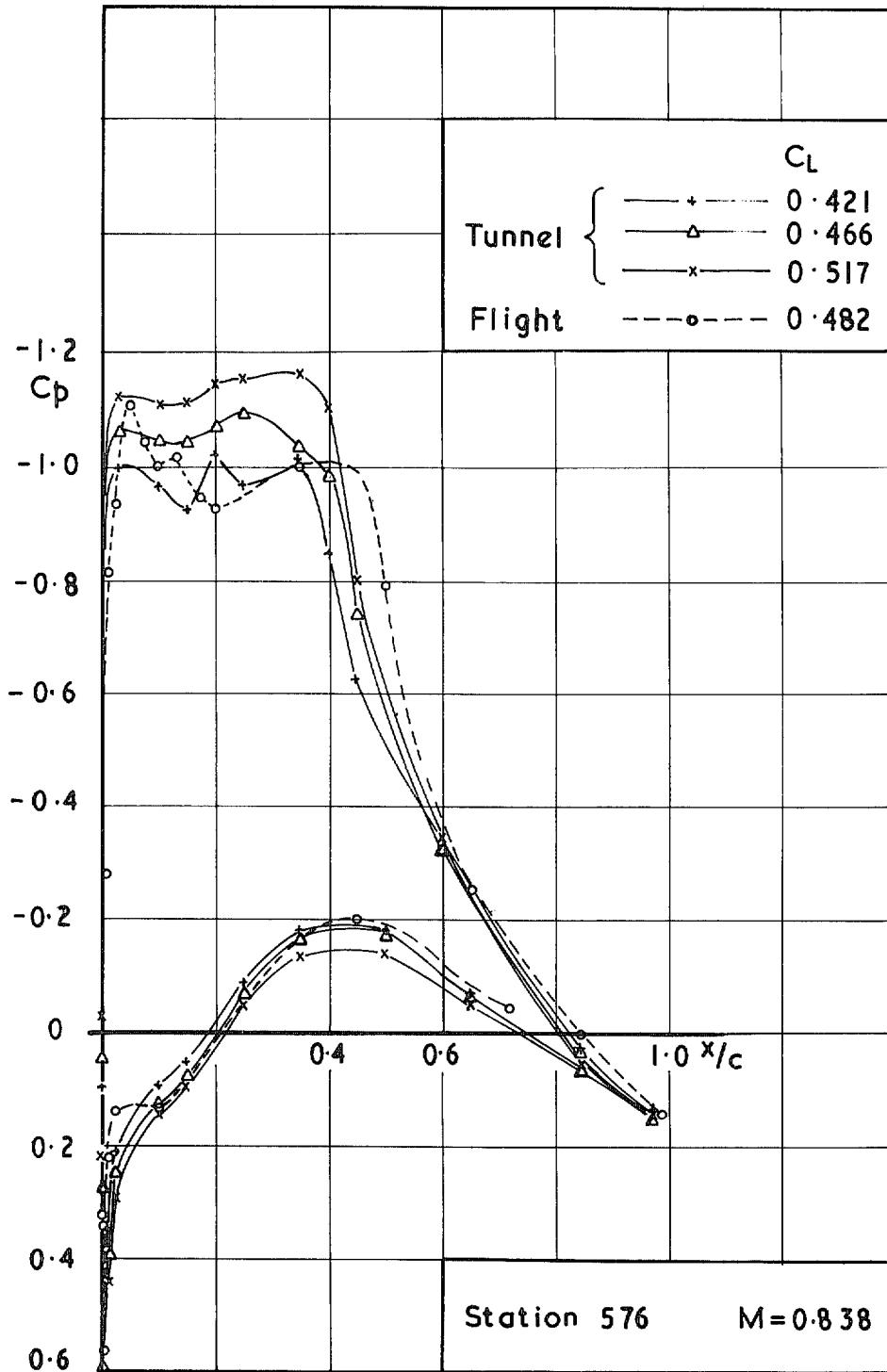


FIG. 9c.  $C_p \sim x/c$  for Station 576.  $M = 0.838$ .

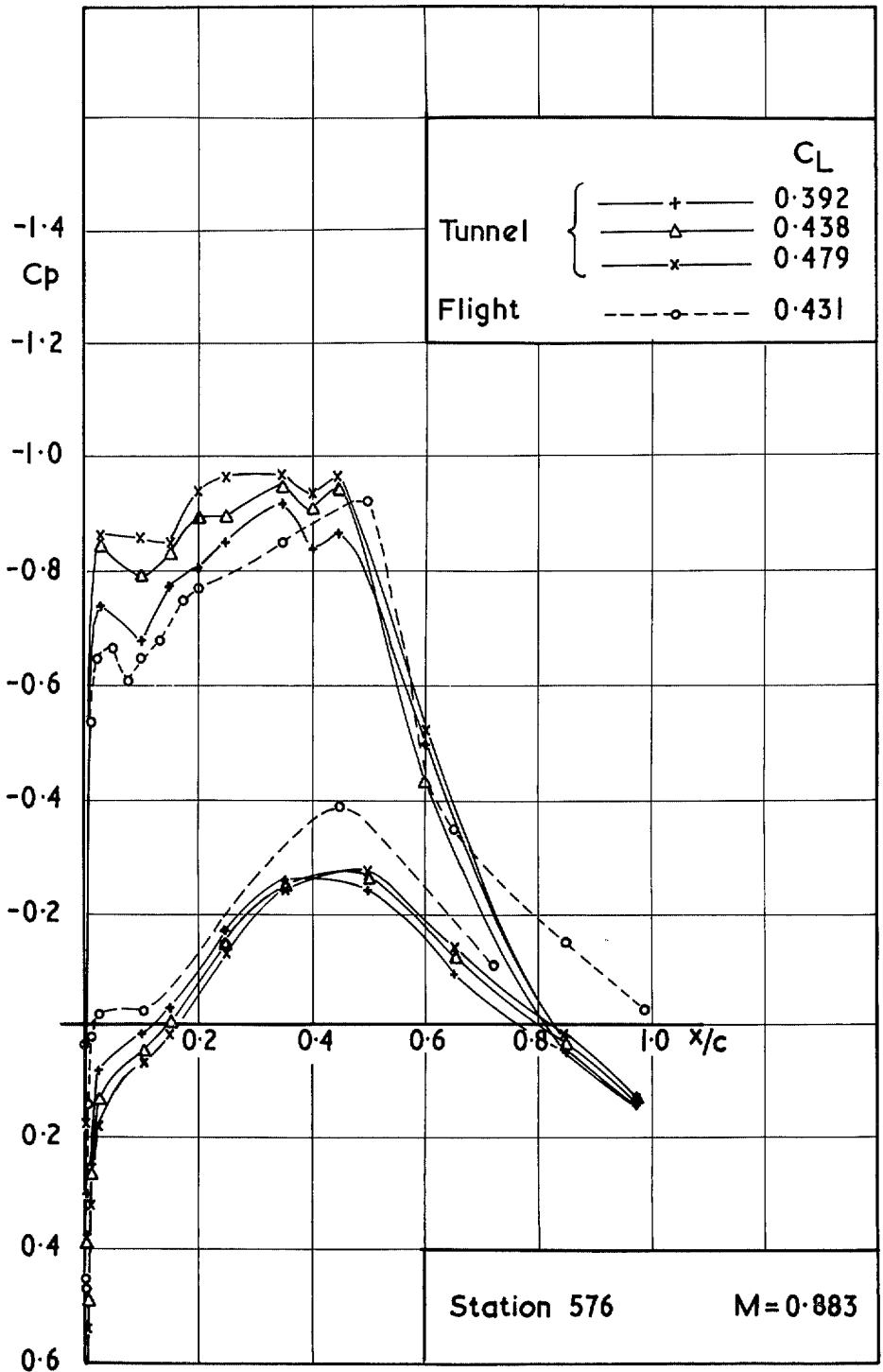


FIG. 9d.  $C_p \sim x/c$  for Station 576.  $M = 0.883$ .

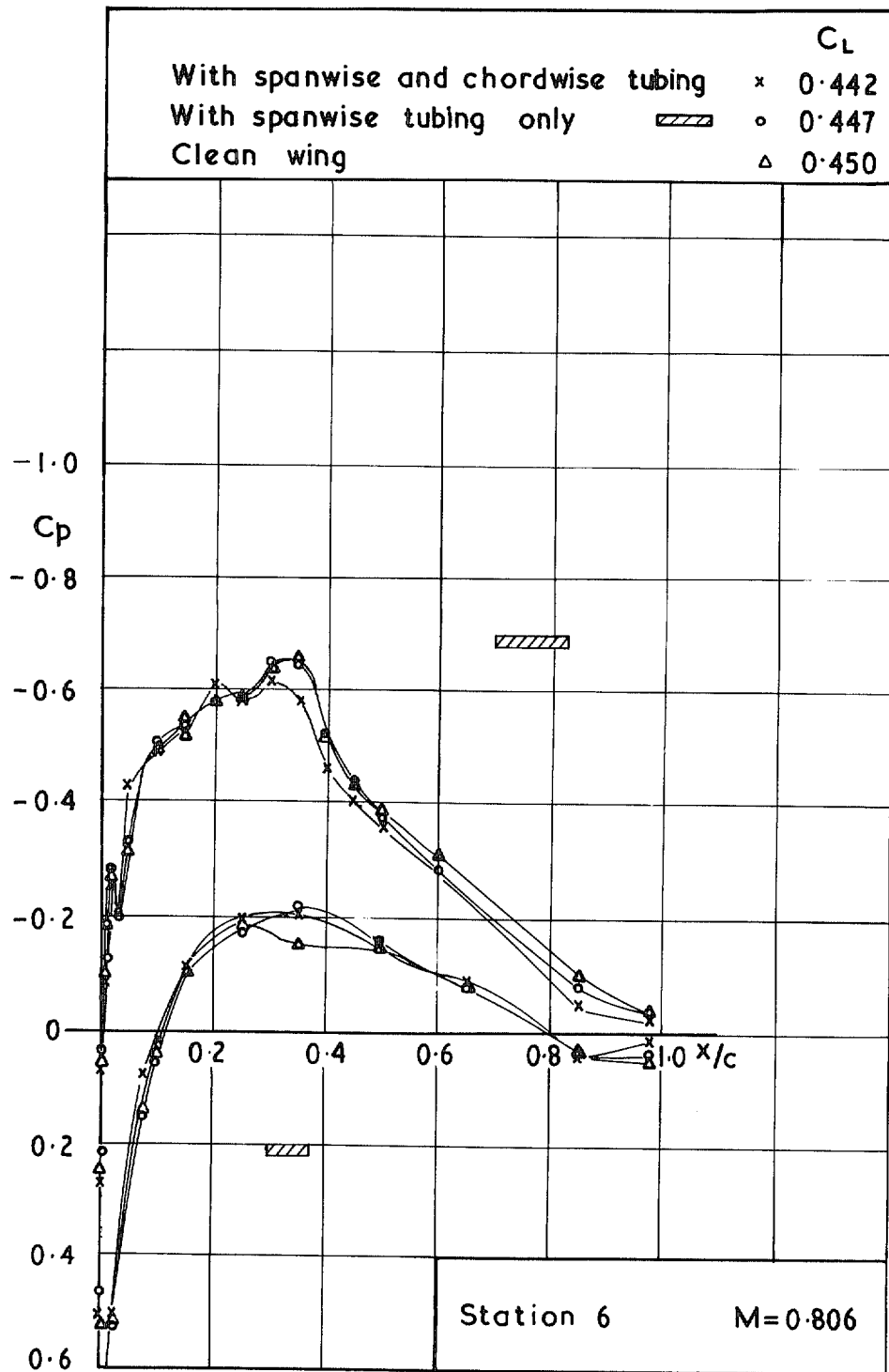


FIG. 10a.  $C_p \sim x/c$  for Station 6.  $M = 0.806$ .  
Effects of simulated pressure tubing.

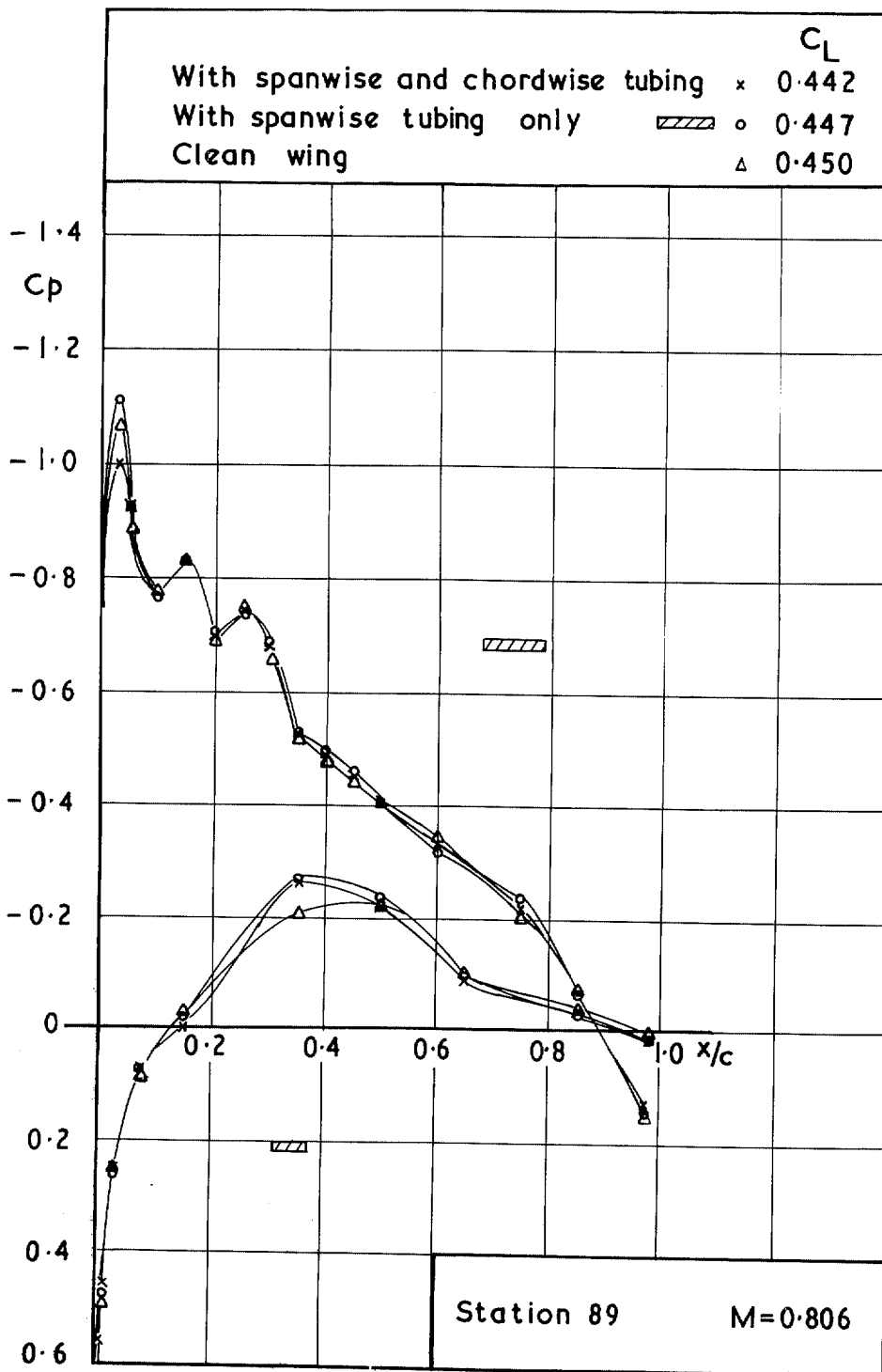


FIG. 10b.  $C_p \sim x/c$  for Station 89.  $M = 0.806$ .  
Effects of simulated pressure tubing.

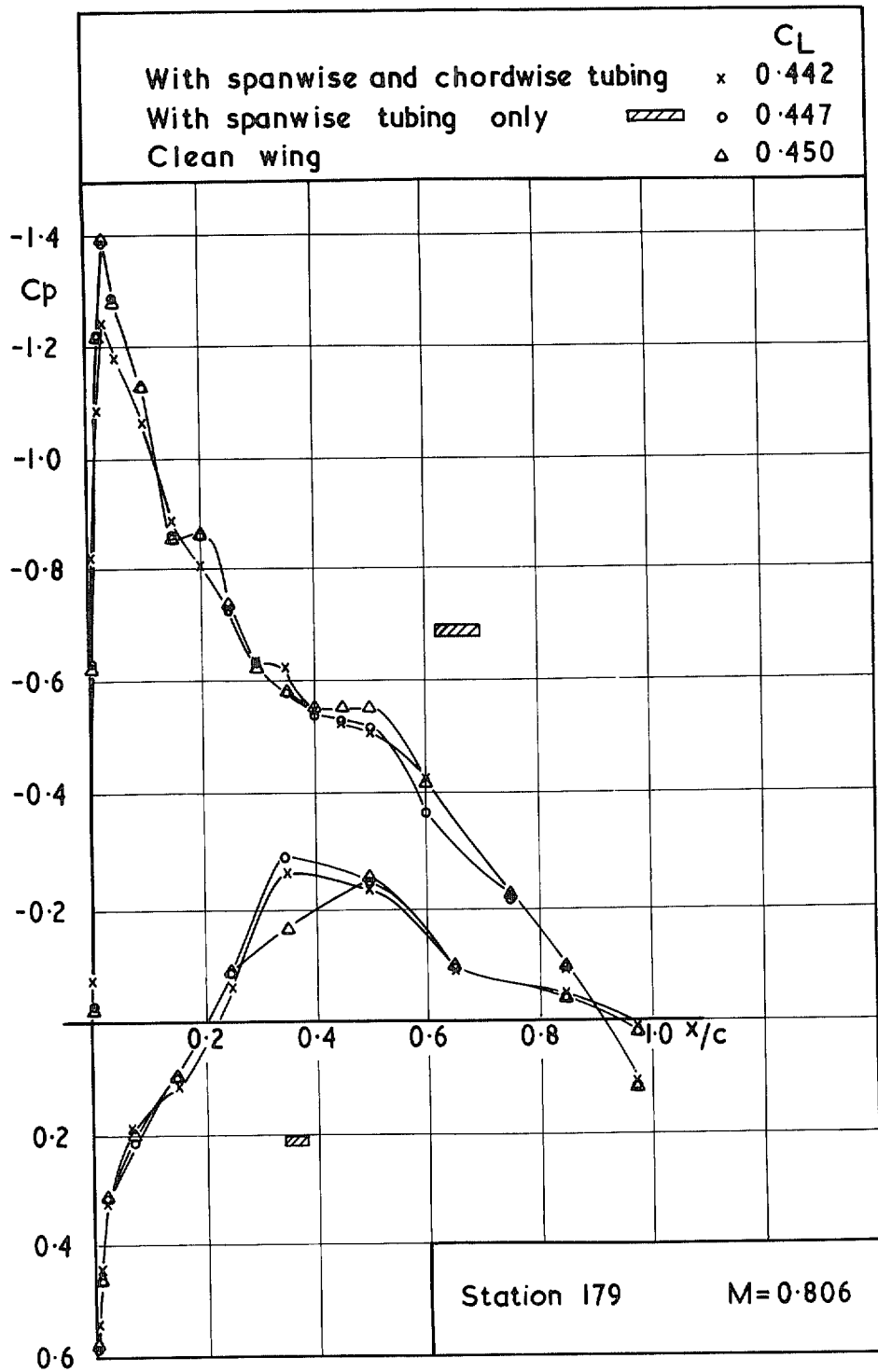


FIG. 10c.  $C_p \sim x/c$  for Station 179.  $M = 0.806$ .  
Effects of simulated pressure tubing.

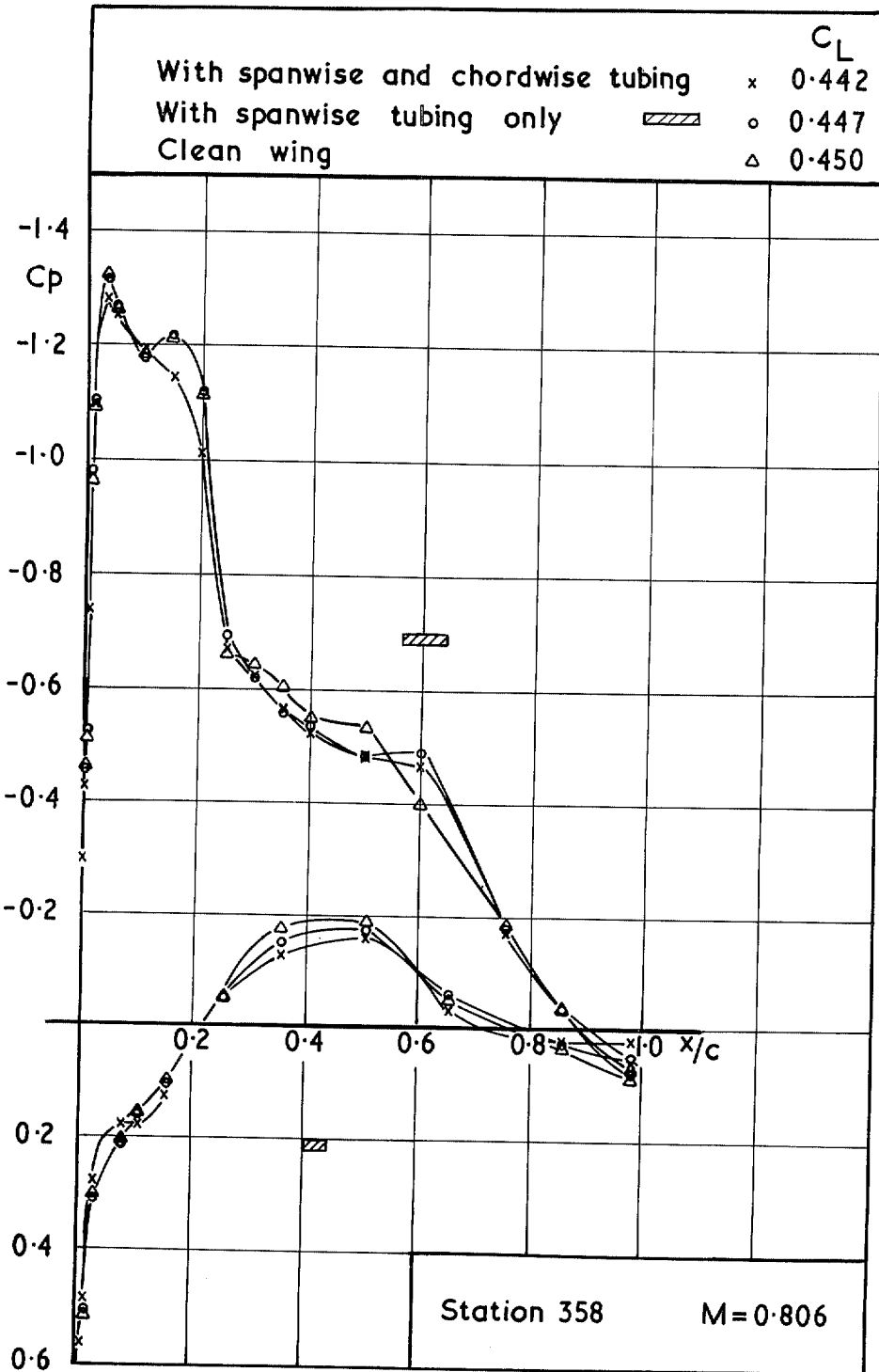


FIG. 10d.  $C_p \sim x/c$  for Station 358.  $M = 0.806$ .  
Effects of simulated pressure tubing.

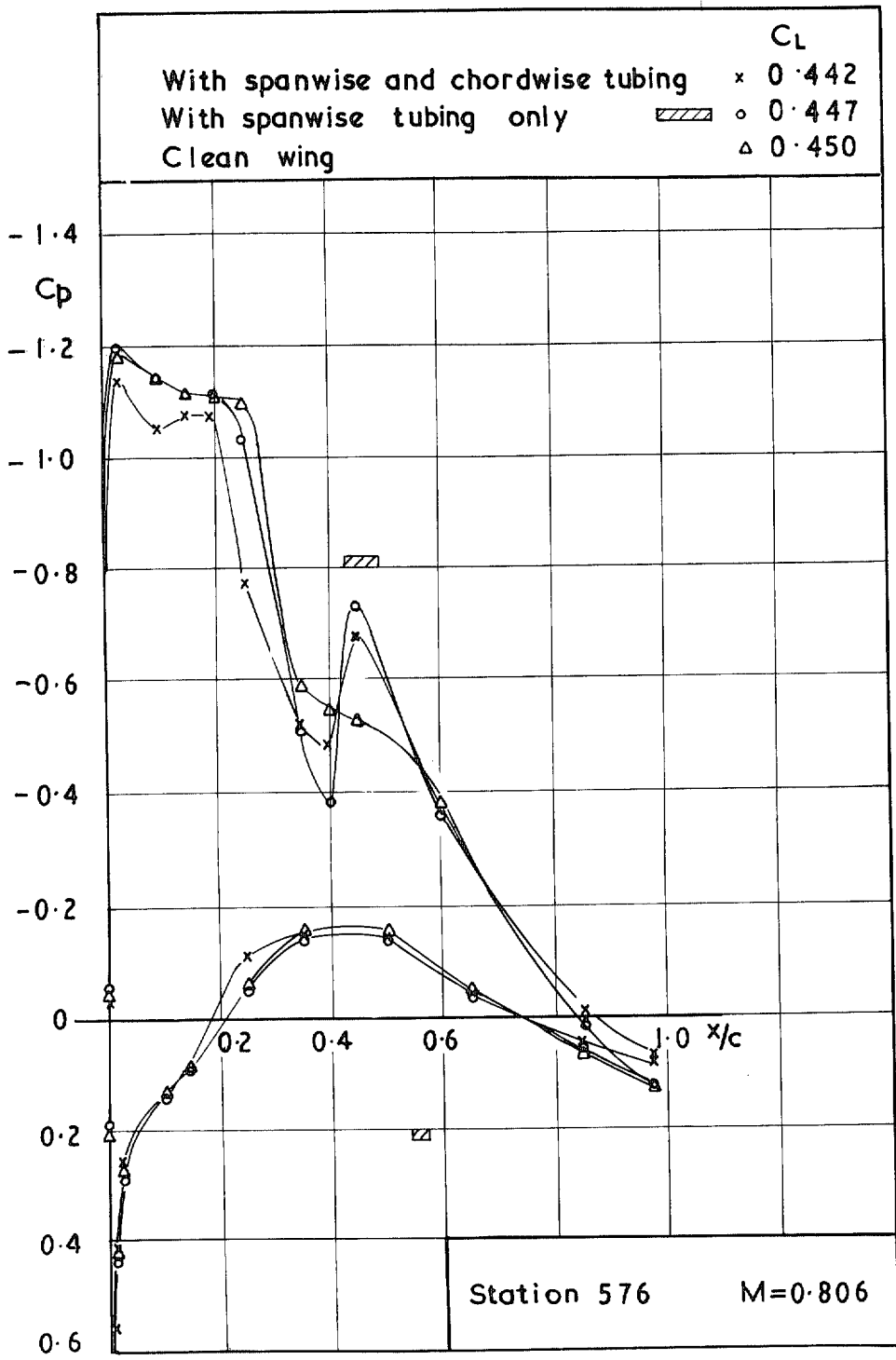


FIG. 10e.  $C_p \sim x/c$  for Station 576.  $M = 0.806$ .  
Effects of simulated pressure tubing.

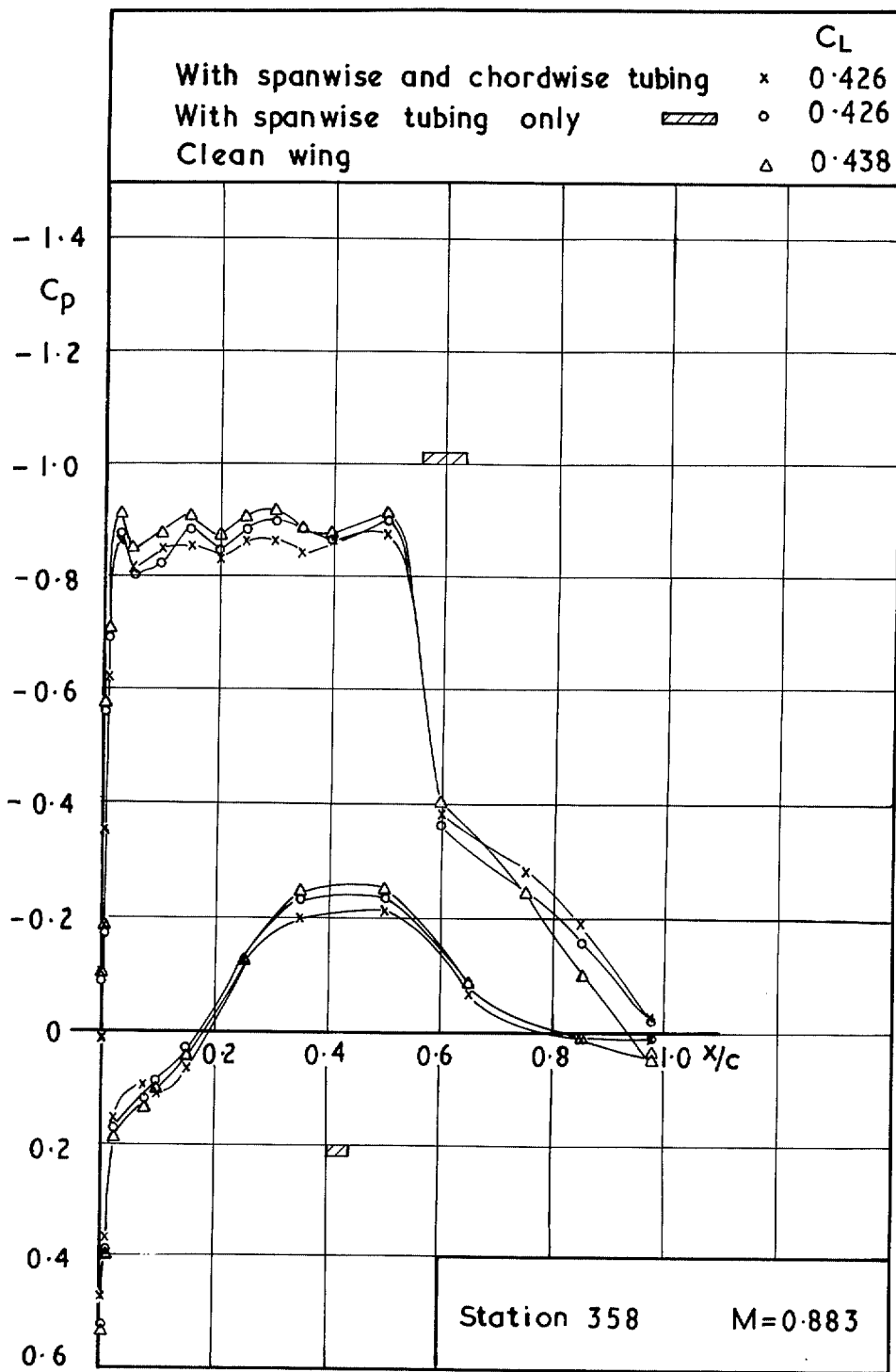


FIG. 10f.  $C_p \sim x/c$  for Station 358.  $M = 0.883$ .  
Effects of simulated pressure tubing.

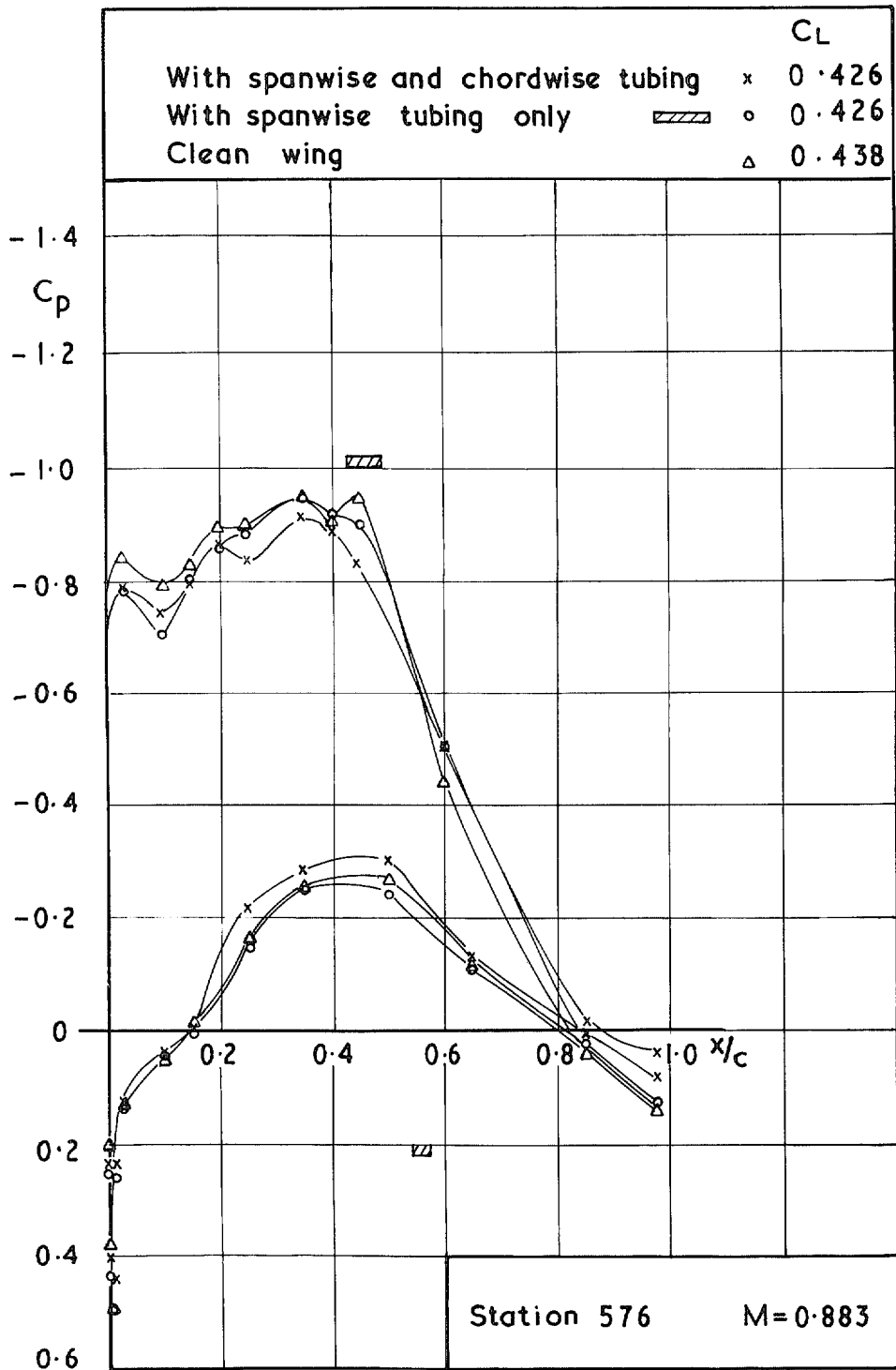


FIG. 10g.  $C_p \sim x/c$  for Station 576.  $M = 0.883$ .  
Effects of simulated pressure tubing.

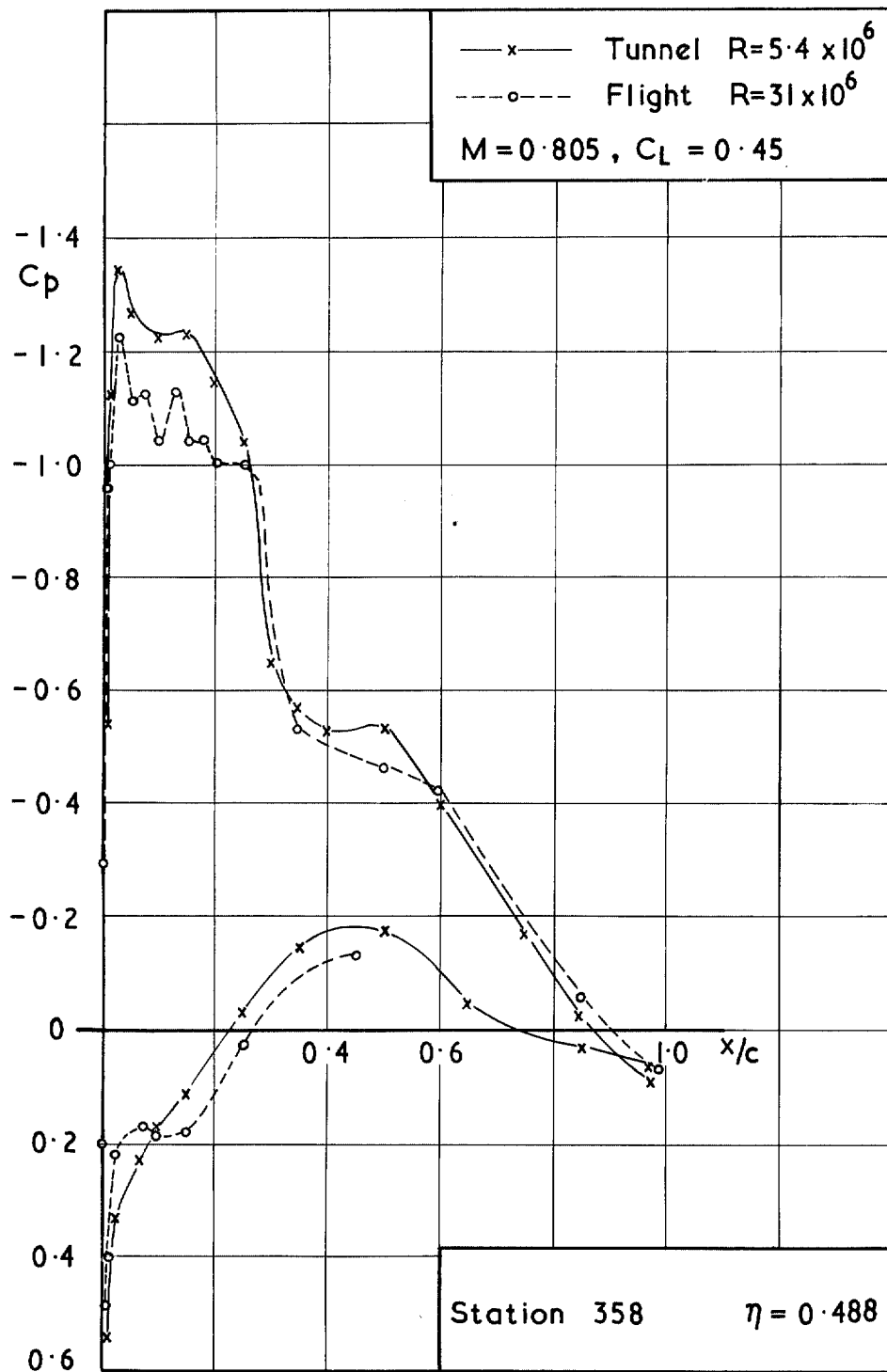


FIG. 11a. Typical flight-tunnel comparison.  $C_p \sim x/c$  for Station 358,  $\eta = 0.488$ .

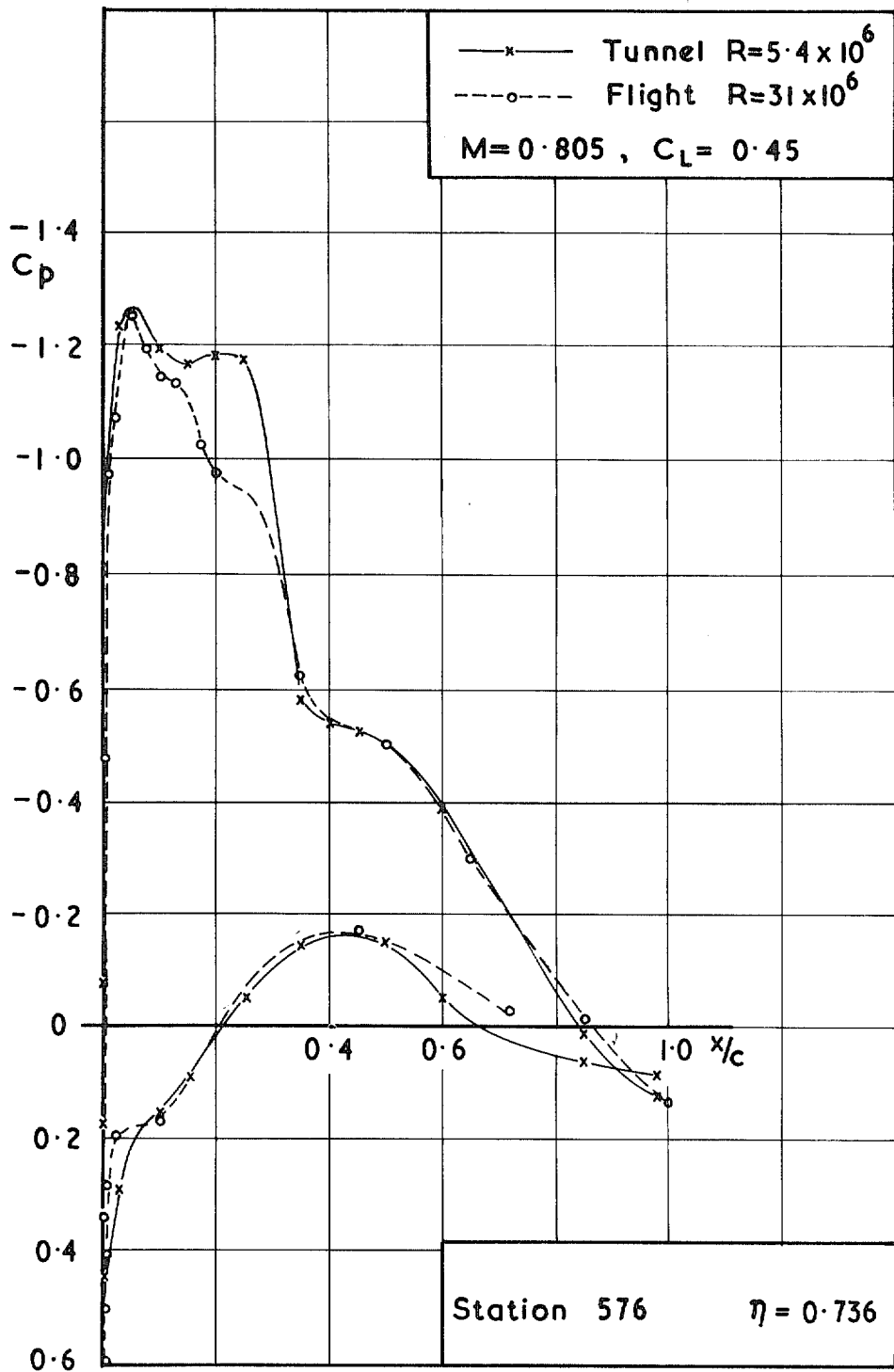


FIG. 11b. Typical flight-tunnel comparison.  $C_p \sim x/c$  for Station 576,  $\eta = 0.736$ .

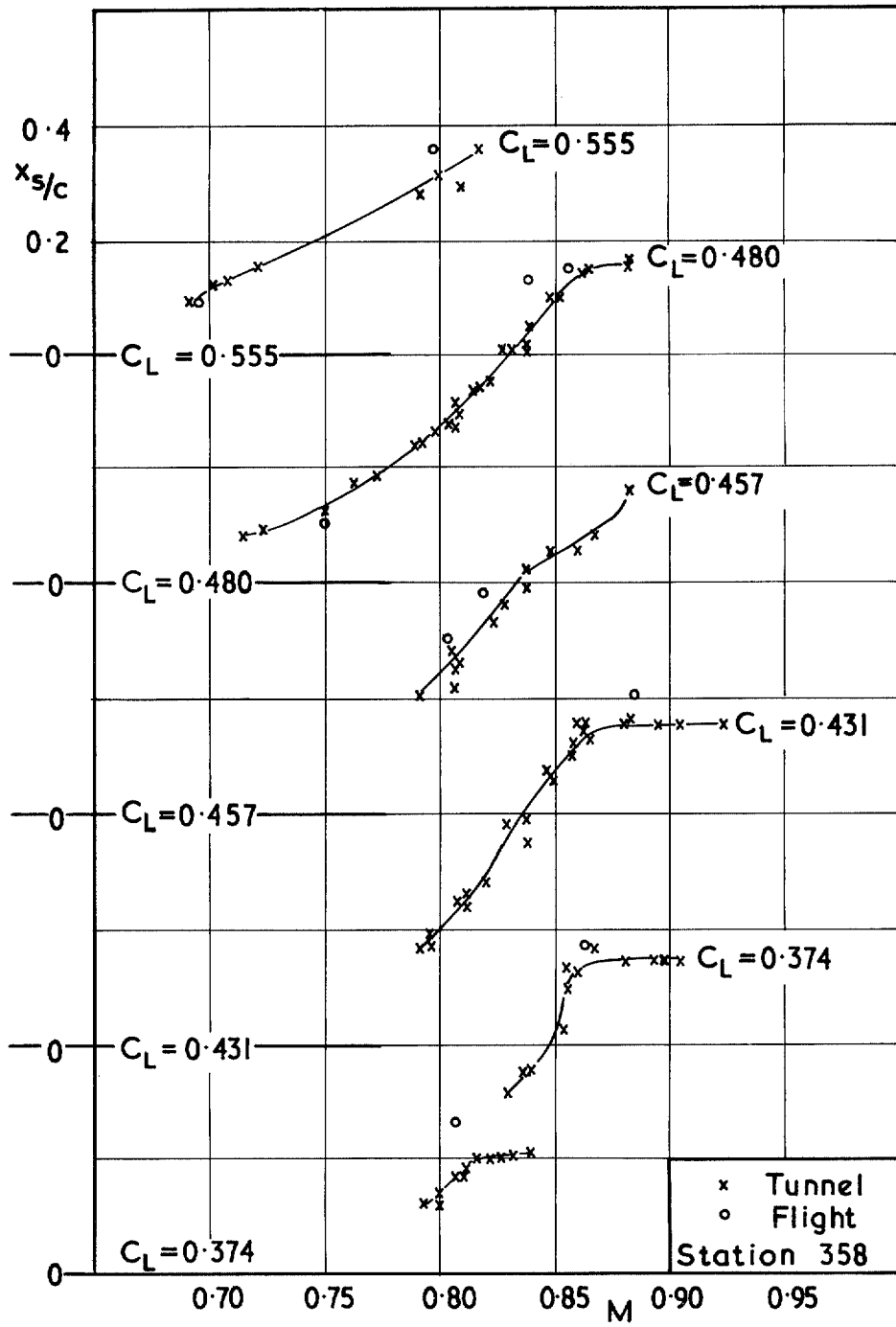


FIG. 12a. Shockwave positions. Station 358.

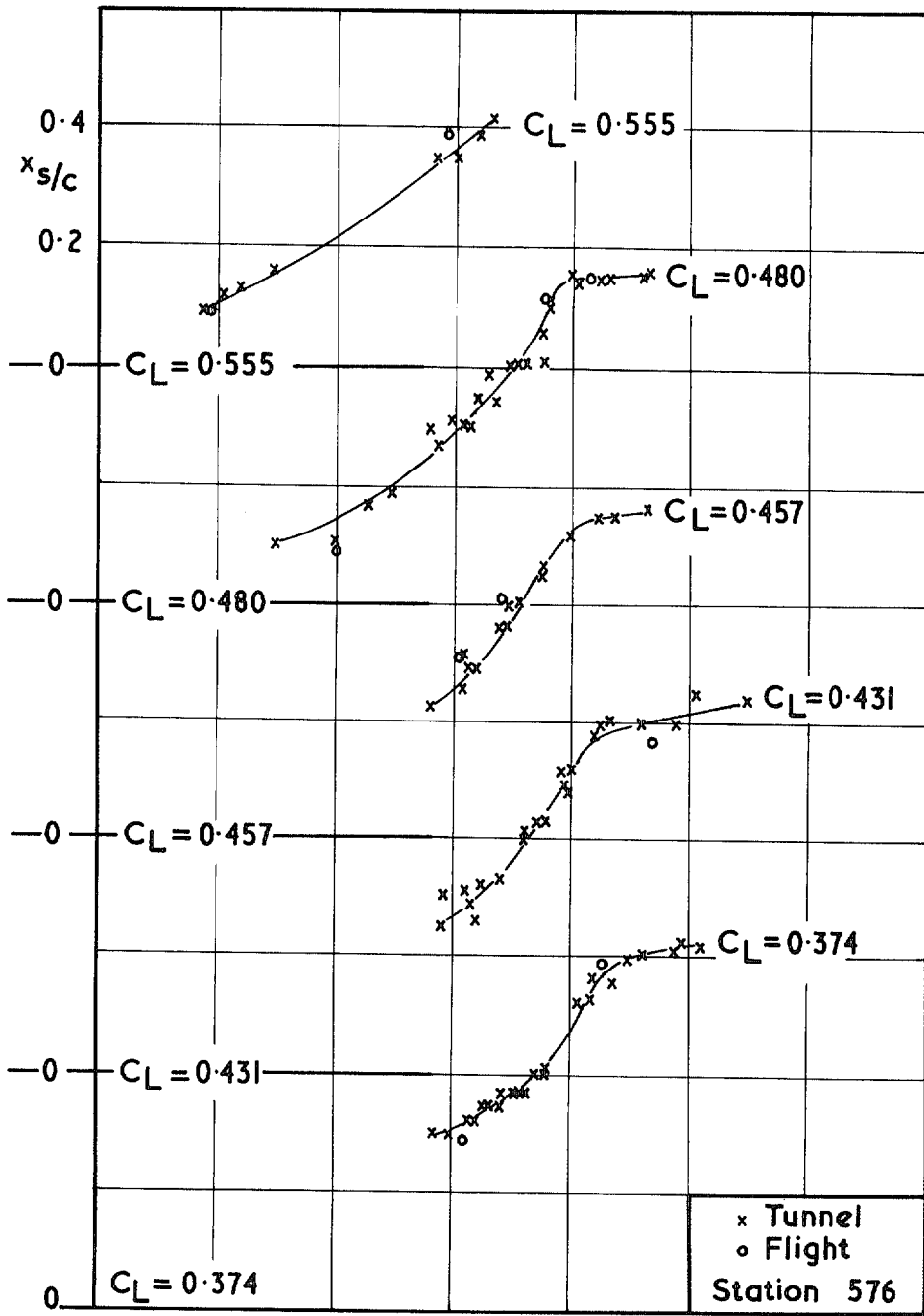


FIG. 12b. Shockwave positions. Station 576.

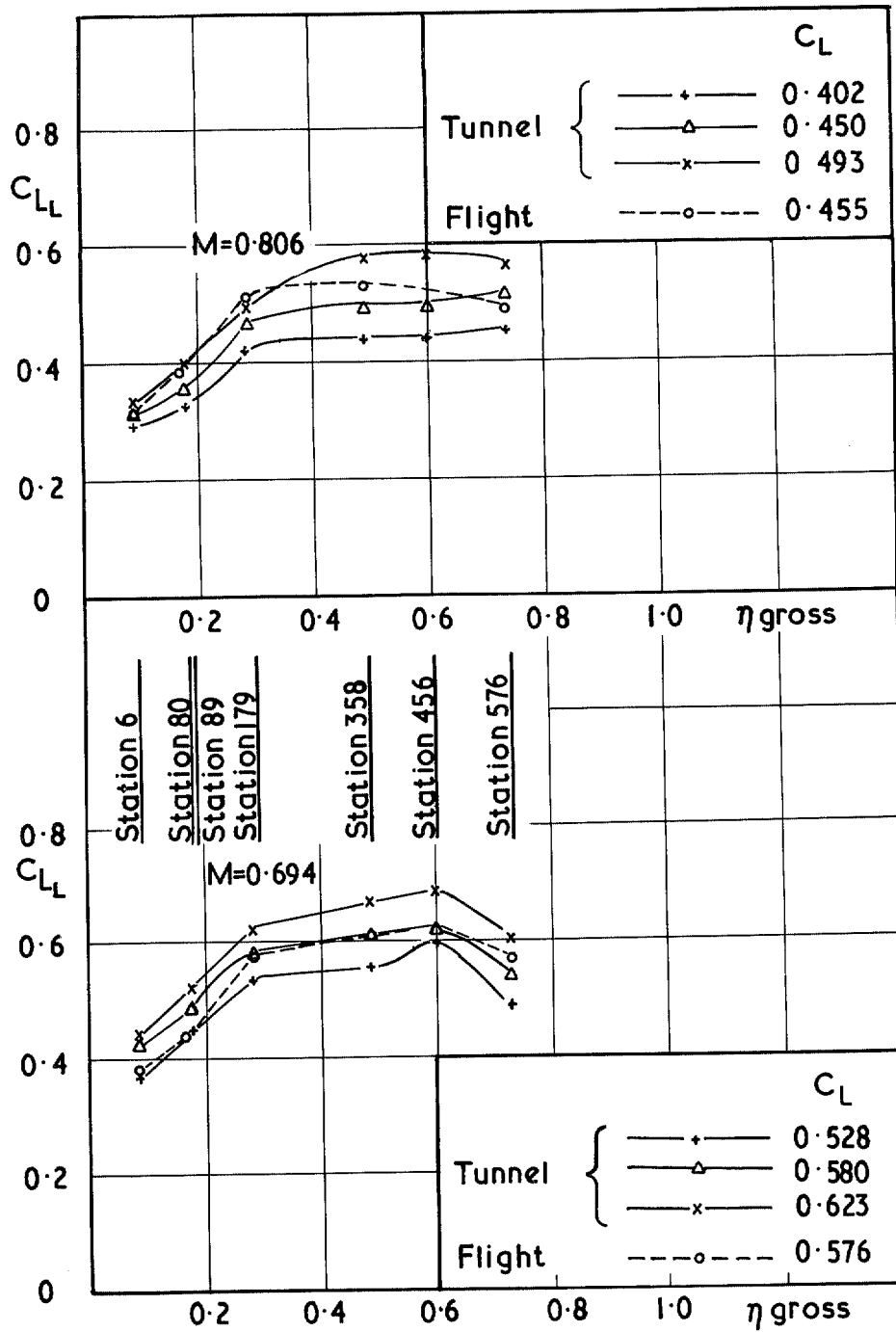


FIG. 13a. Spanwise lift distributions.

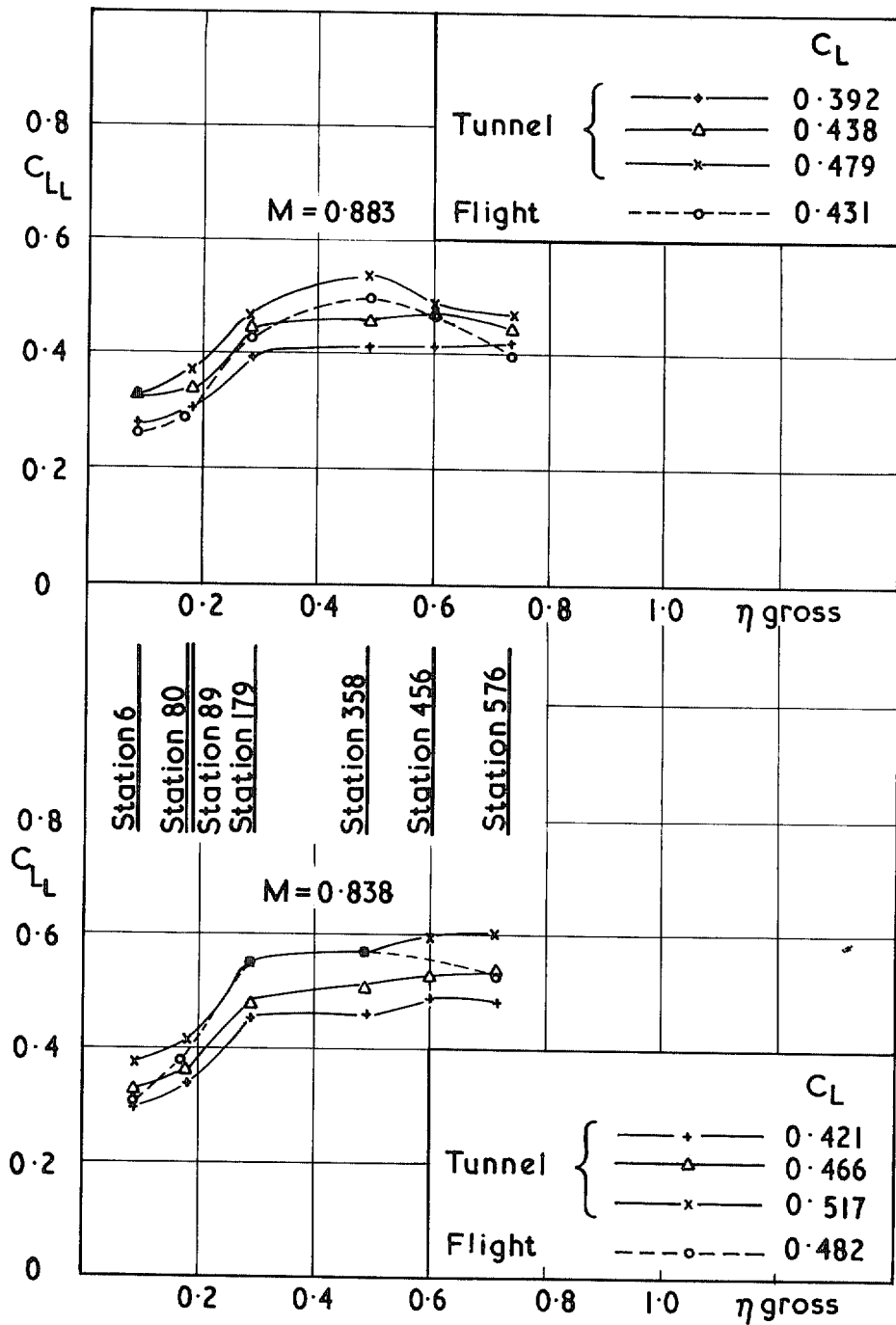


FIG. 13b. Spanwise lift distributions.

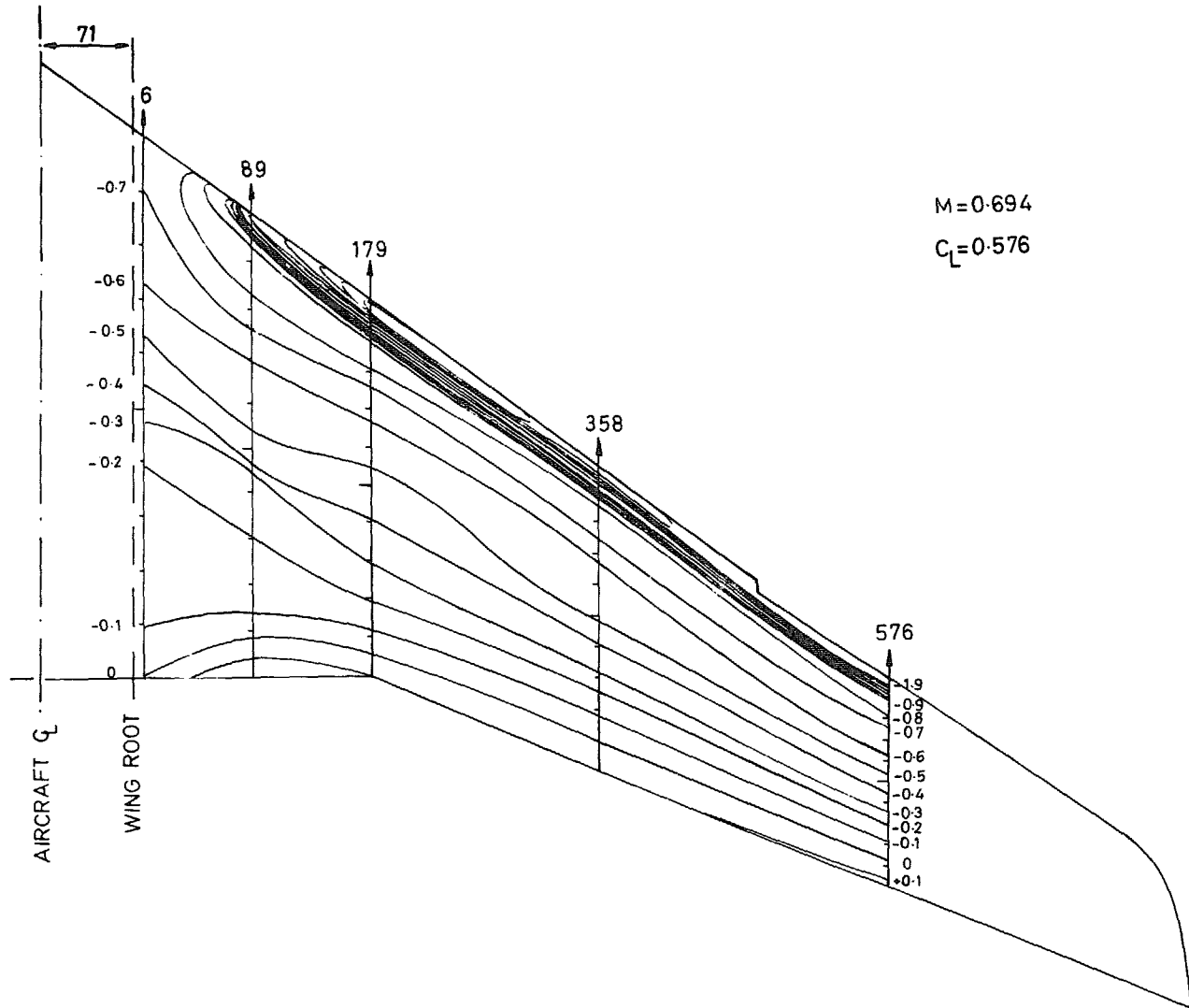


FIG. 14a. Flight isobars





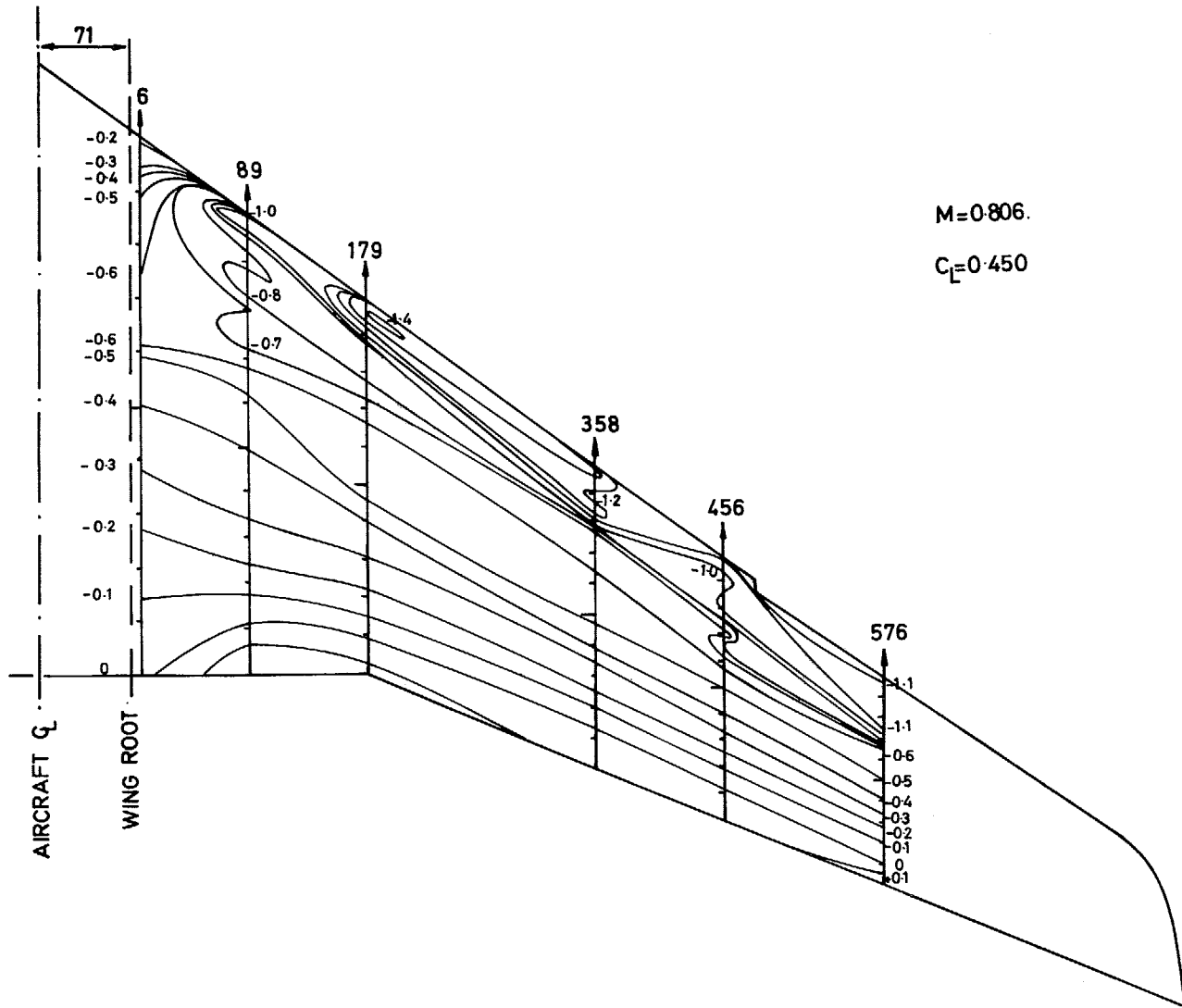


FIG. 15b. Tunnel isobars.

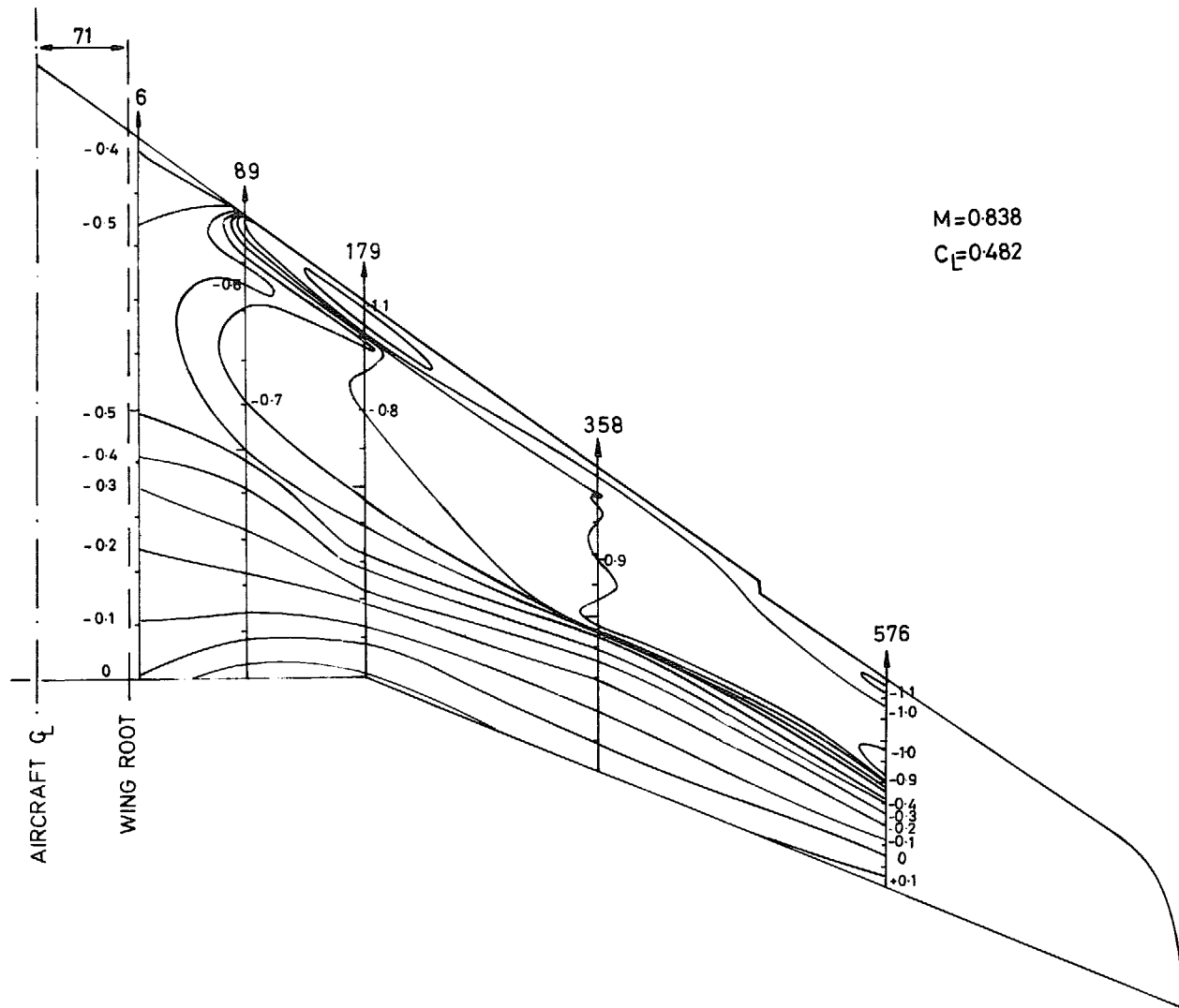


FIG. 16a. Flight isobars.

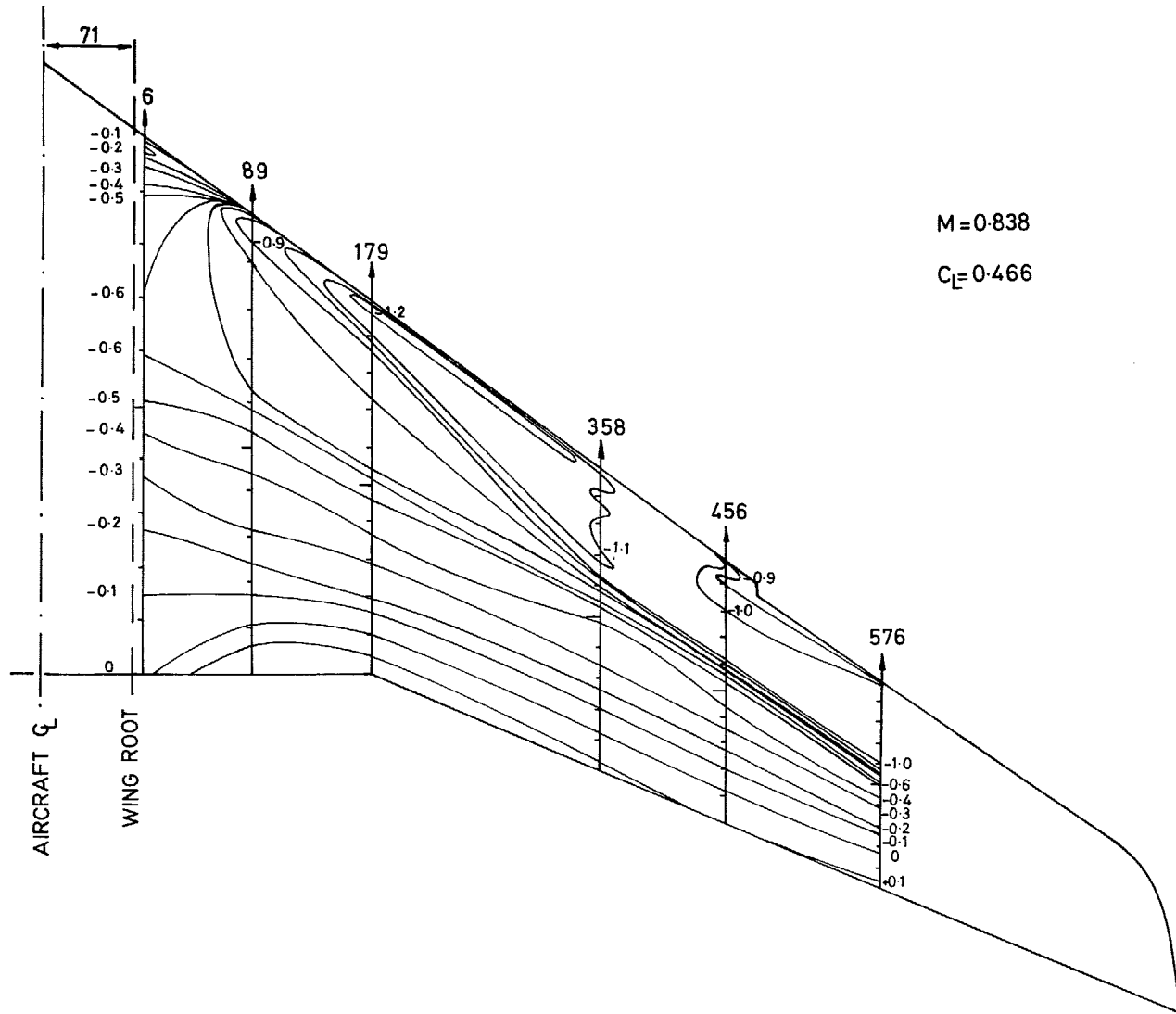


FIG. 16b. Tunnel isobars.



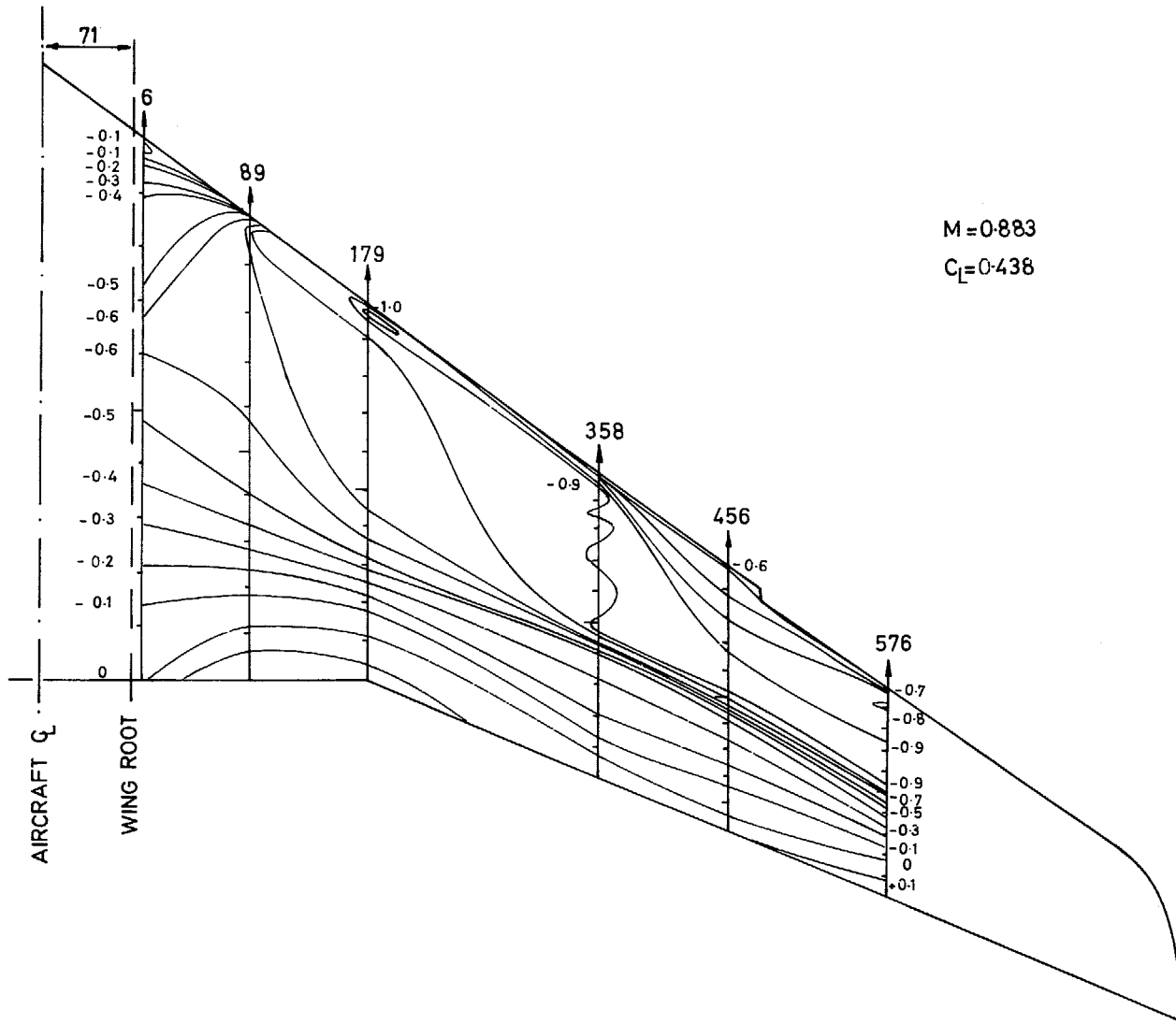


FIG. 17b. Tunnel isobars.

© *Crown Copyright* 1972

HER MAJESTY'S STATIONERY OFFICE

*Government Bookshops*

49 High Holborn, London WC1V 6HB  
13a Castle Street, Edinburgh EH2 3AR  
109 St Mary Street, Cardiff CF1 1JW  
Brazennose Street, Manchester M60 8AS  
50 Fairfax Street, Bristol BS1 3DE  
258 Broad Street, Birmingham B1 2HE  
80 Chichester Street, Belfast BT1 4JY

*Government publications are also available  
through booksellers*